

4-2014

Universal Breakaway Steel Post for Other Applications

Robert W. Bielenberg
University of Nebraska - Lincoln, rbielenberg2@unl.edu

Ronald K. Faller
University of Nebraska - Lincoln, rfaller1@unl.edu

Karla A. Lechtenberg
University of Nebraska - Lincoln, kpolivka2@unl.edu

Craig W. Price
university of Nebraska - Lincoln

Tyler L. Schmidt
University of Nebraska - Lincoln

See next page for additional authors

Follow this and additional works at: <http://digitalcommons.unl.edu/ndor>

 Part of the [Transportation Engineering Commons](#)

Bielenberg, Robert W.; Faller, Ronald K.; Lechtenberg, Karla A.; Price, Craig W.; Schmidt, Tyler L.; and Reid, John D., "Universal Breakaway Steel Post for Other Applications" (2014). *Nebraska Department of Transportation Research Reports*. 98.
<http://digitalcommons.unl.edu/ndor/98>

This Article is brought to you for free and open access by the Nebraska LTAP at DigitalCommons@University of Nebraska - Lincoln. It has been accepted for inclusion in Nebraska Department of Transportation Research Reports by an authorized administrator of DigitalCommons@University of Nebraska - Lincoln.

Authors

Robert W. Bielenberg, Ronald K. Faller, Karla A. Lechtenberg, Craig W. Price, Tyler L. Schmidt, and John D. Reid



TESTING CERT # 2937.01

Midwest States' Regional Pooled Fund Research Program

Fiscal Year 2013 (Year 23)

Research Project Number TPF-5 (193), Suppl. 55

NDOR Sponsoring Agency Code RPF-13-UBSP

UNIVERSAL BREAKAWAY STEEL POST FOR OTHER APPLICATIONS

Submitted by

Craig W. Price
Former Undergraduate Research Assistant

Tyler L. Schmidt
Undergraduate Research Assistant

Robert W. Bielenberg, M.S.M.E., E.I.T.
Research Associate Engineer

Karla A. Lechtenberg, M.S.M.E., E.I.T.
Research Associate Engineer

Ronald K. Faller, Ph.D., P.E.
Research Associate Professor
MwRSF Director

John D. Reid, Ph.D.
Professor

MIDWEST ROADSIDE SAFETY FACILITY

Nebraska Transportation Center
University of Nebraska-Lincoln
130 Whittier Research Center
2200 Vine Street
Lincoln, Nebraska 68583-0853
(402) 472-0965

Submitted to

MIDWEST STATES REGIONAL POOLED FUND PROGRAM

Nebraska Department of Roads
1500 Nebraska Highway 2
Lincoln, Nebraska 68502

MwRSF Research Report No. TRP-03-288-14

April 1, 2014

TECHNICAL REPORT DOCUMENTATION PAGE

1. Report No. TRP-03-288-14	2.	3. Recipient's Accession No.	
4. Title and Subtitle Universal Breakaway Steel Post for Other Applications		5. Report Date April 1, 2014	
7. Author(s) Price, C.W., Schmidt, T.L., Bielenberg, R.W., Lechtenberg, K.A., Faller, R.K., Reid, J.D.		8. Performing Organization Report No. TRP-03-288-14	
9. Performing Organization Name and Address Midwest Roadside Safety Facility (MwRSF) Nebraska Transportation Center University of Nebraska-Lincoln 130 Whittier Research Center 2200 Vine Street Lincoln, Nebraska 68583-0853		10. Project/Task/Work Unit No.	
12. Sponsoring Organization Name and Address Midwest States Regional Pooled Fund Program Nebraska Department of Roads 1500 Nebraska Highway 2 Lincoln, Nebraska 68502		11. Contract © or Grant (G) No. TPF-5 (193), Supplement 55	
13. Type of Report and Period Covered Final Report: 2012-2014		14. Sponsoring Agency Code RPPF-13-UBSP	
15. Supplementary Notes Prepared in cooperation with U.S. Department of Transportation, Federal Highway Administration.			
16. Abstract (Limit: 200 words) The Universal Breakaway Steel Post (UBSP) was developed and evaluated to replace the existing Controlled Release Terminal (CRT) wood posts which were used in the original bullnose guardrail system. Previously, three full-scale crash tests were performed on the thrie beam bullnose barrier with UBSPs, and the UBSP was determined to be a suitable alternative for the CRT posts. However, the UBSP was modified prior to the completion of the full-scale tests, and dynamic component testing was not conducted to compare the post behaviors. Therefore, a series of nine component tests were conducted in soil to compare the weak- and strong-axis properties between the UBSPs and CRT posts. As part of the component testing, one of the weak-axis tests involving the UBSP was conducted with a reused lower section of the post; since, the original development of the UBSP recommended reuse as long as the lower section was undamaged and displaced less than ½ in. (13 mm). From the testing series, it was determined that the performance of the UBSP indicated a strong potential for these posts to be utilized in other applications. However, UBSP should first be evaluated through engineering analysis and full-scale crash testing before implementation.			
17. Document Analysis/Descriptors Highway Safety, Roadside Appurtenances, Dynamic Test, Guardrail Posts, Wood Posts, UBSP, Universal Breakaway Steel Post, Equivalency, Safety, and CRT		18. Availability Statement No restrictions. Document available from: National Technical Information Services, Springfield, Virginia 22161	
19. Security Class (this report) Unclassified	20. Security Class (this page) Unclassified	21. No. of Pages 99	22. Price

DISCLAIMER STATEMENT

This report was completed with funding from the Federal Highway Administration, U.S. Department of Transportation. The contents of this report reflect the views and opinions of the authors who are responsible for the facts and the accuracy of the data presented herein. The contents do not necessarily reflect the official views or policies of the state highway departments participating in the Midwest States Regional Pooled Fund Program nor the Federal Highway Administration, U.S. Department of Transportation. This report does not constitute a standard, specification, regulation, product endorsement, or an endorsement of manufacturers.

UNCERTAINTY OF MEASUREMENT STATEMENT

The Midwest Roadside Safety Facility (MwRSF) has determined the uncertainty of measurements for several parameters involved in standard full-scale crash testing and non-standard testing of roadside safety features. Information regarding the uncertainty of measurements for critical parameters is available upon request by the sponsor and the Federal Highway Administration.

INDEPENDENT APPROVING AUTHORITY

The Independent Approving Authority (IAA) for the data contained herein was Dr. Jennifer Schmidt, P.E., Post-Doctoral Research Associate.

ACKNOWLEDGEMENTS

The authors wish to acknowledge several sources that made a contribution to this project:

(1) the Midwest States' Regional Pooled Fund Program funded by the Illinois Department of Transportation, Iowa Department of Transportation, Kansas Department of Transportation, Minnesota Department of Transportation, Missouri Department of Transportation, Nebraska Department of Roads, Ohio Department of Transportation, South Dakota Department of Transportation, Wisconsin Department of Transportation, and Wyoming Department of Transportation for sponsoring this project; and (2) MwRSF personnel for installing the posts and conducting the bogie tests.

Acknowledgement is also given to the following individuals who made a contribution to the completion of this research project.

Midwest Roadside Safety Facility

J.C. Holloway, M.S.C.E., E.I.T., Research Manager
S.K. Rosenbaugh, M.S.C.E., E.I.T., Research Associate Engineer
C.S. Stolle, Ph.D., E.I.T., Post-Doctoral Research Associate
J.D. Schmidt, Ph.D., P.E., Post-Doctoral Research Associate
A.T. Russell, B.S.B.A., Laboratory Mechanic II
K.L. Krenk, B.S.M.A, Field Operations Manager
D.S. Charroin, Laboratory Mechanic
S.M. Tighe, Laboratory Mechanic
Undergraduate and Graduate Assistants

Illinois Department of Transportation

Tim Sheehan, P.E., Safety Design Engineer
Priscilla A. Tobias, P.E., State Safety Engineer/Bureau Chief
David Piper, P.E., Highway Policy Engineer

Iowa Department of Transportation

David Little, P.E., Assistant District Engineer
Deanna Maifield, P.E., Methods Engineer
Chris Poole, Roadside Safety Engineer

Kansas Department of Transportation

Ron Seitz, P.E., Bureau Chief
Rod Lacy, P.E., Metro Engineer
Scott King, P.E., Road Design Leader

Minnesota Department of Transportation

Michael Elle, P.E., Design Standard Engineer

Missouri Department of Transportation

Joseph G. Jones, P.E., Engineering Policy Administrator

Nebraska Department of Roads

Phil TenHulzen, P.E., Design Standards Engineer
Jodi Gibson, Research Coordinator

Ohio Department of Transportation

Michael Bline, P.E., Standards and Geometrics Engineer
Maria E. Ruppe, P.E., Roadway Standards Engineer

South Dakota Department of Transportation

David Huft, Research Engineer
Bernie Clocksin, Lead Project Engineer

Wisconsin Department of Transportation

Jerry Zogg, P.E., Chief Roadway Standards Engineer
Erik Emerson, P.E., Standards Development Engineer

Wyoming Department of Transportation

William Wilson, P.E., Architectural and Highway Standards Engineer

Federal Highway Administration

John Perry, P.E., Nebraska Division Office
Danny Briggs, Nebraska Division Office

TABLE OF CONTENTS

TECHNICAL REPORT DOCUMENTATION PAGE i

DISCLAIMER STATEMENT ii

UNCERTAINTY OF MEASUREMENT STATEMENT ii

INDEPENDENT APPROVING AUTHORITY..... ii

ACKNOWLEDGEMENTS iii

TABLE OF CONTENTS..... v

LIST OF FIGURES vii

LIST OF TABLES ix

1 INTRODUCTION 1

 1.1 Background 1

 1.2 Objective 4

 1.3 Research Approach 4

2 TEST CONDITIONS..... 5

 2.1 Test Facility 5

 2.2 Equipment 5

 2.2.1 Bogie 5

 2.2.2 Accelerometers 6

 2.2.3 Retroreflective Optic Speed Trap 7

 2.2.4 Digital Photography 7

 2.3 End of Test Determination..... 8

 2.4 Data Processing..... 8

 2.5 Results..... 9

3 DYNAMIC TESTING..... 10

 3.1 Purpose..... 10

 3.2 Scope..... 10

 3.3 Post Details 11

 3.3.1 Test No. UBSPB-1 21

 3.3.2 Test No. UBSPB-2 24

 3.3.3 Test No. UBSPB-3 27

 3.3.4 Test No. UBSPB-4 30

 3.3.5 Test No. UBSPB-5 33

 3.3.6 Test No. UBSPB-6 37

 3.3.7 Test No. UBSPB-7 41

 3.3.8 Test No. UBSPB-8 44

 3.3.9 Test No. UBSPB-8B 49

 3.4 Discussion..... 52

3.4.1 Strong-Axis Testing 52
3.4.2 Weak-Axis Testing 54
3.4.3 Comparison of UBSPs with Reused Lower Section..... 56
3.4.4 Conclusions..... 56

4 SUMMARY, CONCLUSIONS, AND RECOMMENDATIONS 66
4.1 Summary and Conclusions 66
4.2 Recommendations..... 67

5 REFERENCES 69

6 APPENDICES 71
Appendix A. Material Certifications..... 72
Appendix B. Soil Batch Sieve Analysis..... 78
Appendix C. Bogie Test Results 80

LIST OF FIGURES

Figure 1. UBSP Installed in the Thrie Beam Bullnose	2
Figure 2. Rigid Frame Bogie and Guidance Track	6
Figure 3. CRT Bogie Testing Matrix and Setup	13
Figure 4. Breakaway Steel Post Bogie Testing Matrix and Setup	14
Figure 5. CRT Wood Post Details	15
Figure 6. Breakaway Steel Post Details	16
Figure 7. Breakaway Steel Post Assembly Details	17
Figure 8. Breakaway Steel Post Component Details	18
Figure 9. Washer and Plate Components	19
Figure 10. Bill of Materials	20
Figure 11. Force vs. Deflection and Energy vs. Deflection, Test No. UBSPB-1	22
Figure 12. Pre-Test Photograph, Test No. UBSPB-1	22
Figure 13. Time-Sequential and Post-Impact Photographs, Test No. UBSPB-1.....	23
Figure 14. Force vs. Deflection and Energy vs. Deflection, Test No. UBSPB-2	25
Figure 15. Pre-Test Photograph, Test No. UBSPB-2	25
Figure 16. Time-Sequential and Post-Impact Photographs, Test No. UBSPB-2.....	26
Figure 17. Force vs. Deflection and Energy vs. Deflection, Test No. UBSPB-3	28
Figure 18. Pre-Test Photograph, Test No. UBSPB-3	28
Figure 19. Time-Sequential and Post-Impact Photographs, Test No. UBSPB-3.....	29
Figure 20. Force vs. Deflection and Energy vs. Deflection, Test No. UBSPB-4	31
Figure 21. Pre-Test Photograph, Test No. UBSPB-4	31
Figure 22. Time-Sequential and Post-Impact Photographs, Test No. UBSPB-4.....	32
Figure 23. Force vs. Deflection and Energy vs. Deflection, Test No. UBSPB-5	34
Figure 24. Pre-Test Photograph, Test No. UBSPB-5	34
Figure 25. Time-Sequential and Post-Impact Photographs, Test No. UBSPB-5.....	35
Figure 26. Bolts and Lower Base Plate, Test No. UBSPB-5.....	36
Figure 27. Force vs. Deflection and Energy vs. Deflection, Test No. UBSPB-6	38
Figure 28. Pre-Test Photograph, Test No. UBSPB-6	38
Figure 29. Time-Sequential and Post-Impact Photographs, Test No. UBSPB-6.....	39
Figure 30. Fractured Bolts, Test No. UBSPB-6	40
Figure 31. Force vs. Deflection and Energy vs. Deflection, Test No. UBSPB-7	42
Figure 32. Pre-Test Photograph, Test No. UBSPB-7	42
Figure 33. Time-Sequential and Post-Impact Photographs, Test No. UBSPB-7.....	43
Figure 34. Force vs. Deflection and Energy vs. Deflection, Test No. UBSPB-8	45
Figure 35. Pre-Test Photograph, Test No. UBSPB-8	45
Figure 36. Time-Sequential and Post-Impact Photographs, Test No. UBSPB-8.....	46
Figure 37. Lower Section and Base Plate, Test No. UBSPB-8	47
Figure 38. Top Section, Test No. UBSPB-8	48
Figure 39. Force vs. Deflection and Energy vs. Deflection, Test No. UBSPB-8B	50
Figure 40. Pre-Test Photograph, Test No. UBSPB-8B.....	50
Figure 41. Time-Sequential and Post-Impact Photographs, Test No. UBSPB-8B	51
Figure 42. Force vs. Deflection Comparison Plot, Strong-Axis Tests.....	60
Figure 43. Energy vs. Deflection Comparison Plot, Strong-Axis Tests	61
Figure 44. Force vs. Deflection Comparison Plot, Weak-Axis Tests	62

Figure 45. Energy vs. Deflection Comparison Plot, Weak-Axis Tests 63
Figure 46. Force vs. Deflection of the Re-Run Tests, Test Nos. UBSPB-7 and UBSPB-8 64
Figure 47. Energy vs. Deflection of the Re-Run Tests, Test Nos. UBSPB-7 and UBSPB-8..... 65
Figure A-1. CRT Wooden Post, Test Nos. UBSPB-1 through UBSPB-4..... 73
Figure A-2. Washers, Bolts and Nuts, Test Nos. UBSPB-5 through UBSPB-8B..... 74
Figure A-3. Long Foundation Tube, Test Nos. UBSPB-5 through UBSPB-8B..... 75
Figure A-4. Post Material Certification, Test Nos. UBSPB-5 through UBSPB-8B..... 76
Figure A-5. Upper and Lower Shear Plates, Test Nos. UBSPB-5 through UBSPB-8B..... 77
Figure B-1. Soil Gradation for Test Nos. UBSPB-1 through UBSPB-8B..... 79
Figure C-1. Results of Test No. UBSPB-1 (SLICE) 81
Figure C-2. Results of Test No. UBSPB-1 (EDR-3) 82
Figure C-3. Results of Test No. UBSPB-2 (SLICE) 83
Figure C-4. Results of Test No. UBSPB-2 (EDR-3) 84
Figure C-5. Results of Test No. UBSPB-3 (SLICE) 85
Figure C-6. Results of Test No. UBSPB-3 (EDR-3) 86
Figure C-7. Results of Test No. UBSPB-4 (SLICE) 87
Figure C-8. Results of Test No. UBSPB-4 (EDR-3) 88
Figure C-9. Results of Test No. UBSPB-5 (SLICE) 89
Figure C-10. Results of Test No. UBSPB-5 (EDR-3) 90
Figure C-11. Results of Test No. UBSPB-6 (SLICE) 91
Figure C-12. Results of Test No. UBSPB-6 (EDR-3) 92
Figure C-13. Results of Test No. UBSPB-7 (SLICE) 93
Figure C-14. Results of Test No. UBSPB-7 (EDR-3) 94
Figure C-15. Results of Test No. UBSPB-8 (SLICE) 95
Figure C-16. Results of Test No. UBSPB-8 (EDR-3) 96
Figure C-17. Results of Test No. UBSPB-8B (SLICE)..... 97
Figure C-18. Results of Test No. UBSPB-8B (EDR-3) 98

LIST OF TABLES

Table 1. Dynamic Testing Matrix, Test Nos. UBSPB-1 through UBSPB-8B 11
Table 2. Moisture Contents of CRT Wood Posts, Test Nos. UBSPB-1 through UBSPB-4..... 12
Table 3. Results of Bogie Testing..... 59

1 INTRODUCTION

1.1 Background

Between 1997 and 2000, the Midwest Roadside Safety Facility (MwRSF) developed a three-beam bullnose guardrail system to be used to shield hazards located on the median of divided highways [1-3]. After full-scale crash testing, the system passed an evaluation according to the Test Level 3 (TL-3) criteria provided in the National Cooperative Highway Research Program (NCHRP) Report No. 350 [4]. Controlled Release Terminal (CRT) wood posts [5] were used in the original bullnose guardrail system to aid in the energy absorption of the system. Although the three beam bullnose with CRT posts adequately met the TL-3 safety requirements, the use of wood posts was believed to have several drawbacks. First, the properties and performance of wood posts are variable due to knots, checks, and splits, thus requiring grading and inspection of posts. Second, two holes are drilled into the CRT posts that allow them to break away upon impact. These holes expose the interior of the wood to the environment, which may accelerate deterioration. Further, chemical preservatives used to treat the wood posts have been identified as harmful to the environment by some government agencies. Thus, the use of treated wood posts may require special consideration during disposal. Due to these concerns, a need existed for a breakaway steel post option for use in the three beam bullnose guardrail system.

In order to address this need, MwRSF developed the Universal Breakaway Steel Post (UBSP) to replace the CRT wood posts in the three beam bullnose system [6-9]. The design goal of the new, non-proprietary, UBSP was to mimic the strength and behavior of the wooden CRT post. The UBSP, as shown in Figure 1, consisted of a W6x9 (W152x13.4) steel post top section, which was the standard steel section used in strong-post guardrail, and a 6-in. x 8-in. x $\frac{3}{16}$ -in.



Figure 1. UBSP Installed in the Thrie Beam Bullnose

(152-mm x 203-mm x 5-mm) steel tube bottom section. The bottom section was designed with the same cross-section size as the CRT post to ensure similar post-soil resistive forces. The two post sections were welded to base plates and connected by four $\frac{7}{16}$ -in. (11-mm) diameter, ASTM A325 bolts. The new post design released through fracturing the four vertical bolts connecting the top and bottom halves of the post. Different strong- and weak-axis capacities were generated by the spacing of the bolts in the base plates.

During the R&D effort, three successful full-scale crash tests were performed on the thrie beam bullnose barrier with UBSPs. Based on the satisfactory crash performance with UBSPs, the researchers determined that the UBSP was a suitable alternative for wood, CRT post used in the original thrie beam bullnose system.

Following the initial dynamic bogie testing program, design modifications were incorporated into the final UBSP prior to completion of the full-scale crash testing program. These changes consisted of incorporating larger diameter bolts to connect the two halves of the post and changing the spacing of those bolts in order to fine tune the post capacity. While these changes worked well in the full-scale crash testing, the final post design was never component tested to quantify its capacity in the weak and strong axis of bending. Thus, further dynamic component testing of the UBSP will be required and compared to the CRT post behavior. The satisfactory performance of the UBSP in the bullnose median barrier system would indicate a potential for UBSPs to be used as a surrogate in other CRT applications, such as in the long-span guardrail system, guardrail end terminals, guardrail systems installed in subsurface rock foundations or rigid pavement mow strips, future short-radius guardrails, and new, reduced maintenance barrier systems. However, further analysis and testing would be required to verify its performance in these other guardrail applications.

1.2 Objective

The objective of this research project was to investigate the feasibility of the UBSP for use in other guardrail systems and as a replacement to CRT posts. This study would focus on a comparison of the weak- and strong-axis properties of the UBSP with those of CRT posts. If the results from the comparison were positive, a second phase of the research would be conducted to select guardrail systems in which the UBSP could potentially be used in lieu of CRT posts, conduct full-scale crash testing and evaluation, and document the crash testing results.

1.3 Research Approach

The research project began with a series of dynamic component tests of UBSPs and CRT posts in soil. The test matrix consisted of four tests on each post type and included two tests each along the strong axis and weak axis of the posts. All posts were installed in a soil compliant with the Manual for Assessing Safety Hardware (MASH) [10]. The component test data was analyzed and compared. From the test results, MwRSF prepared recommendations regarding the UBSP's use as a potential replacement for timber CRT posts in other barrier systems along with guidance regarding the extent of a future Phase II full-scale crash testing and evaluation program.

2 TEST CONDITIONS

2.1 Test Facility

Physical testing of the 6-in. x 8-in. (152-mm x 203-mm) CRT wood posts and W6x9 (W152x13.4) universal breakaway steel posts was conducted at the MwRSF testing facility which is located at the Lincoln Air Park on the Northwest side of the Lincoln Municipal Airport. The facility is approximately 5 miles (8 km) northwest from the University of Nebraska-Lincoln's city campus.

2.2 Equipment

Equipment and instrumentation utilized to collect and record data during the dynamic bogie tests included a bogie, onboard accelerometers, retroreflective speed trap, high-speed and standard-speed digital cameras, and a still camera.

2.2.1 Bogie

A rigid-frame bogie was used to impact the posts. A variable-height, detachable impact head was used in the testing. The bogie head was constructed of 8-in. (203-mm) diameter, 1/2-in. (13-mm) thick standard steel pipe, with 3/4-in. (19-mm) neoprene belting wrapped around the pipe to prevent local damage to the post from the impact. The impact head was bolted to the bogie vehicle, creating a rigid frame with an impact height of 24⁷/₈ in. (632 mm). The bogie with the impact head is shown in Figure 2. The weight of the bogie with the addition of the mountable impact head and accelerometers was 1,875 lb (850 kg).

A pickup truck with a reverse cable tow system was used to propel the bogie to a target impact speed of 20 mph (32 km/h). When the bogie approached the end of the guidance system, it was released from the tow cable, allowing it to be free rolling when it impacted the post. A remote braking system was installed on the bogie allowing it to be brought safely to rest after the test.



Figure 2. Rigid Frame Bogie and Guidance Track

2.2.2 Accelerometers

Two environmental shock and vibration sensor/recorder systems were mounted on the bogie vehicle near its center of gravity (c.g.) to measure the accelerations in the longitudinal, lateral, and vertical directions. However, only the longitudinal accelerations were processed and reported.

The first accelerometer system, SLICE 6DX was a modular data acquisition system manufactured by Diversified Technical Systems, Inc. (DTS) of Seal Beach, California. The acceleration sensors were mounted inside the body of the custom built SLICE 6DX event data recorder and recorded data at 10,000 Hz to the onboard microprocessor. The SLICE 6DX was configured with 7 GB of non-volatile flash memory, a range of ± 500 g's, a sample rate of 10,000 Hz, and a 1,650 Hz (CFC 1000) anti-aliasing filter. The "SLICEWare" computer software programs and a customized Microsoft Excel worksheet were used to analyze and plot the accelerometer data.

The second accelerometer, Model EDR-3, was a triaxial piezoresistive accelerometer system developed by Instrumental Sensor Technology (IST) of Okemos, Michigan. The EDR-3

was configured with 256 kB of RAM, a range of ± 200 g's, a sample rate of 3,200 Hz, and a 1,120-Hz low-pass filter. The "DynaMax 1 (DM-1)" computer software program and a customized Microsoft Excel worksheet were used to analyze and plot the accelerometer data.

2.2.3 Retroreflective Optic Speed Trap

A retroreflective optic speed trap was used to determine the speed of the bogie vehicle before impact in test nos. UBSPB-1 through UBSPB-8B. Three retroreflective targets, spaced at approximately 4-in. (102-mm) intervals, were applied to the side of the bogie vehicle which reflected the beam of light. When the emitted beam of light was returned to the Emitter/Receiver, a signal was sent to the Optic Control Box, which in turn sent a signal to the data computer as well as activated the External LED box. The computer recorded the signals and the time each occurred. The speed was then calculated using the spacing between the retroreflective targets and the time between the signals. LED lights and high-speed digital video analysis are only used as a backup in the event that vehicle speeds cannot be determined from the electronic data.

2.2.4 Digital Photography

One AOS VITcam high-speed digital video camera and two JVC digital video cameras were used to document each test. The AOS high-speed camera had a frame rate of 500 frames per second and the JVC digital video cameras had frame rates of 29.97 frames per second. The high-speed digital video camera and one digital video camera were placed laterally from the post, with a view perpendicular to the bogie's direction of travel. The second digital video camera was placed on the opposite side of the post with respect to the other two cameras. A Nikon D50 digital still camera was also used to document pre- and post-test conditions for all tests.

2.3 End of Test Determination

When the impact head initially contacted the test article, the force exerted by the surrogate test vehicle was directly perpendicular. However, as the post rotated, the surrogate test vehicle's orientation and path moved further from perpendicular. This introduced two sources of error: (1) the contact force between the impact head and the post has a vertical component and (2) the impact head slides upward along the test article. Therefore, only the initial portion of the accelerometer trace may be used since variations in the data become significant as the system rotates and the surrogate test vehicle overrides the system. For this reason, the end of the test needed to be defined.

Guidelines were established to define the end-of-test time using the high-speed digital video of the crash test. The first occurrence of any one of the following three events was used to determine the end of the test: (1) the test article fractures; (2) the surrogate vehicle overrides/loses contact with the test article; or (3) a maximum post rotation of 45 degrees.

2.4 Data Processing

The electronic accelerometer data obtained in dynamic testing was filtered using the SAE Class 60 Butterworth filter conforming to the SAE J211/1 specifications [11]. The pertinent acceleration signal was extracted from the bulk of the data signals. The processed acceleration data was then multiplied by the mass of the bogie to get the impact force using Newton's Second Law. Next, the acceleration trace was integrated to find the change in velocity versus time. Initial velocity of the bogie, calculated from the optic speed trap data, was then used to determine the bogie velocity, and the calculated velocity trace was integrated to find the bogie's displacement, which is also the deflection of the post. Combining the previous results, a force vs. deflection curve was plotted for each test. Finally, integration of the force vs. deflection curve provided the energy vs. deflection curve for each test.

2.5 Results

The information desired from the bogie tests was the relation between the applied force and deflection of the post at the impact location. This data was then used to find the total energy (the area under the force versus deflection curve) dissipated during each test. The energy curve was used to compute the average force at a specific deflection using the following formula:

$$\bar{F} = \frac{Energy}{Deflection}$$

Although the acceleration data was applied to the impact location, the data came from the c.g. of the bogie. Error was added to the data since the bogie was not perfectly rigid and sustained vibrations. The bogie may have also rotated during impact, causing differences in accelerations between the bogie center of mass and the bogie impact head. While these issues may affect the data, the data was still valid. Filtering procedures were applied to the data to smooth out vibrations, and the rotations of the bogie during test were minor. One useful aspect of using accelerometer data was that it included influences of the post inertia on the reaction force. This was important as the mass of the post would affect barrier performance as well as test results.

The accelerometer data for each test was processed in order to obtain acceleration, velocity, and deflection curves, as well as force vs. deflection and energy vs. deflection curves. The values described herein were calculated from the SLICE data curves.

3 DYNAMIC TESTING

3.1 Purpose

In previous research, MwRSF has conducted successful full-scale crash tests using W6x9 (W152x13.4) Universal Breakaway Steel Posts (UBSP) in a three-beam bullnose guardrail system. However, additional component testing was desired to evaluate the potential for the UBSP posts to be used in other applications. Therefore, bogie tests were undertaken on both controlled releasing terminal (CRT) wood posts and the UBSPs in order to compare their dynamic properties.

3.2 Scope

Nine bogie tests were conducted on 6-in. x 8-in. (152-mm x 203-mm) CRT wood posts and W6x9 (W152x13.4) UBSPs in soil. All of the tests used an embedment depth of 40 in. (1,016 mm). The target impact speed for all tests was 20 mph (32 km/h) and the posts were impacted $24\frac{7}{8}$ in. (632 mm) above the ground line perpendicular to the face of the post. Four of the tests used an impact angle of 90 degrees, creating a classical “head-on” or full-frontal impact and strong-axis bending. The remaining five tests used an impact angle of 0 degrees, creating weak-axis bending. The bogie testing matrix is shown in Table 1 and the test setup is shown in Figures 3 through 10. Material specifications, mill certificates, and certificates of conformity for the post materials used in all nine tests are shown in Appendix A.

Table 1. Dynamic Testing Matrix, Test Nos. UBSPB-1 through UBSPB-8B

Test No.	Post Type	Impact Axis	Foundation Type	Post Length in. (mm)	Embedment Depth in. (mm)	Target Impact Velocity mph (km/h)
UBSPB-1	CRT	Strong	Soil	72 (1,829)	40 (1,016)	20 (32)
UBSPB-2	CRT	Strong	Soil	72 (1,829)	40 (1,016)	20 (32)
UBSPB-3	CRT	Weak	Soil	72 (1,829)	40 (1,016)	20 (32)
UBSPB-4	CRT	Weak	Soil	72 (1,829)	40 (1,016)	20 (32)
UBSPB-5	Steel Breakaway	Strong	Soil	72 (1,829)	40 (1,016)	20 (32)
UBSPB-6	Steel Breakaway	Strong	Soil	72 (1,829)	40 (1,016)	20 (32)
UBSPB-7	Steel Breakaway	Weak	Soil	72 (1,829)	40 (1,016)	20 (32)
UBSPB-8	Steel Breakaway	Weak	Soil	72 (1,829)	40 (1,016)	20 (32)
UBSPB-8B	Steel Breakaway	Weak	Soil	72 (1,829)	40 (1,016)	20 (32)

3.3 Post Details

CRT wood posts were fabricated from grade No. 1 or better, non-dense southern yellow pine (SYP) material. The moisture content for each post is listed in

. A 72-in. (1,829-mm) long, CRT wood post with a standard 6-in. x 8-in. (152-mm x 203-mm) cross section was utilized during testing and weakened by drilling out two 3½-in. (89-mm) holes in the middle region of the post, as shown in Figure 5. The CRT post was impacted at a height of 24⅞ in. (632 mm) above the ground line with an embedment depth of 40 in. (1,016 mm) rather than the longer CRT posts which were used in the original bullnose system. The goal of this effort was to determine the feasibility of UBSP to replace CRT wood posts in other systems. The other systems that will be researched will most likely be MGS type systems and thus, the 72-in. (1,829-mm) long CRT post was tested.

Table 2. Moisture Contents of CRT Wood Posts, Test Nos. UBSPB-1 through UBSPB-4

Test No.	Moisture Content (%)*		
	Top of the Post	Groundline	Bottom of the Post
UBSPB-1	12	17	15
UBSPB-2	12	17	8
UBSPB-3	11	25	12
UBSPB-4	13	16	13

*Measured at impact face

The UBSP was comprised of an upper W6x9 (W152x13.4) beam which was connected to the lower 6-in. x 8-in. (152-mm x 203-mm) foundation tube. A ¾-in. (19-mm) thick steel plate was rigidly welded to the bottom of the W6x9 (W152x13.4) beam and a ½-in. (13-mm) thick steel plate was rigidly welded to the top of the foundation tube. Four breakaway steel bolts, four nuts and sixteen washers were used to connect the two different components as shown in Figure 6. It should be noted that the testing detailed herein used F844 standard washers for the four washers located at each of the bolts connecting the top and bottom halves of the UBSP. Previous component testing and full-scale crash testing have demonstrated that F844 and F436 washers both perform acceptably when used in the UBSP.

A compacted, coarse, crushed limestone material, as recommended by MASH, was utilized for all tests [10]. Soil specifications are shown in Appendix B. MASH adheres to the general philosophy that testing longitudinal barriers in stiff soil results in higher impact and barrier loads, increased occupant risk values, and increased propensity for rail rupture, pocketing, and snag. Therefore, MASH has established a minimum post-soil resistance force standard to ensure systems are installed in strong, stiff soil. Thus, using heavily compacted soils was justified by MASH. Therefore, all tests utilized heavily compacted soil.

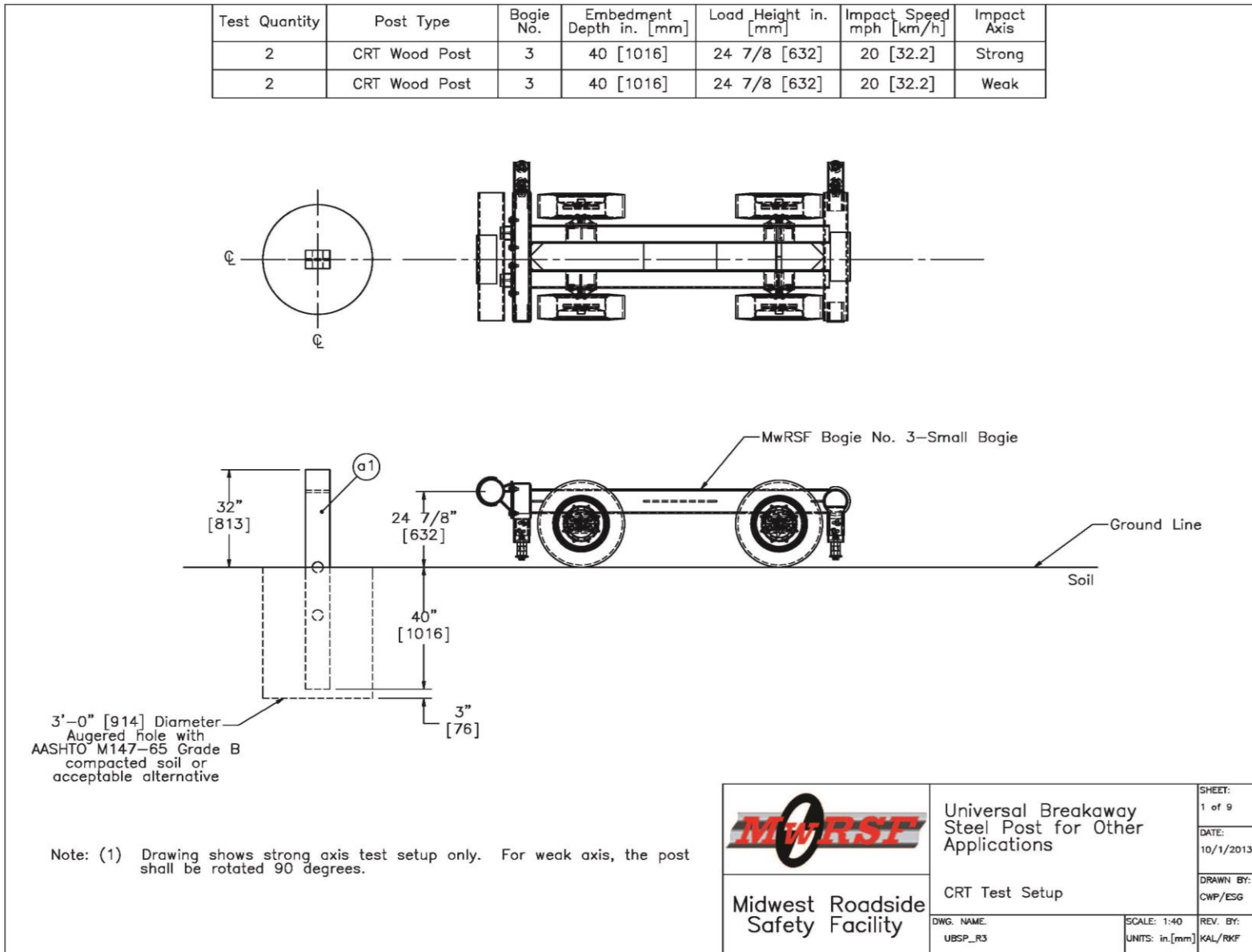


Figure 3. CRT Bogie Testing Matrix and Setup

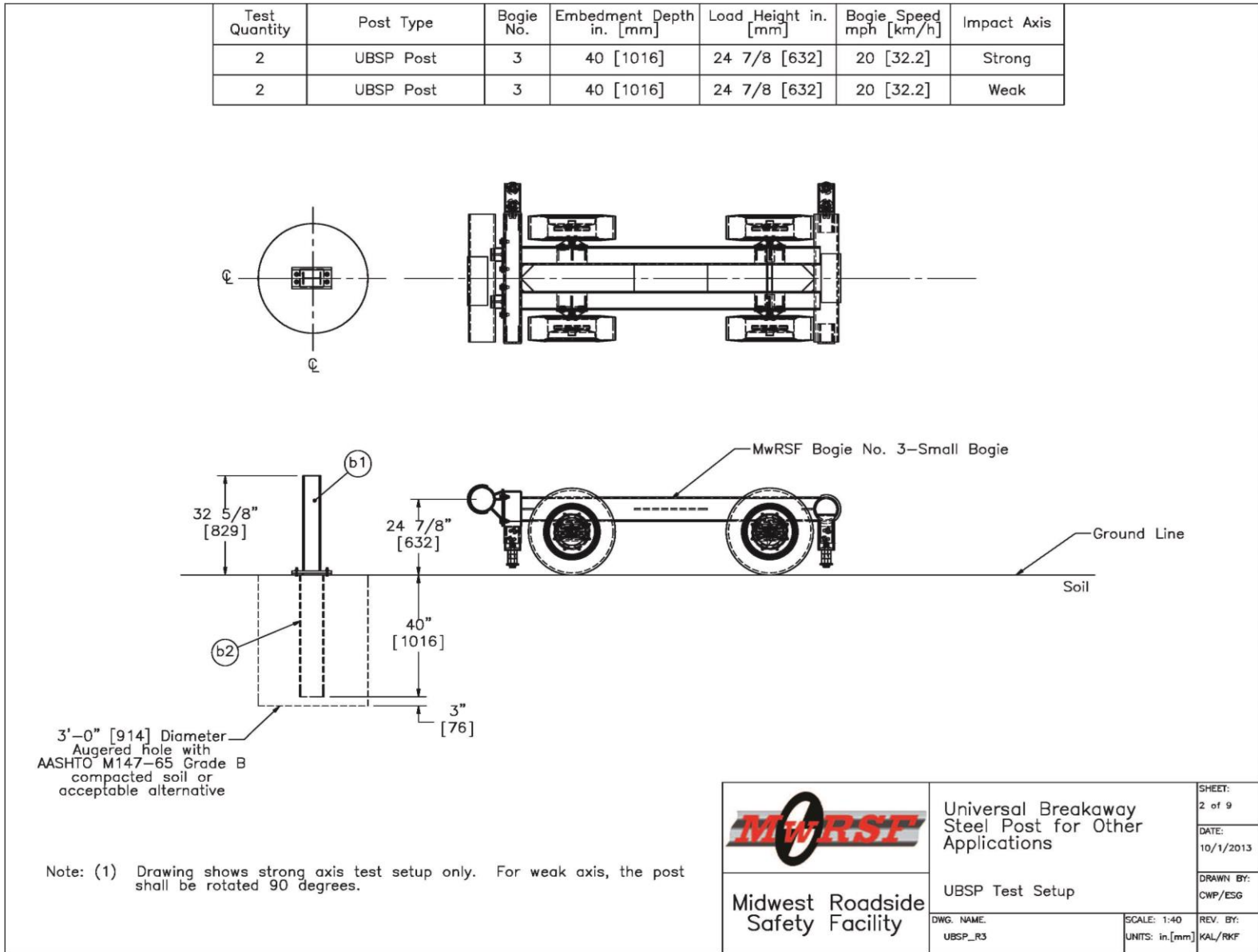


Figure 4. Breakaway Steel Post Bogie Testing Matrix and Setup

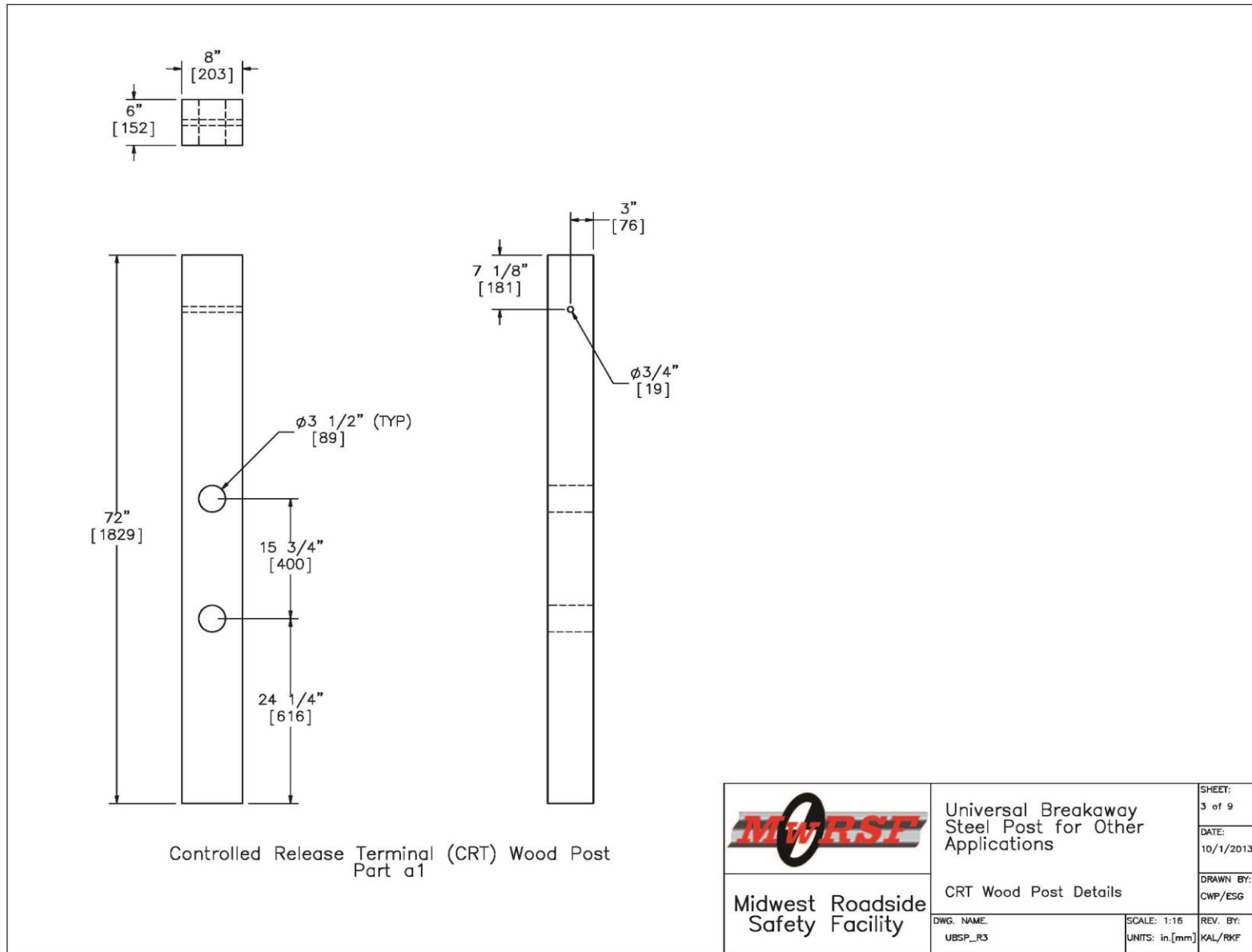


Figure 5. CRT Wood Post Details

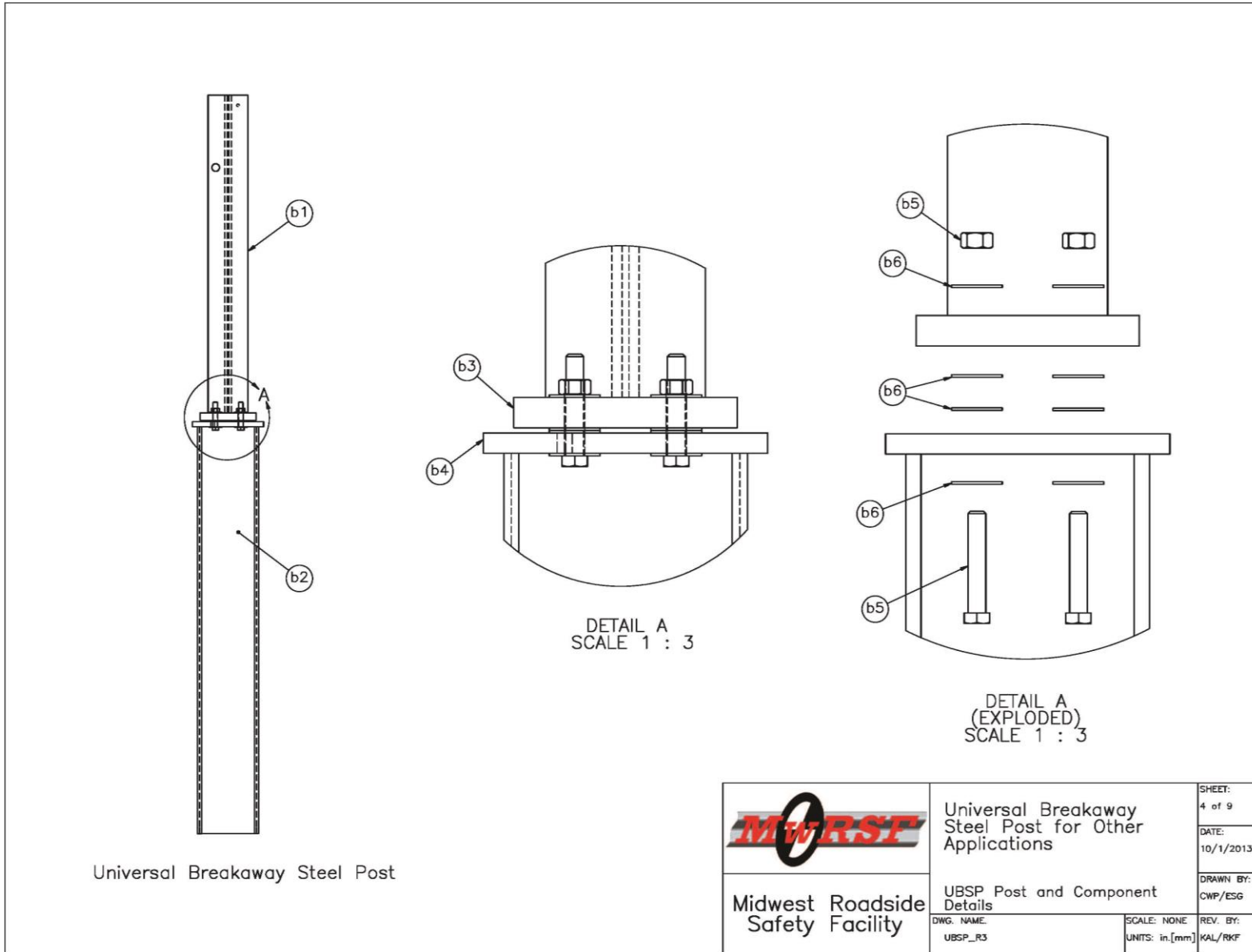


Figure 6. Breakaway Steel Post Details

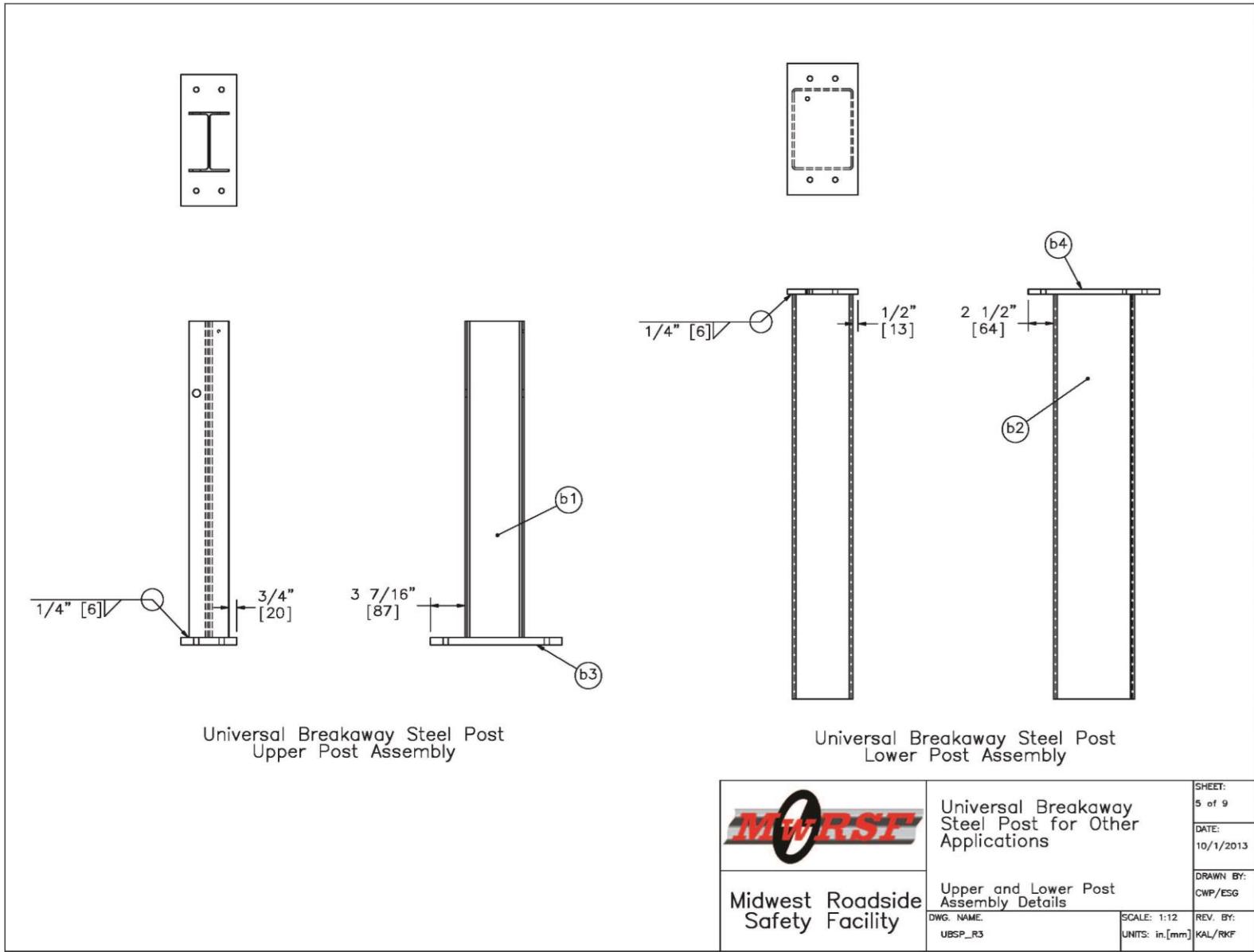


Figure 7. Breakaway Steel Post Assembly Details

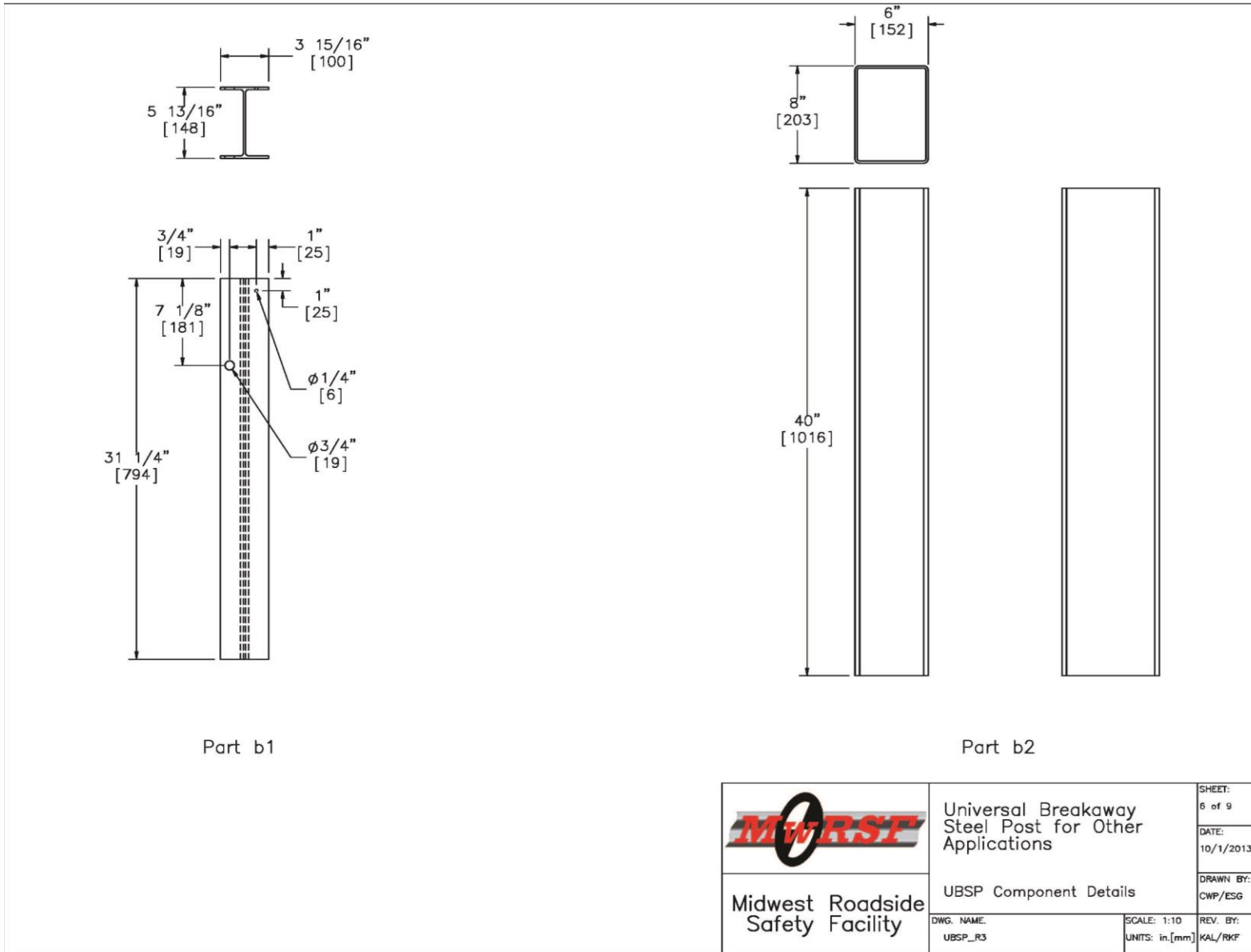


Figure 8. Breakaway Steel Post Component Details

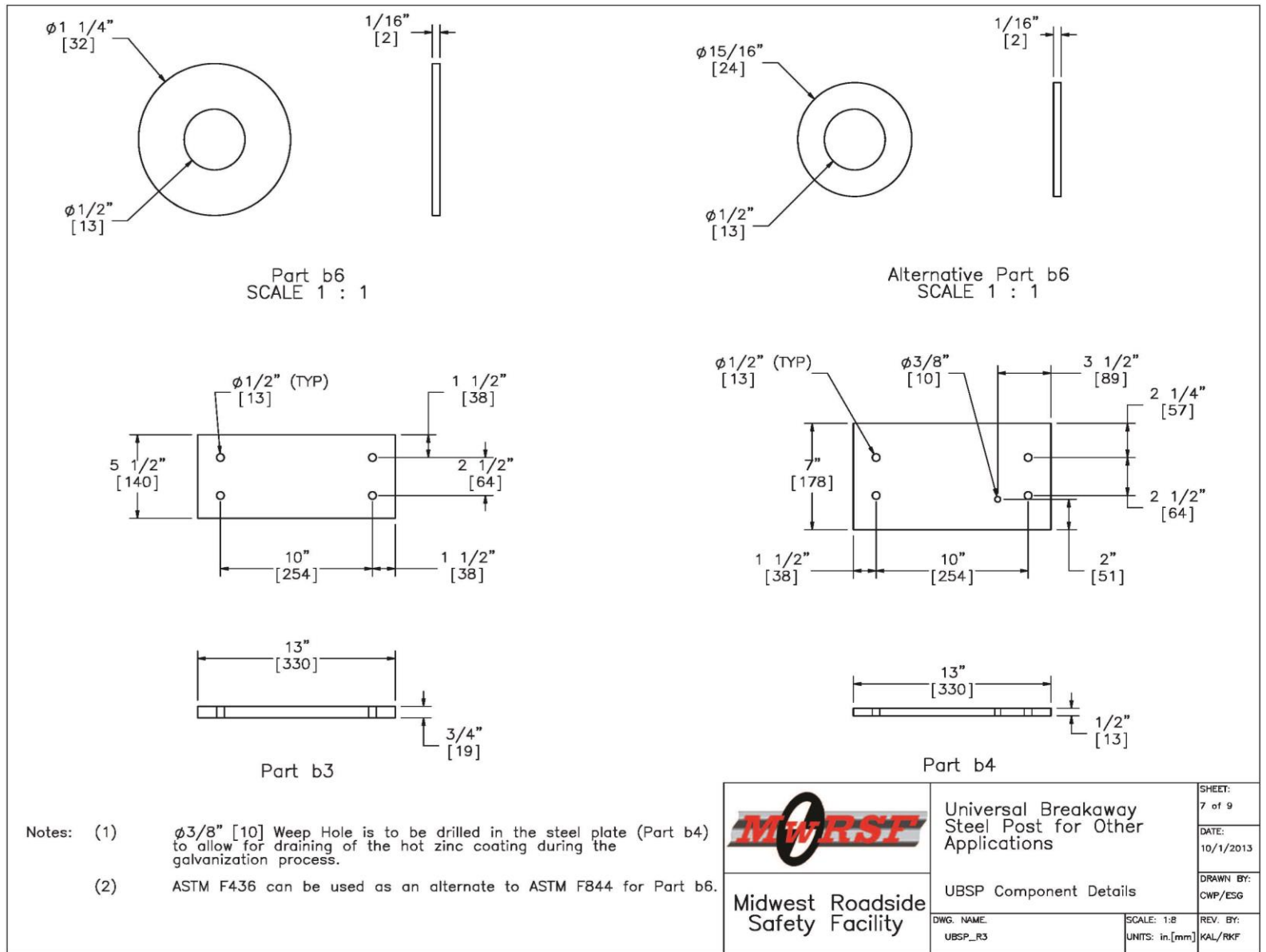


Figure 9. Washer and Plate Components

3.3.1 Test No. UBSPB-1

During test no. UBSPB-1, the bogie impacted the CRT wood post, which created strong-axis bending a speed of 21.1 mph (34.0 km/h). Initially, the post began to rotate backward. However, by 8 ms, the post began to fracture. The top of the post continued to rotate backward until the bogie overrode it. Upon post-test examination, the post was found to have fractured through the hole at ground level.

Force vs. deflection and energy vs. deflection curves created from the SLICE accelerometer data are shown in Figure 11. The post reached a peak force of 14.5 kips (64.5 kN) at 3.3 in. (84 mm) of deflection. At this point, the post began to fracture, and the resistive forces rapidly declined. By the completion of fracture, the post absorbed 35.9 kip-in. (4.1 kJ) of energy at a deflection of 4.9 in. (124 mm). A pre-test photograph is shown in Figure 12. Time-sequential and post-impact photographs are shown in Figure 13.

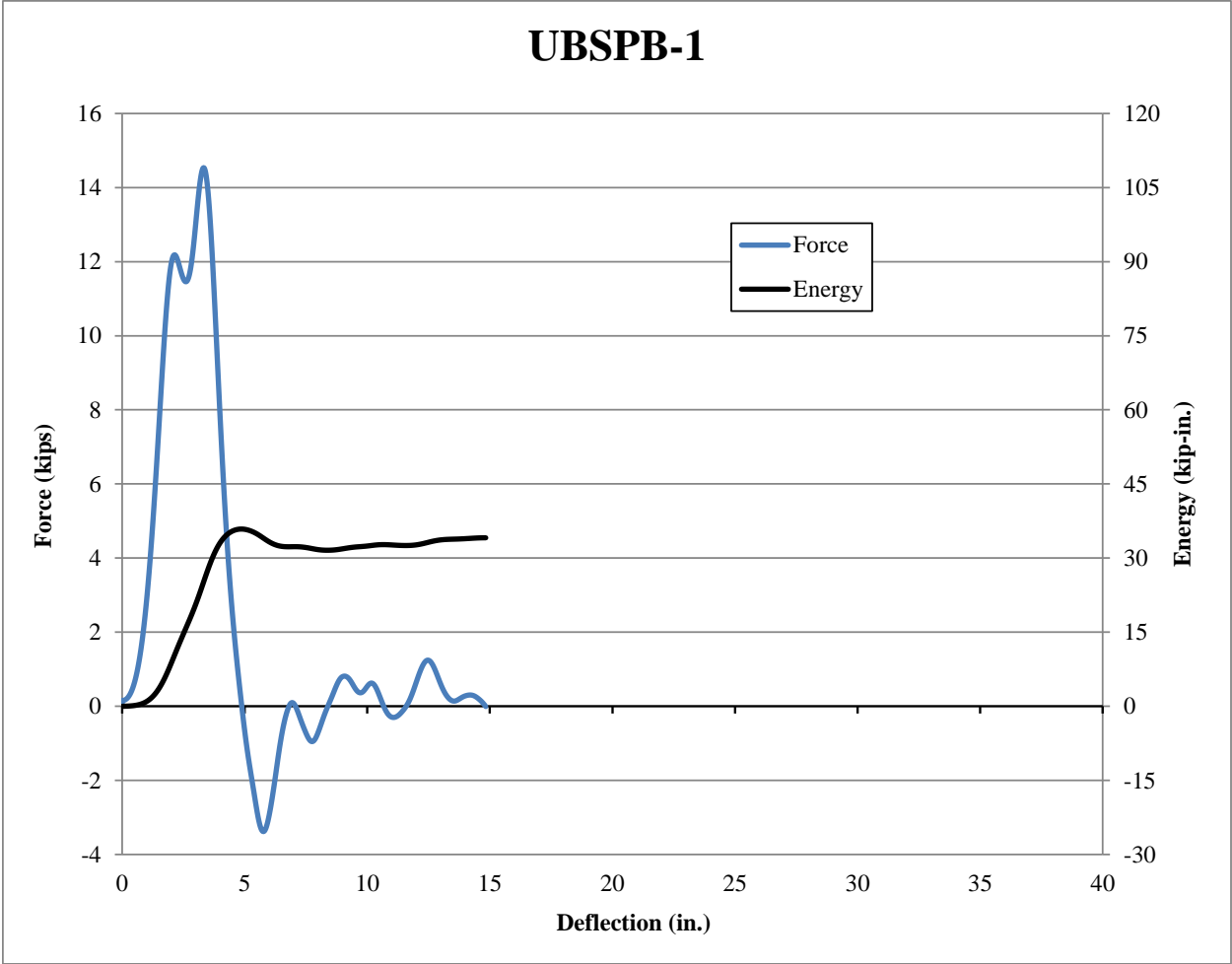


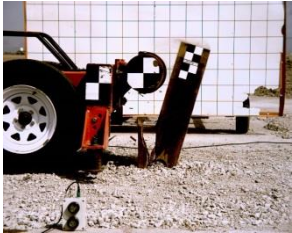
Figure 11. Force vs. Deflection and Energy vs. Deflection, Test No. UBSPB-1



Figure 12. Pre-Test Photograph, Test No. UBSPB-1



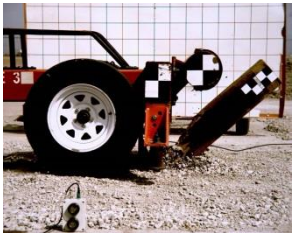
IMPACT



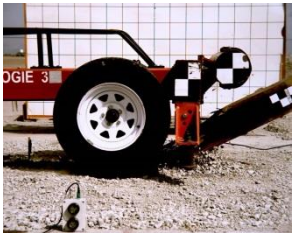
0.020 sec



0.040 sec



0.060 sec



0.080 sec



0.100 sec



Figure 13. Time-Sequential and Post-Impact Photographs, Test No. UBSPB-1

3.3.2 Test No. UBSPB-2

During test no. UBSPB-2, the bogie impacted the CRT wood post, which created strong-axis bending at a speed of 21.2 mph (34.1 km/h). Initially, the post began to rotate backward. However, by 13 ms, the post began to fracture. The top of the post continued to rotate backward until the bogie lost contact with it and overrode it. Upon post-test examination, the post fractured through the hole at ground level.

Force vs. deflection and energy vs. deflection curves created from the SLICE accelerometer data are shown in Figure 14. The post reached a peak force of 14.4 kips (64.1 kN) at 4.4 in. (112 mm) of deflection. Due to fracture of the post, the force quickly dropped to zero as the bogie lost contact with the post momentarily, followed by a second force spike. By the completion of fracture at a deflection of 11.4 in. (290 mm), the post absorbed 48.6 kip-in. (5.5 kJ) of energy. A pre-test photograph is shown in Figure 15. Time-sequential and post-impact photographs are shown in Figure 16.

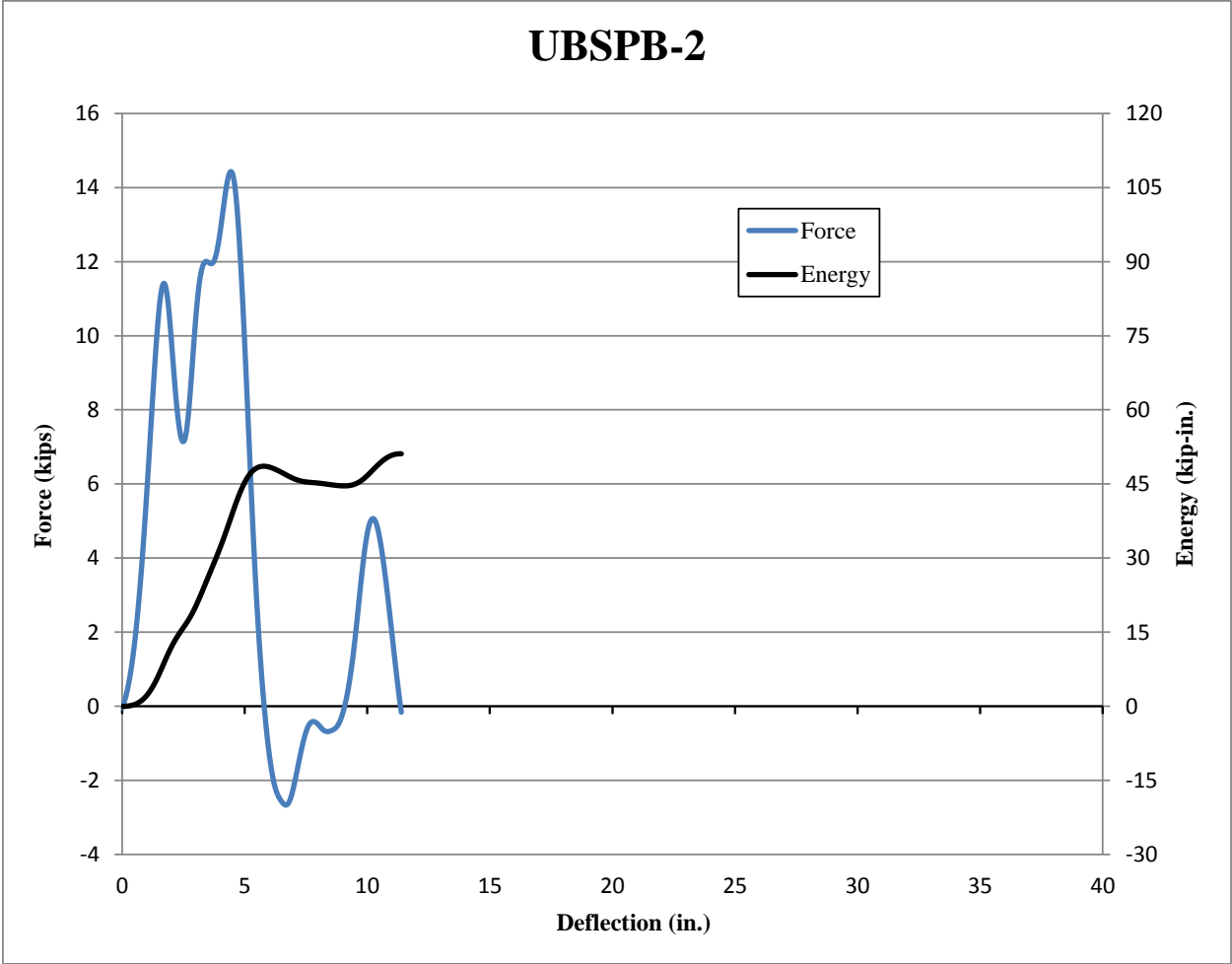
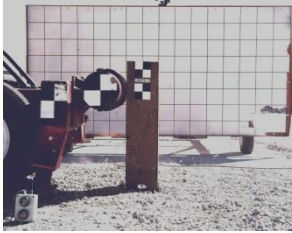


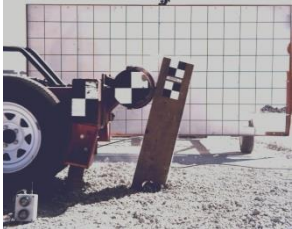
Figure 14. Force vs. Deflection and Energy vs. Deflection, Test No. UBSPB-2



Figure 15. Pre-Test Photograph, Test No. UBSPB-2



IMPACT



0.020 sec



0.040 sec



0.060 sec



0.080 sec



0.100 sec



Figure 16. Time-Sequential and Post-Impact Photographs, Test No. UBSPB-2

3.3.3 Test No. UBSPB-3

During test no. UBSPB-3, the bogie impacted the CRT wood post, which created weak-axis bending at a speed of 20.0 mph (32.2 km/h). Initially, the post began to rotate backward. However, by 20 ms, the post began to fracture. The top of the post continued to rotate backward until the bogie lost contact with it and overrode it at 120 ms. Upon post-test examination, the post was found to have fractured along a diagonal line extending from the lower CRT hole on the back side of the post to the upper CRT hole on the impact side of the post.

Force vs. deflection and energy vs. deflection curves created from the SLICE accelerometer data are shown in Figure 17. The post reached a peak force of 11.1 kips (49.4 kN) at 1.7 in. (43 mm) of deflection. Around 7 in. (178 mm) of deflection, the force quickly dropped and then gradually decreased to zero. At a deflection of 36.4 in. (925 mm), the post absorbed 101.8 kip-in. (11.5 kJ) of energy. A pre-test photograph is shown in Figure 18. Time-sequential and post-impact photographs are shown in Figure 19.

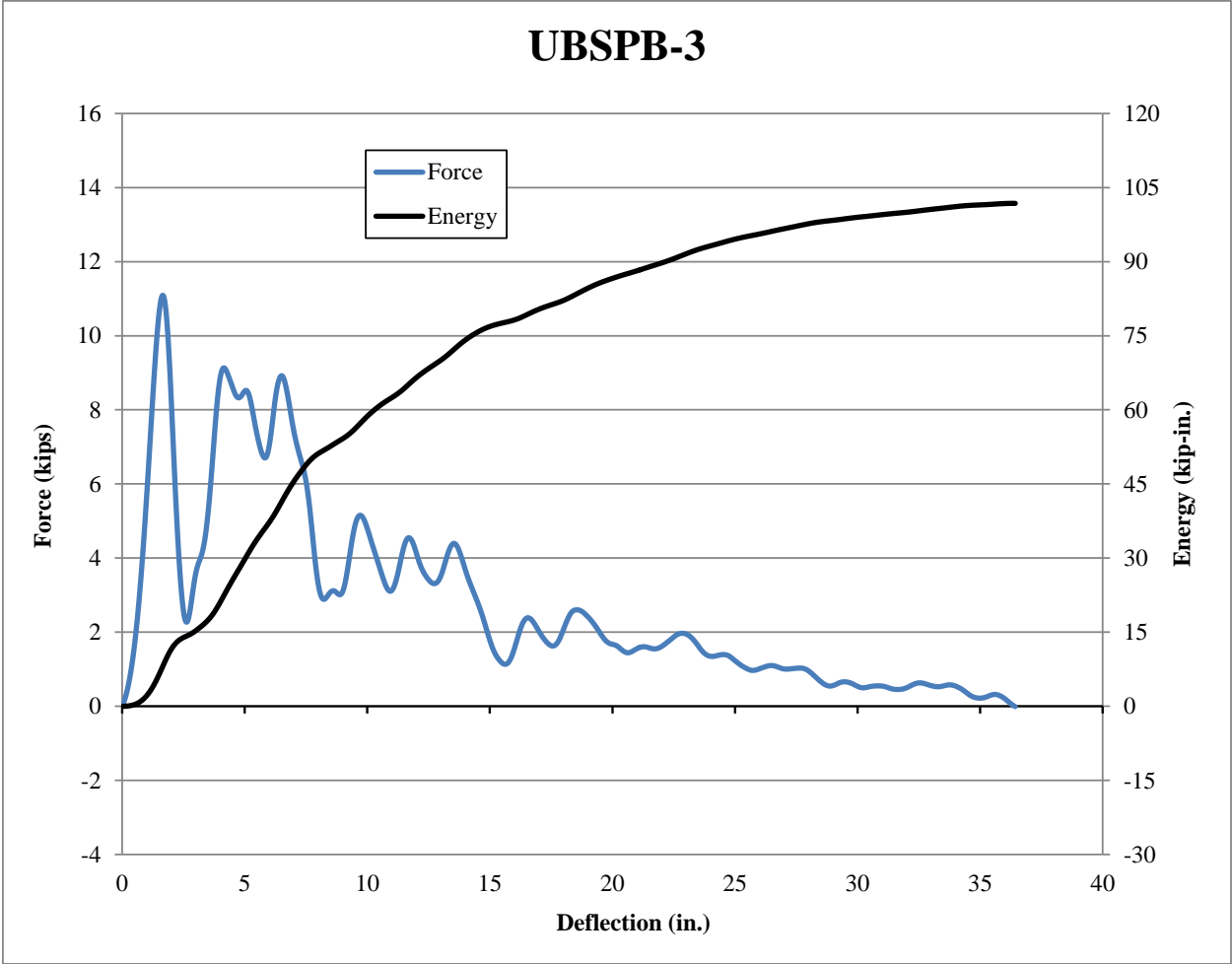


Figure 17. Force vs. Deflection and Energy vs. Deflection, Test No. UBSPB-3

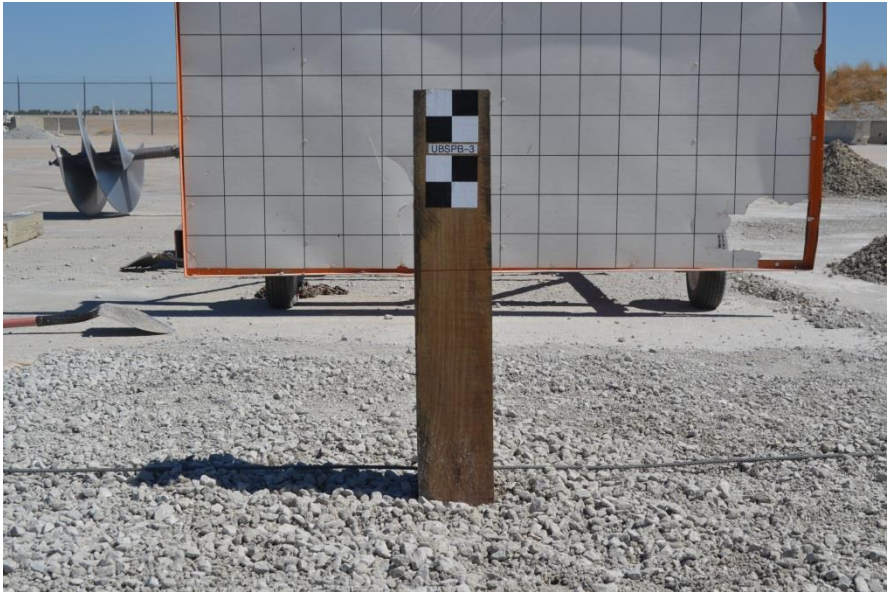


Figure 18. Pre-Test Photograph, Test No. UBSPB-3



IMPACT



0.020 sec



0.040 sec



0.060 sec



0.080 sec



0.100 sec



Figure 19. Time-Sequential and Post-Impact Photographs, Test No. UBSPB-3

3.3.4 Test No. UBSPB-4

During test no. UBSPB-4, the bogie impacted the CRT wood post, which created weak-axis bending at a speed of 20.9 mph (33.6 km/h). Initially, the post began to rotate backward. However, by 13 ms, the post began to fracture. The top of the post continued to rotate backward until the bogie lost contact with it at 54 ms. Upon post-test examination, the post fractured on the front face through the hole at ground level, but it did not fracture completely through the post and remained attached on the backside.

Force vs. deflection and energy vs. deflection curves created from the SLICE accelerometer data are shown in Figure 20. The post reached a peak force of 10.8 kips (48.0 kN) at 1.6 in. (41 mm) of deflection. Around 5 in. (127 mm) of deflection, the force quickly dropped and then gradually decreased to zero at the end of the impact event. At a deflection of 18.3 in. (465 mm), the post absorbed 54.3 kip-in. (6.1 kJ) of energy. A pre-test photograph is shown in Figure 21. Time-sequential and post-impact photographs are shown in Figure 22.

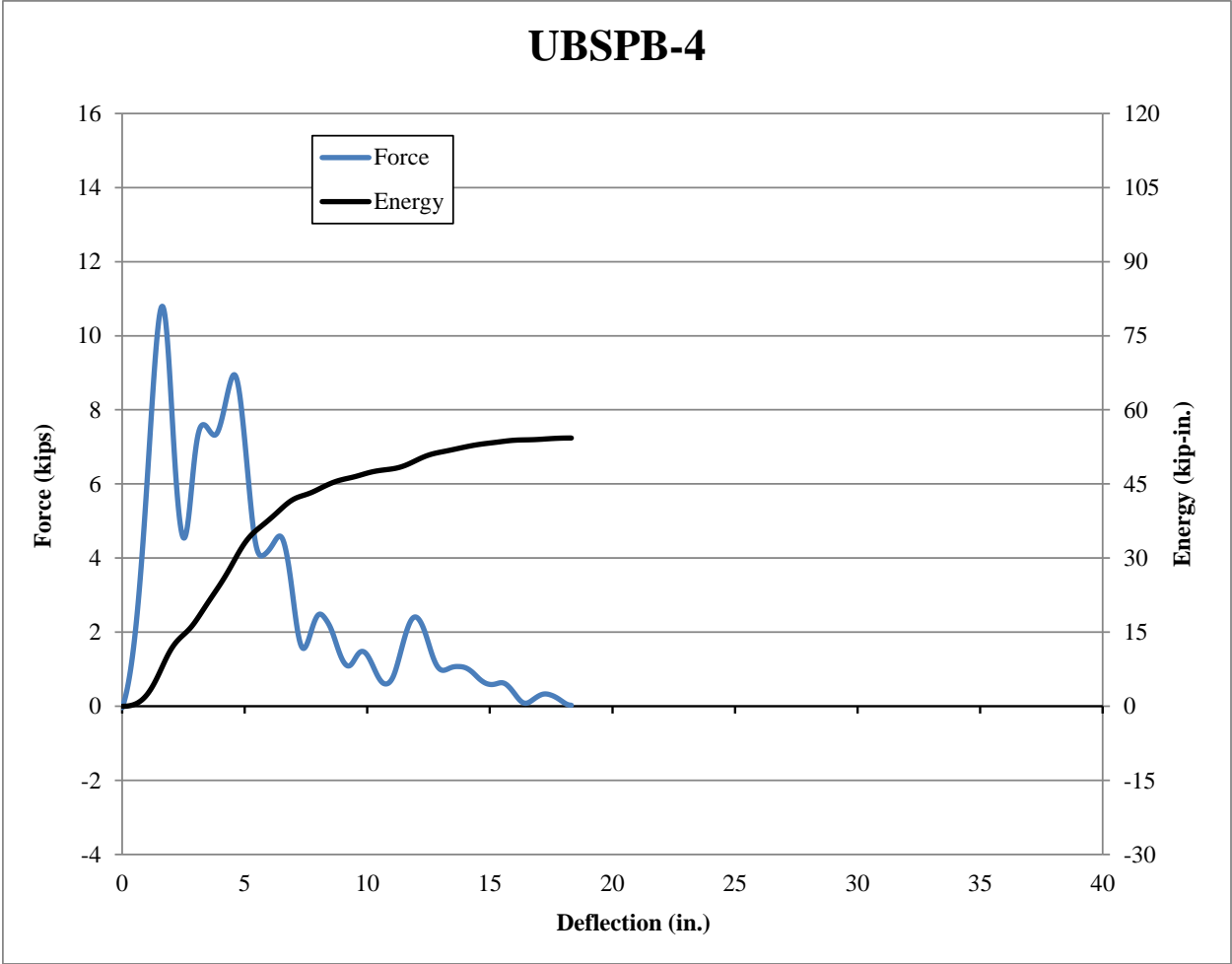


Figure 20. Force vs. Deflection and Energy vs. Deflection, Test No. UBSPB-4

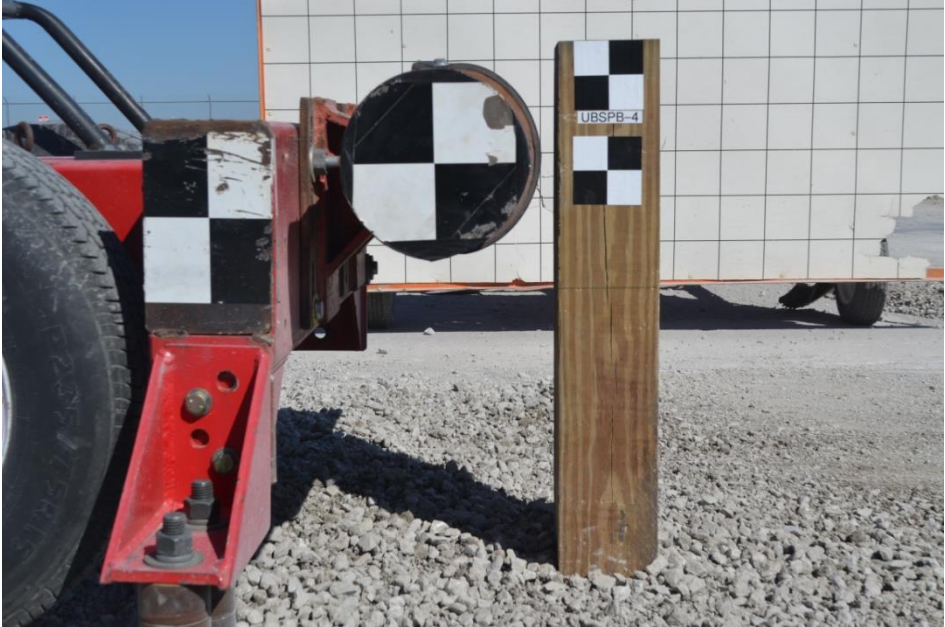
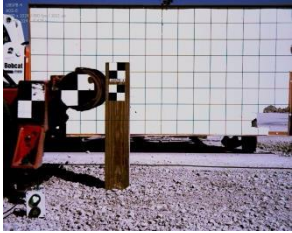


Figure 21. Pre-Test Photograph, Test No. UBSPB-4



IMPACT



0.020 sec



0.040 sec



0.060 sec



0.080 sec



0.100 sec



Figure 22. Time-Sequential and Post-Impact Photographs, Test No. UBSPB-4

3.3.5 Test No. UBSPB-5

Test no. UBSPB-5 was a strong-axis impact on the UBSP. The bogie impacted the UBSP at a speed of 21.3 mph (34.3 km/h). Upon impact, the UBSP began to rotate in the soil until the impact-side bolts released in tension at approximately 12 ms. The bogie continued to rotate the top section of the UBSP until the non-impact-side bolts fractured at approximately 66 ms, which corresponded to a deflection of approximately 23.9 in. (607 mm). Following the release of the post, the bogie continued downstream and overrode the post.

Force vs. deflection and energy vs. deflection curves created from the SLICE accelerometer data are shown in Figure 23. A pre-test photograph is shown in Figure 24. Time-sequential and post-impact photographs are shown in Figure 25. The post reached a peak force of 14.6 kips (64.9 kN) at 2.9 in. (74 mm) of deflection. Due to breakaway of the top post, the resistive force rapidly declined. At a maximum deflection of 23.9 in. (607 mm), the post absorbed 64.9 kip-in. (7.3 kJ) of energy.

Damage to the UBSP is shown in Figure 26. Upon post-test examination, it was found that three of the four bolts had fractured in tension. The remaining bolt, which was located on the impact-side, was stripped of its threads as the nut slid off. The non-impact side of the bottom post plate was bent downward. The upper section and lower tube section did not experience noticeable deformation.

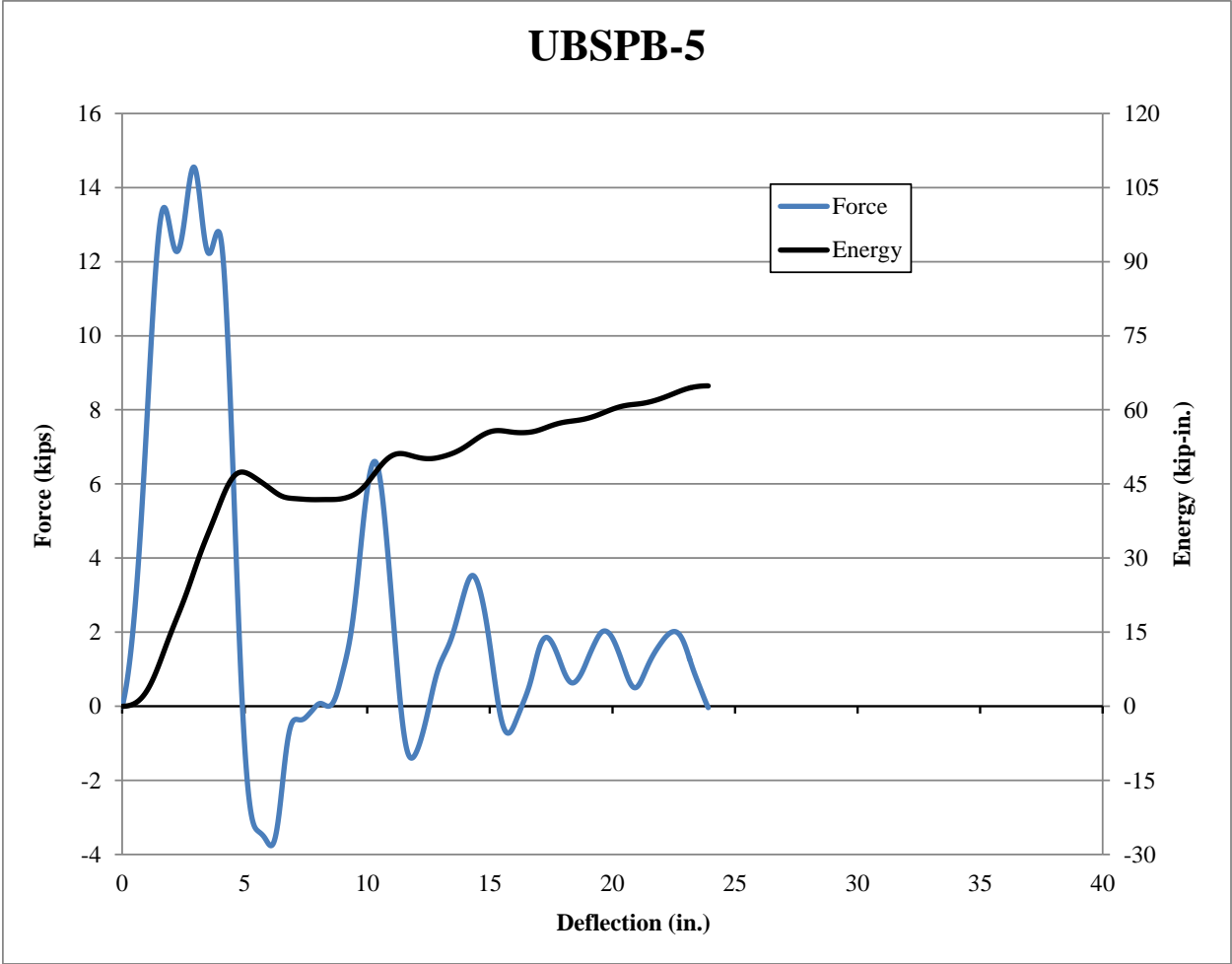


Figure 23. Force vs. Deflection and Energy vs. Deflection, Test No. UBSPB-5

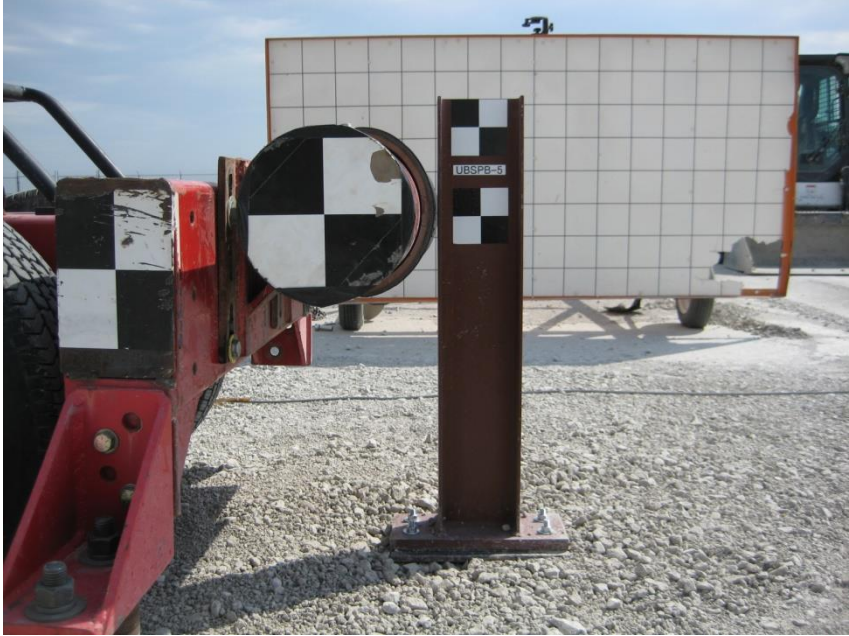
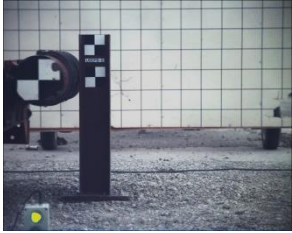


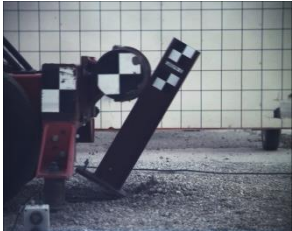
Figure 24. Pre-Test Photograph, Test No. UBSPB-5



IMPACT



0.020 sec



0.040 sec



0.060 sec



0.080 sec



0.100 sec



Figure 25. Time-Sequential and Post-Impact Photographs, Test No. UBSPB-5

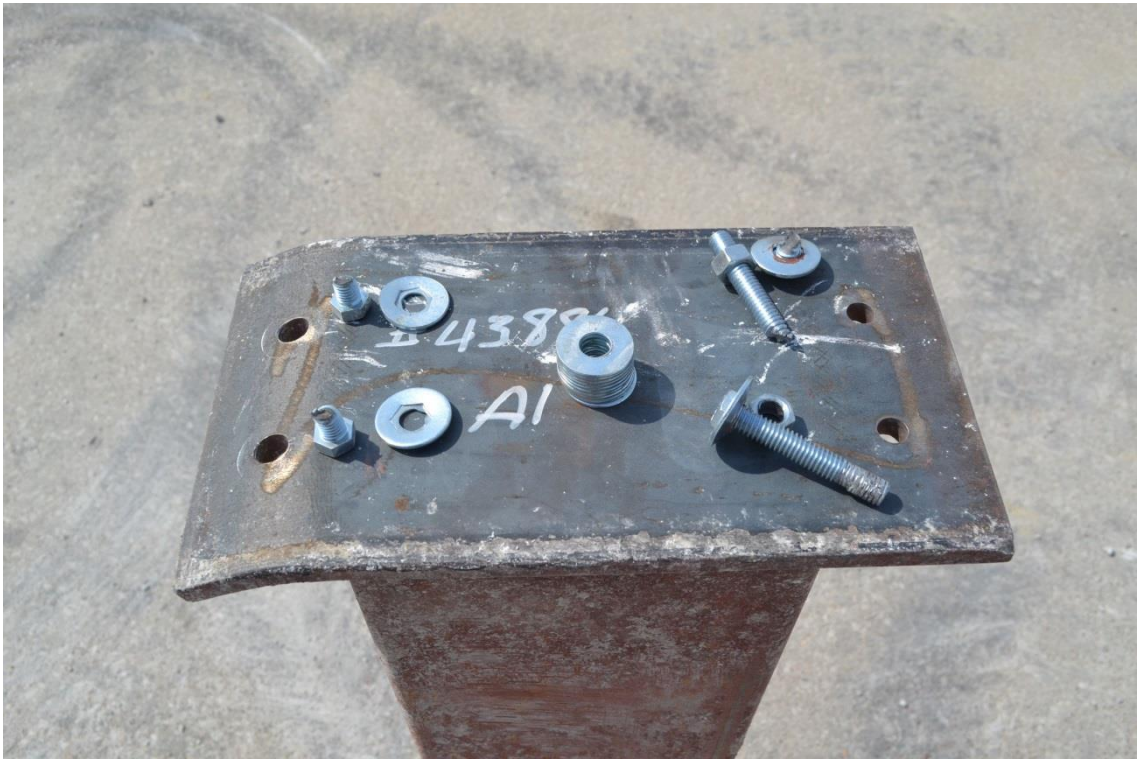


Figure 26. Bolts and Lower Base Plate, Test No. UBSPB-5

3.3.6 Test No. UBSPB-6

Test no. UBSPB-6 was a strong-axis impact on the UBSP. The bogie impacted the UBSP at a speed of 21.0 mph (33.8 km/h). Upon impact, the UBSP began to rotate in the soil until the impact-side bolts fractured in tension at approximately 14 ms. The bogie continued to rotate the top section of the UBSP until the non-impact-side bolts fractured at approximately 72 ms, which corresponded to a deflection of approximately 26.0 in. (660 mm).

Force vs. deflection and energy vs. deflection curves created from the SLICE accelerometer data are shown in Figure 27. A pre-test photograph is shown in Figure 28. Time-sequential and post-impact photographs are shown in Figure 29. The post reached a peak force of 14.6 kips (64.9 kN) at 4.2 in. (107 mm) of deflection. When the top of the post broke away, the resistive force rapidly decreased. At the maximum deflection of 26.0 in. (660 mm), the post absorbed 77.1 kip-in. (8.7 kJ) of energy.

Damage to the UBSP is shown in Figure 29, and the fractured bolts are shown in Figure 30. Upon post-test examination, all four bolts had fractured in tension. The non-impact side of the bottom post plate was bent downward. The top post plate and lower tube did not experience noticeable deformation.

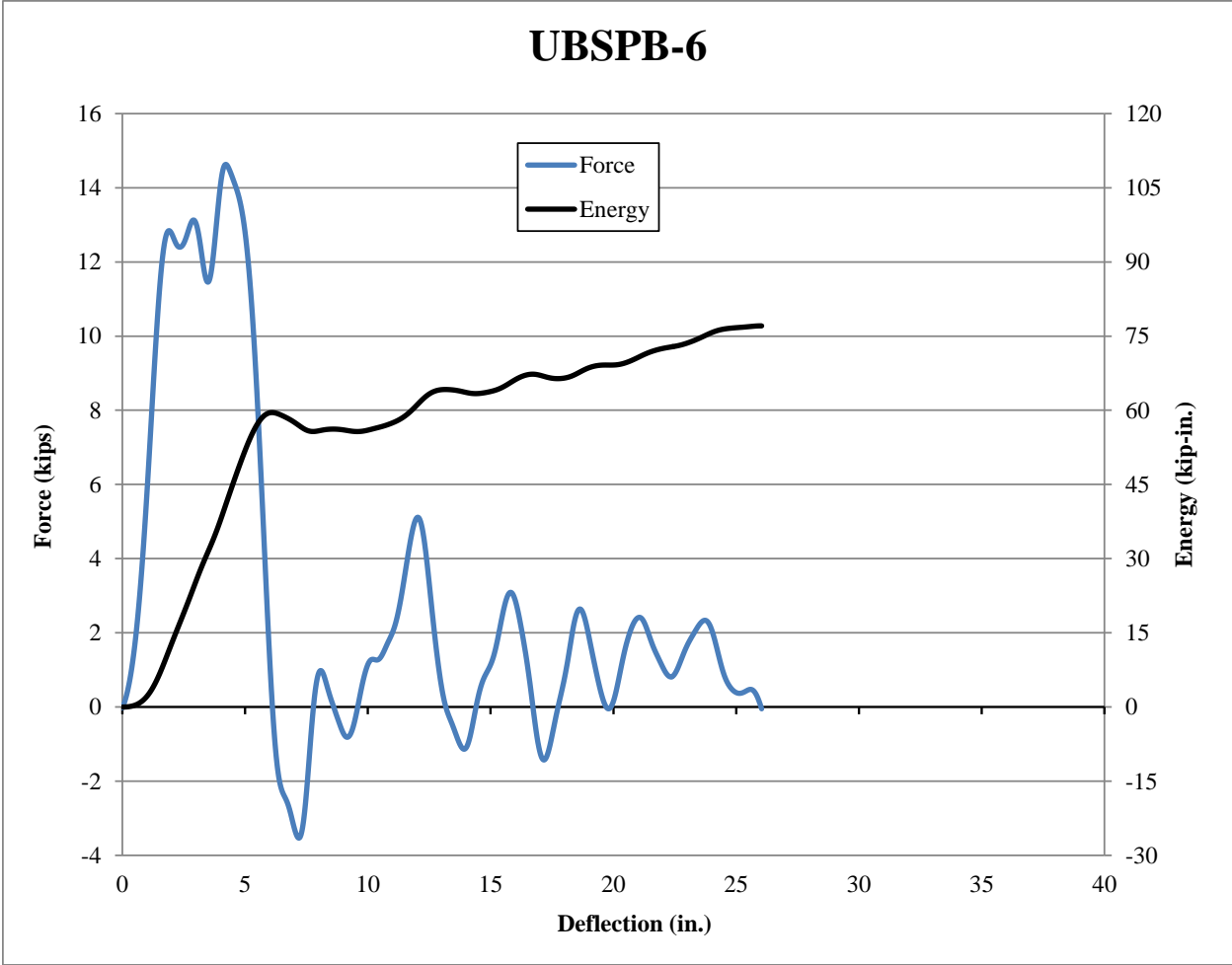
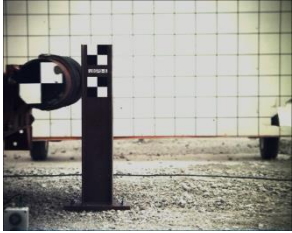


Figure 27. Force vs. Deflection and Energy vs. Deflection, Test No. UBSPB-6



Figure 28. Pre-Test Photograph, Test No. UBSPB-6



IMPACT



0.020 sec



0.040 sec



0.060 sec



0.080 sec



0.100 sec



Figure 29. Time-Sequential and Post-Impact Photographs, Test No. UBSPB-6



Figure 30. Fractured Bolts, Test No. UBSPB-6

3.3.7 Test No. UBSPB-7

Test no. UBSPB-7 was a weak-axis impact of the UBSP. The bogie impacted the UBSP at a speed of 20.2 mph (32.5 km/h). Upon impact, the UBSP began to rotate in the soil until the impact-side bolts fractured in tension at approximately 14 ms. The bogie continued to rotate the top section of the UBSP until the non-impact-side bolts fractured at approximately 26 ms, which corresponded to a deflection of approximately 12.7 in. (323 mm).

Force vs. deflection and energy vs. deflection curves created from the SLICE accelerometer data are shown in Figure 31. A pre-test photograph is shown in Figure 32. Time-sequential and post-impact photographs are shown in Figure 33. The post reached a peak force of 7.0 kips (31.1 kN) at 1.6 in. (41 mm) of deflection. The force peaked again near 4 in. (102 mm) of deflection, and then began to decrease due to breakaway of the top of the post. At a maximum deflection of 12.7 in. (323 mm), the post absorbed 32.4 kip-in. (3.7 kJ) of energy.

Fractured bolts are shown in Figure 33. Upon post-test examination, all four bolts had fractured in tension, and the top of the post was bent slightly. The top post plate did not experience noticeable deformation. The lower section of the post was undamaged and displaced very little in the soil. The previous research with the UBSP in the three beam bullnose had noted similar behavior in the full-scale testing [9]. At that time, the researchers noted that if the lower section was undamaged and had displaced less than ½ in. (13 mm), then the bottom section could be reset without removing the post by tamping around the base. In order to further investigate this recommendation, test no. UBSPB-8 was conducted with the same base as UBSPB-7 after re-compacting the soil around the post.

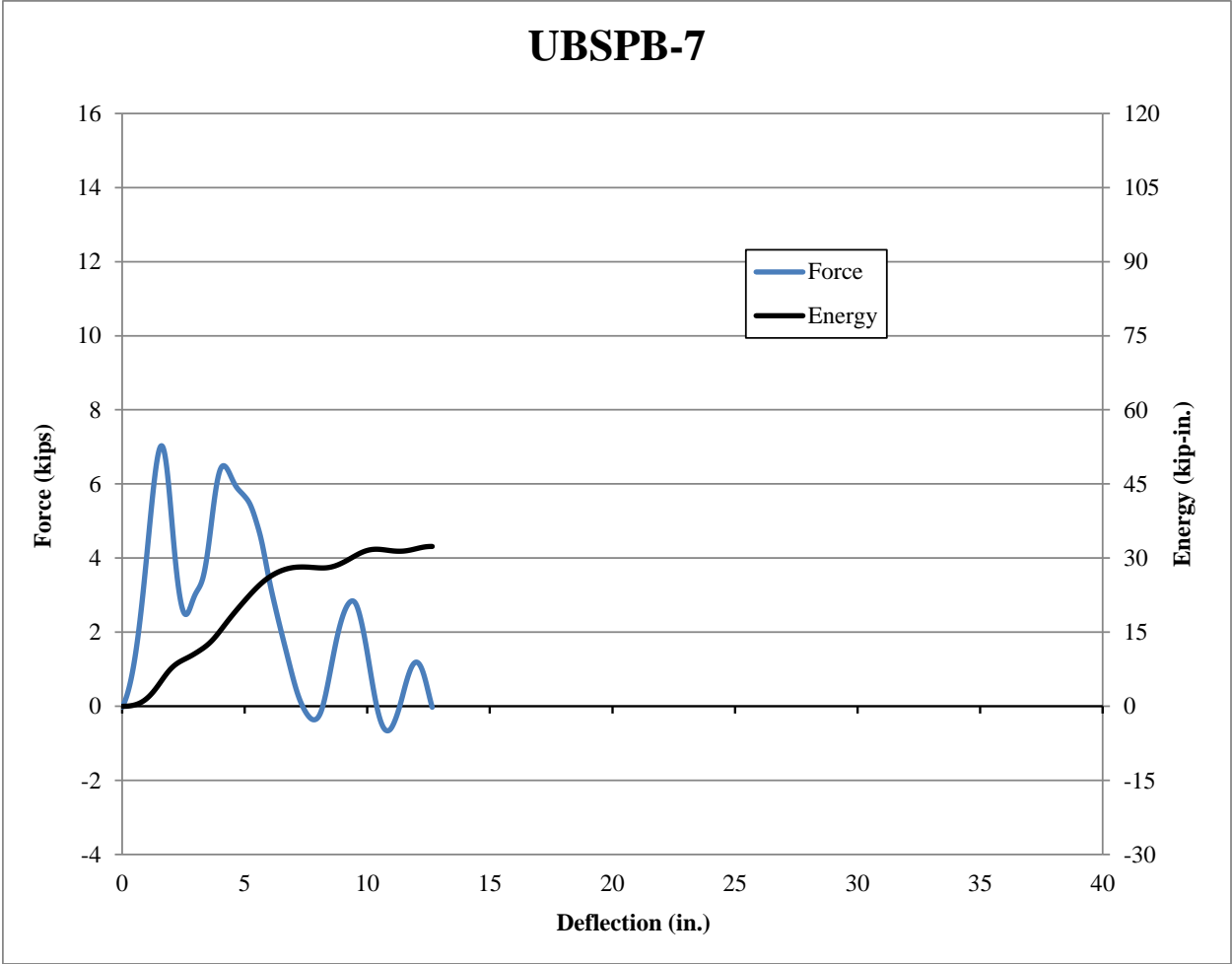
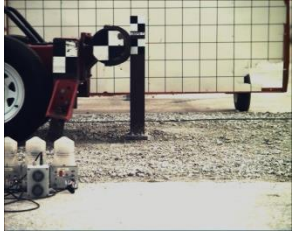


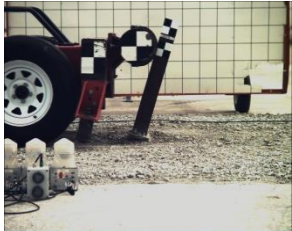
Figure 31. Force vs. Deflection and Energy vs. Deflection, Test No. UBSPB-7



Figure 32. Pre-Test Photograph, Test No. UBSPB-7



IMPACT



0.020 sec



0.040 sec



0.060 sec



0.080 sec



0.100 sec



Figure 33. Time-Sequential and Post-Impact Photographs, Test No. UBSPB-7

3.3.8 Test No. UBSPB-8

Test no. UBSPB-8 was a weak-axis impact on the UBSP after re-compacting the soil around the lower section of the post from test no. UBSPB-7. The bogie impacted the UBSP at a speed of 19.4 mph (31.2 km/h). Upon impact, the UBSP began to rotate in the soil until the impact-side bolts fractured in tension at approximately 12 ms. The bogie continued to rotate the top section of the UBSP until the non-impact-side bolts fractured at approximately 24 ms, which corresponded to a deflection of approximately 13.9 in. (353 mm).

Force vs. deflection and energy vs. deflection curves created from the SLICE accelerometer data are shown in Figure 34. A pre-test photograph is shown in Figure 35. Time-sequential and post-impact photographs are shown in Figure 36. The post reached a peak force of 7.6 kips (33.8 kN) at 1.9 in. (48 mm) of deflection. The force peaked again at 4.5 in. (114 mm) of deflection, and then quickly dropped to zero due to breakaway of the top of the post. At a maximum deflection of 13.9 in. (353 mm), the post absorbed 29.5 kip-in. (3.3 kJ) of energy.

Damage to the UBSP is shown in Figures 37 and 38. Upon post-test examination, it was found that all four bolts had fractured in tension. The top of the post and bottom of the post did not experience noticeable deformation.

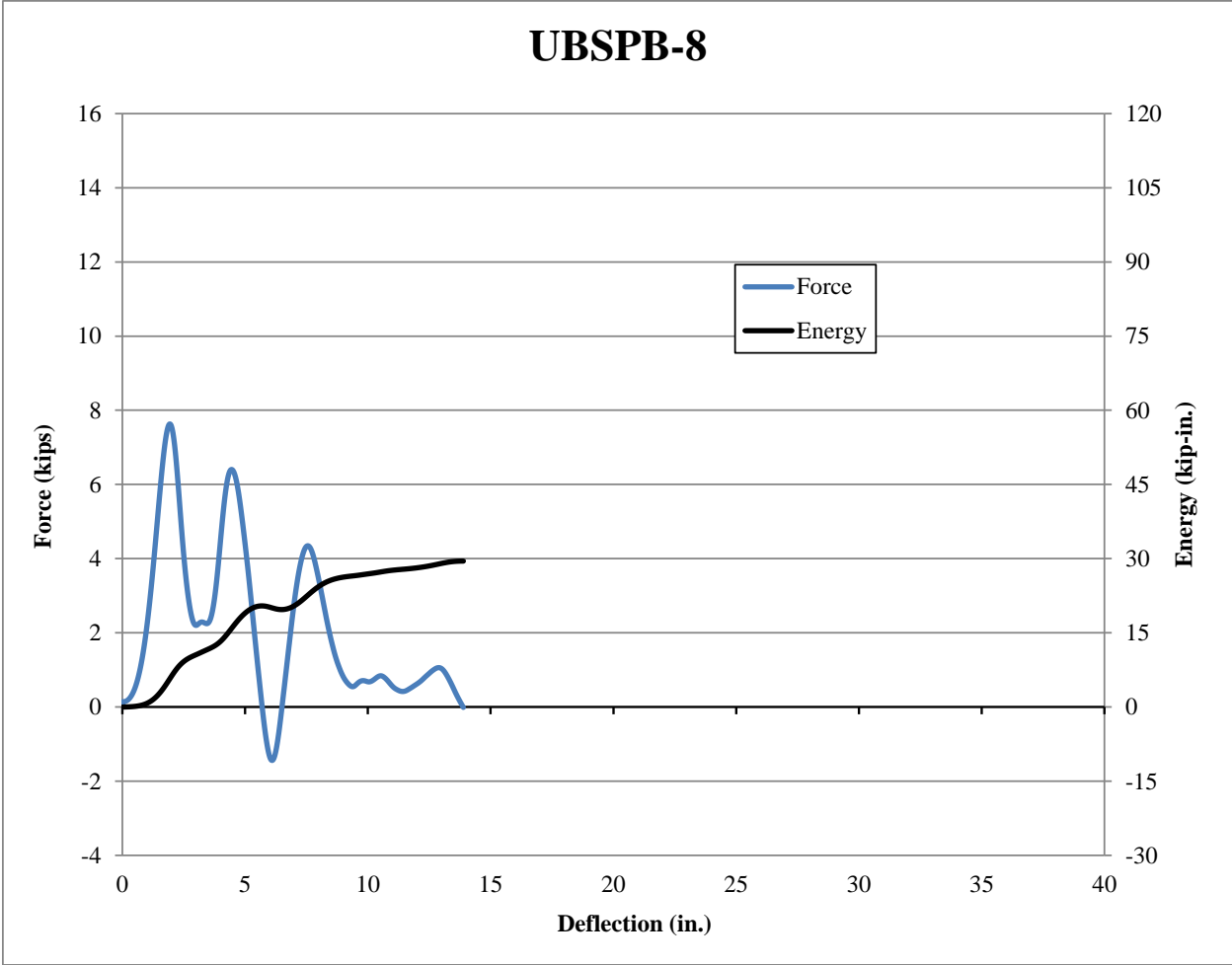
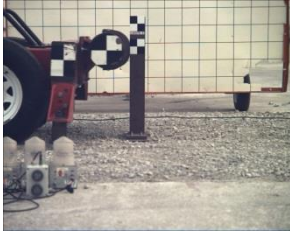


Figure 34. Force vs. Deflection and Energy vs. Deflection, Test No. UBSPB-8



Figure 35. Pre-Test Photograph, Test No. UBSPB-8



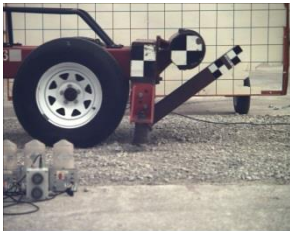
IMPACT



0.020 sec



0.040 sec



0.060 sec



0.080 sec



0.100 sec



Figure 36. Time-Sequential and Post-Impact Photographs, Test No. UBSPB-8



Figure 37. Lower Section and Base Plate, Test No. UBSPB-8



Figure 38. Top Section, Test No. UBSPB-8

3.3.9 Test No. UBSPB-8B

Test no. UBSPB-8B was a weak-axis impact on the UBSP. The bogie impacted the UBSP at a speed of 21.3 mph (34.3 km/h). Upon impact, the UBSP began to rotate in the soil until the impact-side bolts fractured in tension at approximately 12 ms. The bogie continued to rotate the top section of the UBSP until the non-impact-side bolts fractured at approximately 22 ms, which corresponded to a deflection of approximately 17.3 in. (439 mm).

Force vs. deflection and energy vs. deflection curves created from the SLICE accelerometer data are shown in Figure 39. A pre-test photograph is shown in Figure 40. Time-sequential and post-impact photographs are shown in Figure 41. The post reached a peak force of 8.9 kips (39.6 kN) at 1.9 in. (48 mm) of deflection. The force peaked again around 4.5 in. (114 mm) of deflection, and then quickly dropped to zero. At a maximum deflection of 17.3 in. (439 mm), the post absorbed 33.1 kip-in. (3.7 kJ) of energy.

Upon post-test examination, all four bolts had fractured in tension. The top of the post and bottom of the post did not experience noticeable deformation.

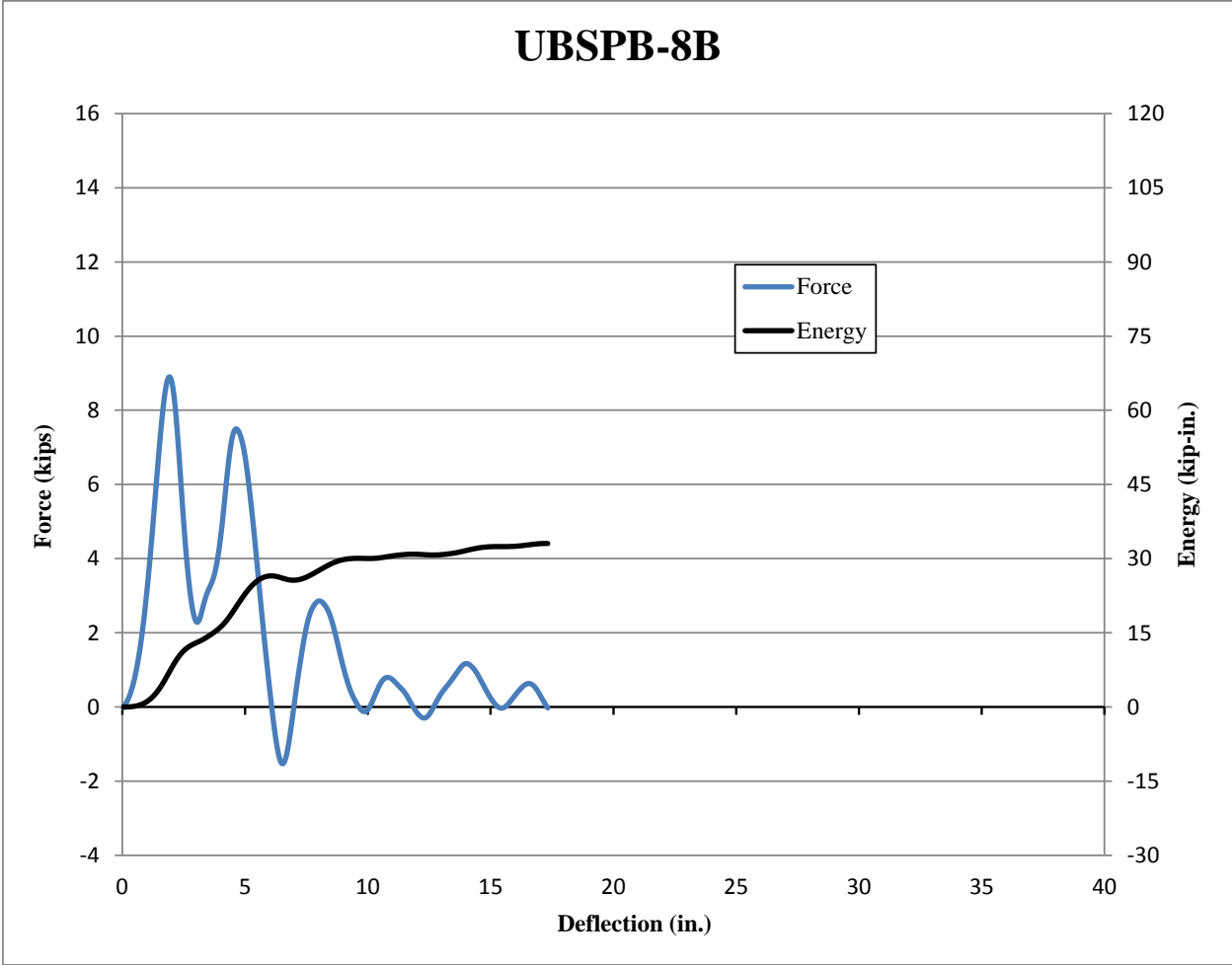
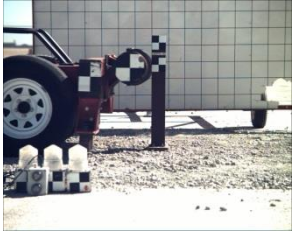


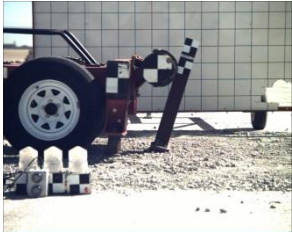
Figure 39. Force vs. Deflection and Energy vs. Deflection, Test No. UBSPB-8B



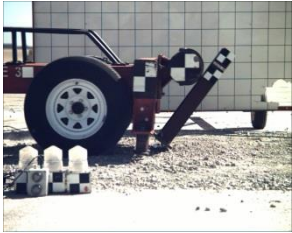
Figure 40. Pre-Test Photograph, Test No. UBSPB-8B



IMPACT



0.020 sec



0.040 sec



0.060 sec



0.080 sec



0.100 sec



Figure 41. Time-Sequential and Post-Impact Photographs, Test No. UBSPB-8B

3.4 Discussion

Following the completion of the component testing, the results from test nos. USBPB-1 through USBPB-8B were analyzed to determine how well the UBSP design compared with the wood CRT post. The results from the strong-axis and weak-axis tests are summarized in Table 3 respectively. The bogie impact speed was relatively consistent throughout the testing matrix as the impact velocity varied between 19.4 mph (31.2 km/h) and 21.3 mph (34.3 km/h). The difference in force and energy versus deflection for all tests, grouped by the impacted axis, can be seen in the force-deflection and energy-deflection comparison plots shown in Figures 42 through 45.

3.4.1 Strong-Axis Testing

Test nos. UBSPB-1, UBSPB-2, UBSPB-5, and UBSPB-6 were conducted with the bogie impacting along the strong axis of the posts. Test results are summarized in Table 3 and shown graphically in Figure 42 and Figure 43. The forces developed by the UBSPs and CRT posts appeared to be similar and suggested that the UBSP correlated well with the CRT posts. All four tests displayed very similar peak loads ranging from 14.4 kips (64.1 kN) to 14.6 kips (64.9 kN) during the first 3½ in. (89 mm) to 4 in. (102 mm) of post deflection. Average post forces through 5 in. (127 mm) and 10 in. (254 mm) of post deflection were slightly higher for the UBSP. The UBSPs displayed average forces at 5 in. (127 mm) and 10 in. (254 mm) of deflection that were 21.8 percent and 28.0 percent higher than the CRT posts, respectively. The difference in average forces was believed largely due to two factors. First, small differences in the fracture force and time between the posts caused the average forces to vary during the first 5 in. (127 mm) of deflection. However, this level of discrepancy in the average forces was not unexpected due to variability in post material properties and soil-resistive forces from test to test. In general, the

overall shape and magnitude of the force versus deflection curves were very similar for the two post types. Second, the CRT posts tended to fracture and develop only minimal resistive forces after fracture occurred in the 5 in. (127 mm) of post deflection, while the UBSPs tended to develop slightly more resistive force over larger post deflections due to the back bolts remaining in place for approximately 24 in. (610 mm) to 26 in. (660 mm) of deflection. As a result, it caused a slightly higher variation in the average forces as post deflections increased. Thus, a review of strong-axis force vs. deflection showed that the UBSPs and CRT posts compared well with minor variations.

A comparison of energy dissipated by the UBSPs and CRT posts when impacted along the strong axis displayed similar results. Total energy for the UBSP was slightly higher than that of the CRT post, but this finding was attributed to the CRT post disengaging in a more brittle fashion, while the UBSP required more deflection prior to disengaging the back side connection bolts. When compared to typical posts used in W-beam guardrails, the energy for all tests on the UBSP and CRT posts was considerably lower than typically observed in tests on the strong axis of standard, strong post guardrail posts.

The physical behavior of the posts was generally similar when impacted along the strong axis. The failure mode for both posts was similar in that both the UBSP and CRT post fractured near the ground line after minimal displacement in the soil foundation. The UBSP did appear to require an increased time to fully disengage the top of the post due to the separate release times of the front and back bolts. This differed somewhat from the CRT post, which failed in a brittle manner and over a relatively-short time duration.

Based on the comparison of the UBSP and CRT post behaviors, it was believed that the UBSP and CRT posts performed in a similar manner when impacted along the strong axis. The

differences in the force and energy absorbed by the two posts were minimal and were not cause for concern. Additionally, the UBSP required slightly longer time to disengage due to the bolt fracture mechanism used by the design. However, the behavior of the posts was judged to be very comparable.

It should be noted that the UBSP displayed permanent deflection in the base plate on the lower section of the post during strong-axis testing. However, this minor deflection was limited to less than ½ in. (13 mm) during all of the tests and did not affect the performance of the post. Previous full-scale testing of the UBSP design with the bullnose noted that the base of the post could be reused if the lower section was undamaged and the post did not display more than ½-in. (13-mm) of deflection in the foundation soil [6]. Thus, the current testing indicates that UBSP bases installed in strong soil conditions may be able to be reused without having to pull the bases out of the ground and resetting them.

It appears from these tests that strong-axis impacts in a sufficiently stiff soil can cause permanent deformation in the form of bending on the back side of the base plates. Thus, it may be worthwhile to explore a slight increase in the thickness of the lower base plate in future research to increase the reusability of the lower section of the post. It is not believed that a slight increase in base plate thickness would adversely affect the performance of the UBSP.

3.4.2 Weak-Axis Testing

Test nos. UBSPB-3, UBSPB-4, UBSPB-7, UBSPB-8, and UBSPB-8B were conducted with the bogie impacting along the weak axis of the posts. Test results are summarized in Table 3 and shown graphically in Figure 44 and Figure 45. The forces developed in the weak axis by the UBSPs and CRT posts displayed more variation than was observed in the strong-axis testing. Peak forces for the UBSPs were 28.2 percent lower on average as compared to the CRT post.

Average post forces through 5 in. (127 mm) and 10 in. (254 mm) of post deflection were also lower for the UBSP. The UBSPs displayed average forces at 5 in. (127 mm), 10 in. (254 mm), and 15 in. (381 mm) of deflection that were 32.9 percent, 44.2 percent, and 51.7 percent lower than the CRT posts, respectively.

A comparison of the energy dissipated by the UBSPs and CRT posts when impacted in the strong axis displayed similar results. Total energy for the UBSP was also significantly lower than observed for the CRT post. The energy for all of the UBSP and CRT post tests was considerably lower than typically observed in tests on the weak axis of standard, strong post guardrail posts.

The physical behavior of the posts was again generally similar when impacted along the weak axis. The failure mode for both posts was similar in that both the UBSP and CRT post fractured near the ground line after minimal displacement in the soil. In the case of the weak-axis impact, the UBSP required less time to fully disengage the top of the post. The UBSP tended to fracture and disengage both the front and back pairs of bolts shortly after impact, while the CRT post tended to fracture relatively slowly and absorb more energy during the post fracture. In fact, the CRT post in test no. UBSPB-4 did not fully disengage the upper and lower sections of the post, and the post sections remained attached by the fibers on the back side of the post.

Based on the comparisons of the UBSP and CRT post behaviors when impacted along the weak axis, two conclusions were evident. First, the UBSP released or disengaged at lower forces than a CRT post in terms of both peak and average loads. Additionally, the UBSP developed significantly lower energy during disengagement along the weak axis as compared to the standard CRT post due to decreased resistive forces and more rapid disengagement of the top and bottom sections of the post.

3.4.3 Comparison of UBSPs with Reused Lower Section

In test no. UBSPB-7, no damage or permanent deformation of the lower section of the UBSP was observed, including the foundation tube and lower base plate. As noted previously, it was recommended during the original development of the UBSP that, if the lower section of the post was undamaged and had not deflected more than ½ in. (13 mm) in the soil, then the lower section of the post could be reused by re-compacting the soil around the post [9]. In order to evaluate this recommendation more fully, test no. UBSPB-8 was conducted by reusing the lower section of the post from test no. UBSPB-7 and re-compacting the soil surrounding the post.

A comparison of the force versus deflection and energy versus deflection data from test nos. UBSPB-7 and UBSPB-8 is shown in Figure 46 and Figure 47, respectively. The results of the tests found that reusing the base of the post produced only a minimal difference in the performance of the UBSP. Peak force increased 8.5 percent from test no. UBSPB-7 to test no. UBSPB-8, while average forces and energies between 5 in. (127 mm) and 10 in. (254 mm) of deflection varied by 10.8 percent and 14.6 percent, respectively. The disengagement of the top and bottom section of the post was identical in both tests with all four bolts fracturing in tension and releasing the post. Thus, performance differences between the two tests were minimal, and the behavior of the UBSP with a reused and re-compacted base was found to be very similar to a newly installed post.

3.4.4 Conclusions

Following the comparison of the strong and weak axis testing of UBSPs and CRT posts in test nos. UBSPB-1 through UBSPB-8B, the researchers determined that the UBSP had the potential to be a surrogate for CRT posts currently used in a variety of guardrail systems and end terminals. CRT posts are currently designed to limit the forces and energy developed by the post

when impacted in the weak axis while providing an increased level of resistance when the strong axis of the post is loaded. The UBSP meets these design criteria when compared to the current CRT post.

A comparison of the strong-axis behavior of the posts found that the UBSP nearly matched the performance of the CRT post. Peak loads on the two post types were nearly identical and the variation in average forces and energies was minimal. In addition, both the UBSPs and CRT posts fractured at the ground line and cleanly disengaged the top section of the post. Thus, it was determined that the UBSP performed very well in terms of the strong-axis behavior of the post.

When considering the weak axis performance, the UBSP met the design intention of the current CRT post. While the UBSP did not replicate the performance of the current CRT post design, it did provide reduced weak-axis impact forces and energies and disengaged cleanly from the lower section of the post at ground line. Thus, the UBSP functioned as intended by limiting the forces and energy developed during weak-axis impacts on the post. The fact that the post develops lower forces and energy than the CRT post does not detract from the design, but rather improves upon its weak-axis performance in most scenarios.

The UBSP demonstrated a great deal of promise for use in other barrier systems based on these component tests, but a conservative approach to implementation of the post into these systems is warranted. Component testing cannot always indicate performance of a hardware component when implemented in various barrier systems due to differences in loading and additional interactions between the new hardware and the impacting vehicle or other system components that may occur when the component is installed. Therefore, while the component testing and analysis provided herein suggested that the UBSP was a suitable surrogate for CRT

posts, implementation of the UBSP into applications other than the bullnose system would likely require full-scale crash testing in order to evaluate their safety performance.

Table 3. Results of Bogie Testing

Test No.	Post Type	Impact Velocity mph (km/h)	Peak		Forces kips (kN)			Energies kip-in. (kJ)			Maximum Deflection in. (mm)	Failure Type
			Deflection in. (mm)	Force kips (kN)	@ 5 in. (127 mm)	@ 10 in. (254 mm)	@ 15 in. (381 mm)	@ 5 in. (127 mm)	@ 10 in. (254 mm)	@ 15 in. (381 mm)		
Stong-Axis Testing												
UBSPB-1	CRT Wood	21.1 (34.0)	3.3 (84)	14.5 (64.5)	7.2 (32.0)	3.2 (14.2)	NA	35.8 (4.0)	32.4 (3.7)	NA	14.8 (376)	Post Fracture
UBSPB-2	CRT Wood	21.2 (34.1)	4.4 (112)	14.4 (64.2)	9.1 (40.5)	4.7 (20.9)	NA	45.3 (5.1)	46.6 (5.3)	NA	11.4 (290)	Post Fracture
Averages			3.9 (99)	14.5 (64.5)	8.1 (36.0)	4.0 (17.8)	NA	40.6 (4.6)	39.5 (4.5)	NA	13.1 (333)	
UBSPB-5	UBSP	21.3 (34.3)	2.9 (74)	14.6 (64.9)	9.5 (42.3)	4.5 (20.0)	3.7 (16.5)	47.4 (5.4)	45.2 (5.1)	55.5 (6.3)	23.9 (607)	Bolts Fractured in Tension
UBSPB-6	UBSP	21.0 (33.8)	4.2 (107)	14.6 (64.9)	10.3 (45.8)	5.6 (24.9)	4.3 (19.1)	51.5 (5.8)	56.0 (6.3)	63.8 (7.2)	26.0 (660)	Bolts Fractured in Tension
Averages			3.6 (91)	14.6 (64.9)	9.9 (44.0)	5.1 (22.7)	4.0 (17.8)	49.5 (5.6)	50.6 (5.7)	59.7 (6.7)	25.0 (635)	
Weak-Axis Testing												
UBSPB-3	CRT Wood	20.0 (32.2)	1.7 (43)	11.1 (49.4)	5.9 (26.2)	5.9 (26.2)	5.1 (22.7)	29.5 (3.3)	58.6 (6.6)	76.8 (8.7)	36.4 (925)	Post Fracture
UBSPB-4	CRT Wood	20.9 (33.6)	1.6 (41)	10.8 (48.0)	6.6 (29.4)	4.7 (20.9)	3.6 (16.0)	33.0 (3.7)	47.2 (5.3)	53.3 (6.0)	18.3 (465)	Post Fracture
Averages			1.7 (43)	10.9 (48.5)	6.3 (28.0)	5.3 (23.6)	4.3 (19.1)	31.3 (3.5)	52.9 (6.0)	65.1 (7.4)	27.4 (696)	
UBSPB-7	UBSP	20.2 (32.5)	1.6 (41)	7.0 (31.3)	4.3 (19.1)	3.2 (14.2)	NA	21.2 (2.4)	31.5 (3.6)	NA	12.7 (323)	Bolts Fractured in Tension
UBSPB-8	UBSP	19.4 (31.2)	1.9 (48)	7.6 (33.8)	3.8 (16.9)	2.7 (12.0)	NA	18.9 (2.1)	26.9 (3.0)	NA	13.9 (353)	Bolts Fractured in Tension
UBSPB-8B	UBSP	21.3 (34.3)	1.9 (48)	8.9 (39.6)	4.6 (20.5)	3.0 (13.3)	2.2 (9.8)	22.8 (2.6)	30.0 (3.4)	32.4 (3.7)	17.3 (439)	Bolts Fractured in Tension
Averages			1.8 (46)	7.9 (35.1)	4.2 (18.7)	3.0 (13.3)	2.1 (9.3)	21.0 (2.4)	29.5 (3.3)	32.4 (3.7)	14.6 (371)	

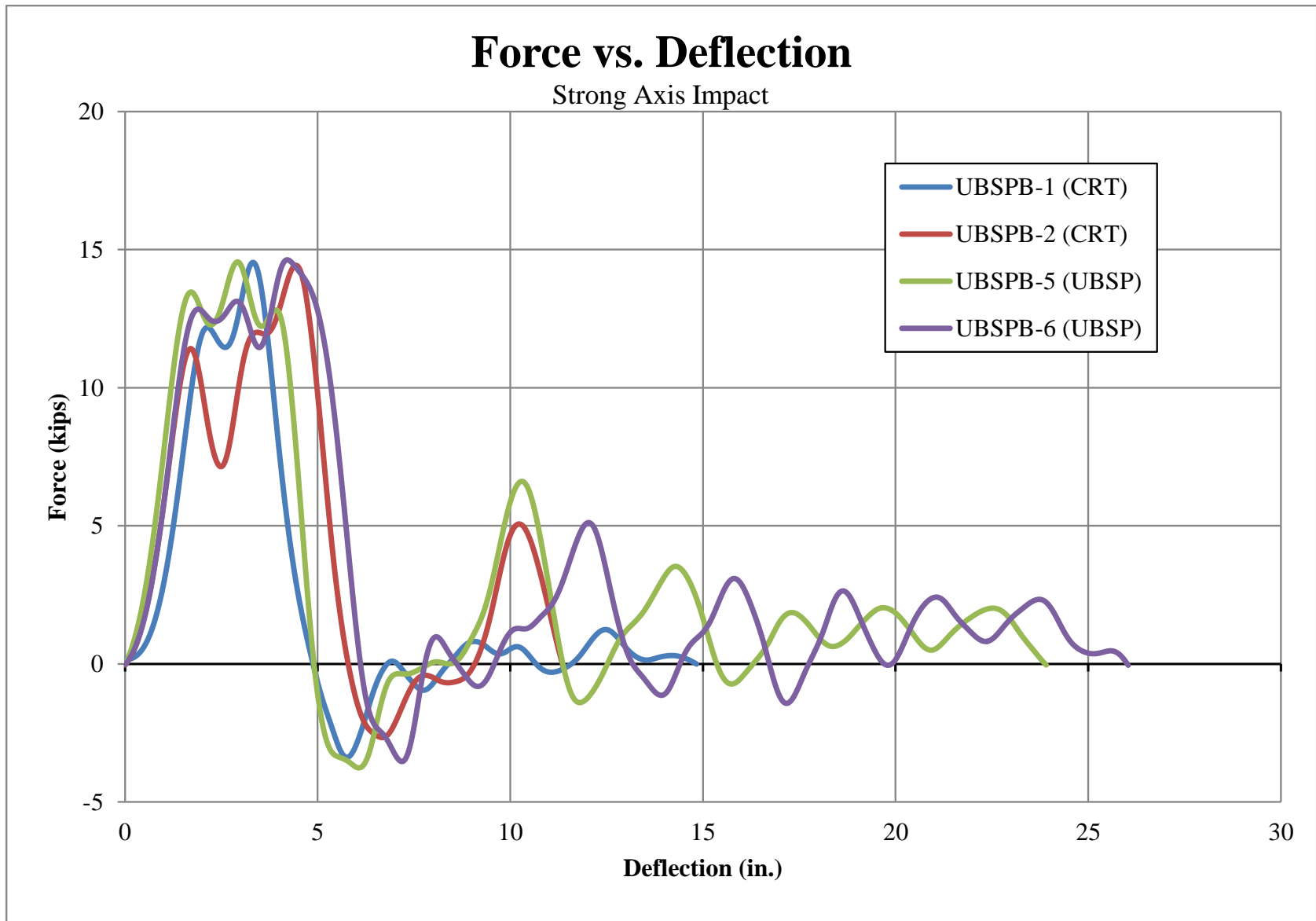


Figure 42. Force vs. Deflection Comparison Plot, Strong-Axis Tests

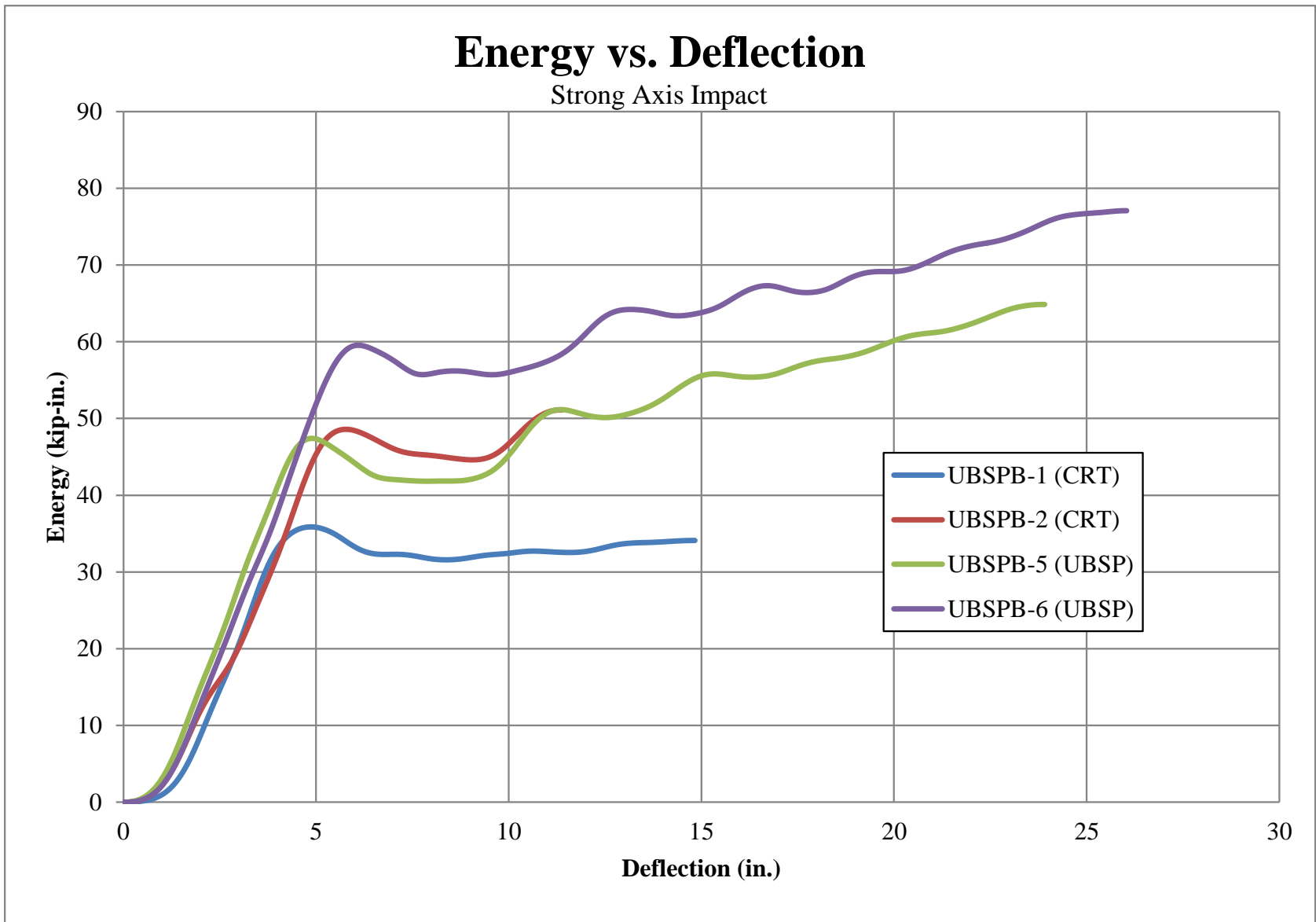


Figure 43. Energy vs. Deflection Comparison Plot, Strong-Axis Tests

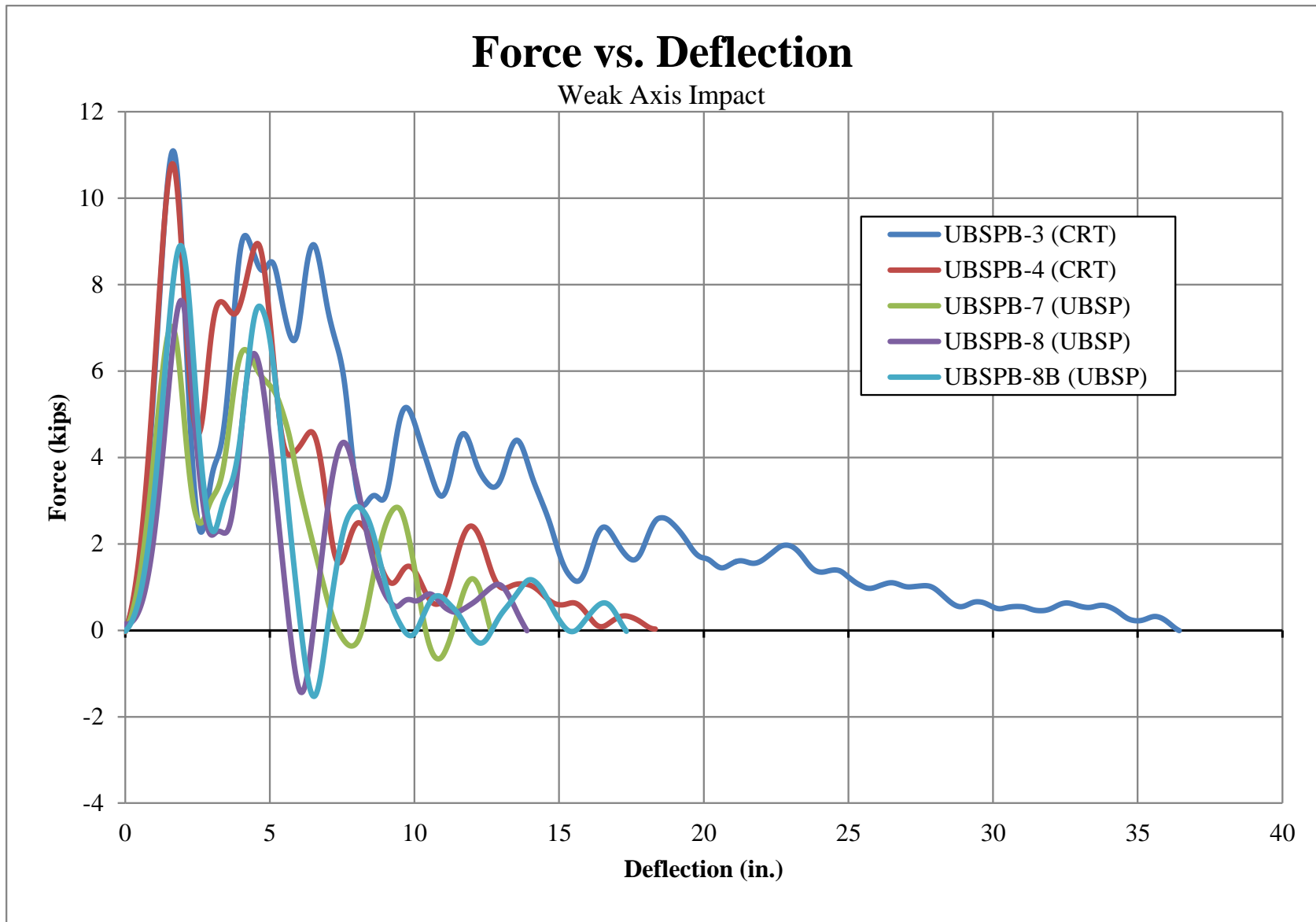


Figure 44. Force vs. Deflection Comparison Plot, Weak-Axis Tests

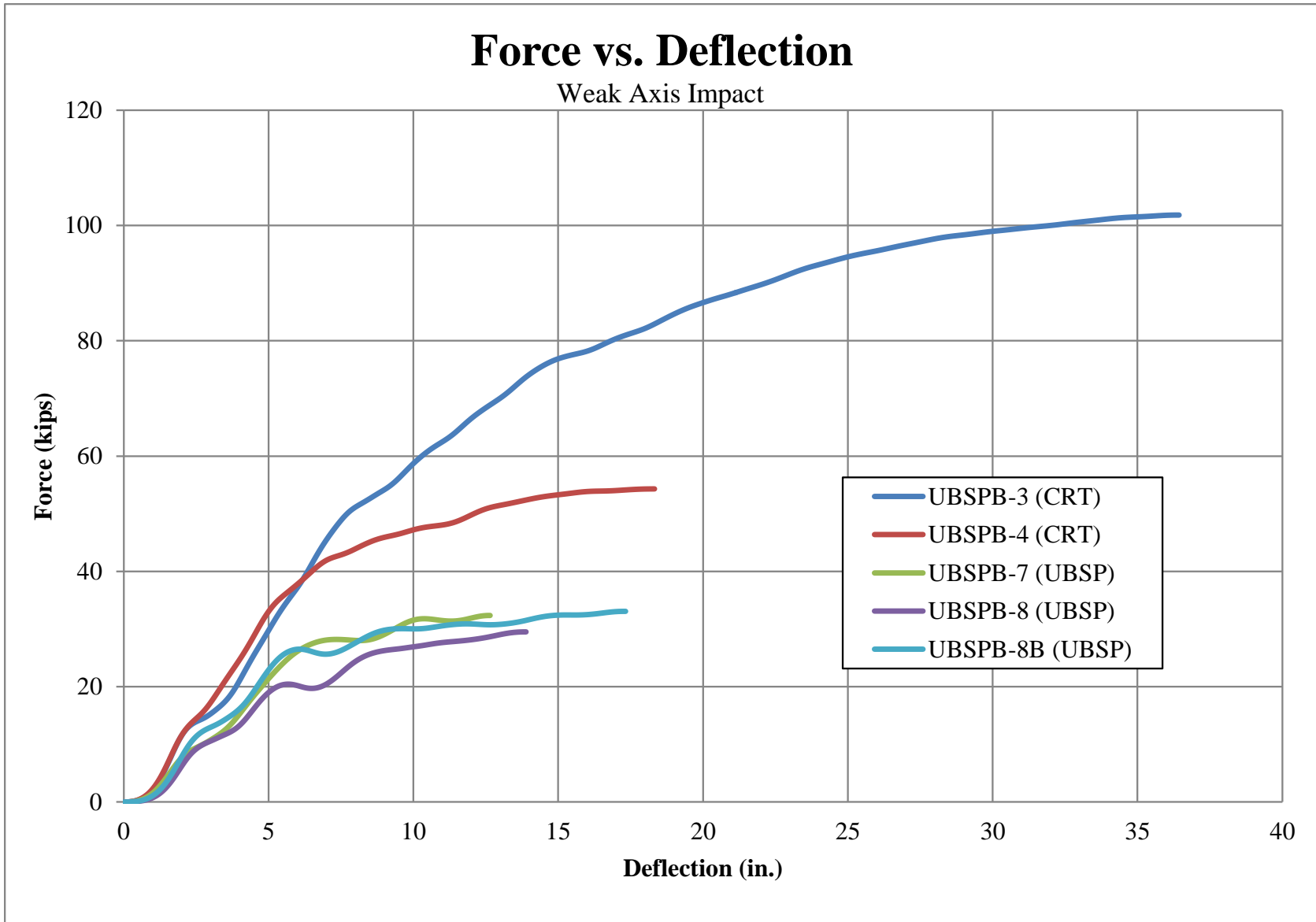


Figure 45. Energy vs. Deflection Comparison Plot, Weak-Axis Tests

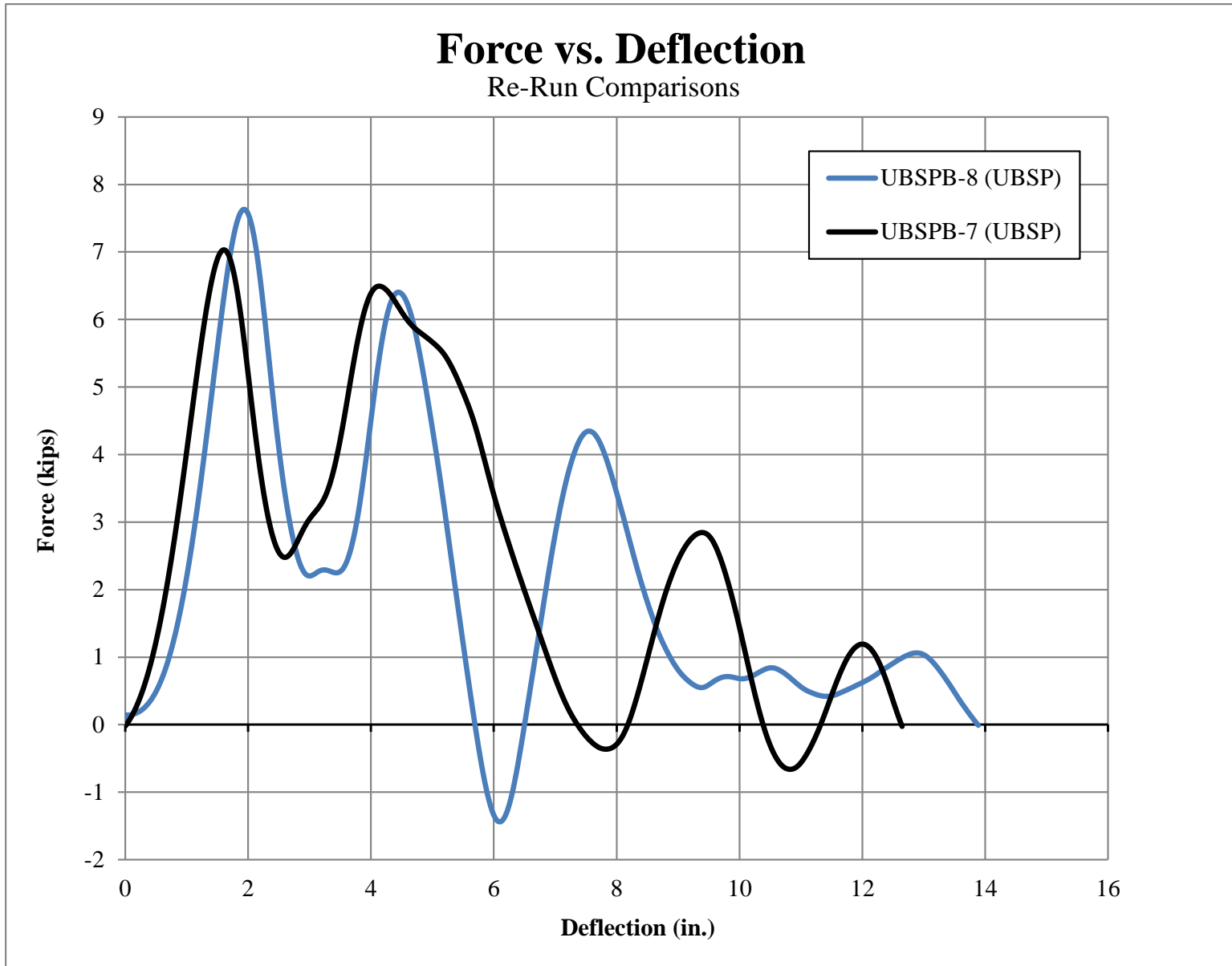


Figure 46. Force vs. Deflection of the Re-Run Tests, Test Nos. UBSPB-7 and UBSPB-8

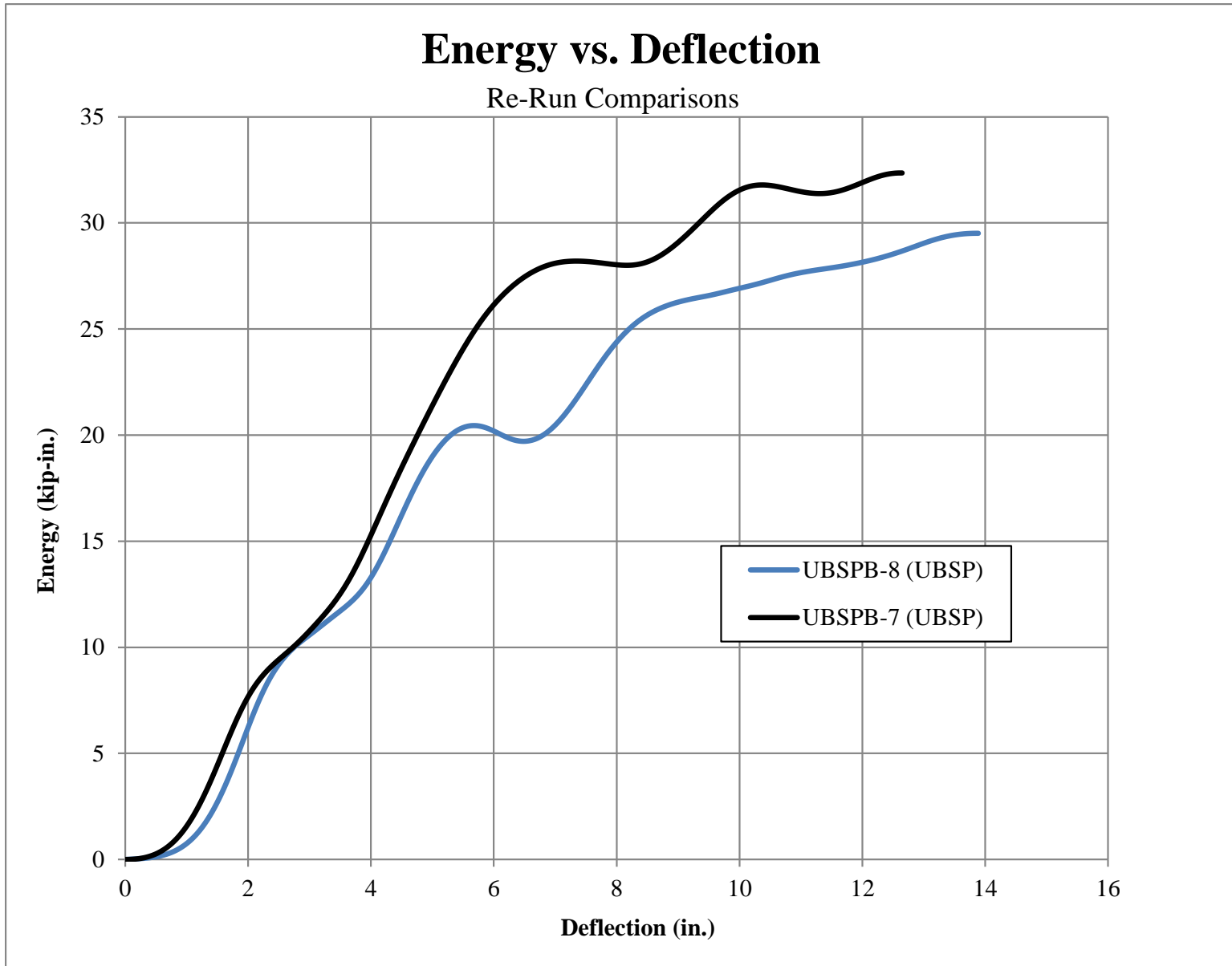


Figure 47. Energy vs. Deflection of the Re-Run Tests, Test Nos. UBSPB-7 and UBSPB-8

4 SUMMARY, CONCLUSIONS, AND RECOMMENDATIONS

4.1 Summary and Conclusions

A breakaway steel post design was recently developed and evaluated for use as a replacement for CRT posts in the three beam bullnose system. The UBSP was believed to perform similarly to a CRT post based on its initial development and its use in the three beam bullnose system. However, further research into the performance of the new design was warranted to determine if the post could serve as a surrogate for CRT posts in other guardrail systems. In order to further evaluate the UBSP, this study included a series of nine component tests of UBSPs and CRT posts installed in soil and impacted in both the strong and weak axis. The test results were compared and contrasted to provide a detailed evaluation of the UBSP and CRT posts.

The results from the component tests found that the UBSP had the potential to serve as a surrogate for CRT posts in other systems. The UBSP demonstrated similar strong-axis behavior in terms of disengagement and force and energy levels when compared to the CRT post. The weak-axis behavior of the UBSP was found to provide similar post disengagement, but the post released at lower force and energy levels than the CRT posts. The lower force and energy levels generated by the UBSP were not believed to negatively affect performance, as CRT and other breakaway posts are used to limit the force and energy during weak-axis impacts. Thus, the reduced forces and energies in the UBSP were not found to be an issue and may even improve performance in certain applications. Thus, the UBSP was determined to be a potential replacement of CRT posts used in applications other than the three beam bullnose. However, it was noted that full-scale testing of the UBSP was recommended to ensure that implementation of

the post in other barrier systems did not adversely affect the safety performance due to post behaviors outside the scope of this component testing.

As part of the component testing conducted in this research, one of the UBSP weak-axis tests was conducted with a reused lower section of the post. The reuse of the lower section was considered based on a prior recommendation from the original development effort which indicated that the lower section could be reused without reinstalling the post if the lower section was undamaged and the embedded stub displaced less than ½ in. (13 mm). The lower section was reset by re-compacting the soil around the post and installing a new top section. A comparison of the test results from the new and reused lower post sections showed very little difference in the performance of the UBSPs. This finding suggested that the recommendation to reuse undamaged and moderately displaced lower posts sections was acceptable.

4.2 Recommendations

The performance of the UBSP indicated that there is a strong potential for these posts to be utilized in other CRT post applications. Thus, a need exists to identify which applications are the most desirable for use of the UBSP and then to design, test, and evaluate those other barrier systems. The most likely systems where UBSPs may replace CRT posts would be the MGS long-span system and guardrail end terminal designs or crash cushions which use CRT posts or other breakaway posts. The use of the UBSP in these types of applications would provide states with a non-propriety steel-post option and decrease concerns for wood post disposal. Thus, further evaluation of the UBSP in these applications may be warranted.

In addition to the use of the UBSP as a replacement for CRT posts, there are other potential applications that may consider this post design. These applications may include: (1) guardrail end terminals which use Breakaway Cable Terminal posts; (2) Midwest Guardrail

Systems installed in subsurface rock foundations, rigid pavement mow strips, or rigid concrete structures such as bridge decks or culverts; and (3) a new reduced-maintenance, barrier system. While these alternative uses of the UBSP have not been fully developed, it is believed that the new post design could provide inroads to advancements in these applications and may warrant further study.

5 REFERENCES

1. Bielenberg, B.W., Faller, R.K., Reid, J.D., Rohde, J.R., Sicking, D.L., and Keller, E.A., *Concept Development of a Bullnose Guardrail System for Median Applications*, Final Report to the Midwest States' Regional Pooled Fund Program, MwRSF Research Report No. TRP-03-73-98, Midwest Roadside Safety Facility, University of Nebraska-Lincoln, Lincoln, Nebraska, May 1998.
2. Bielenberg, B.W., Faller, R.K., Reid, J.D., Rohde, J.R., Sicking, D.L., Keller, E.A., and Holloway, J.C., *Phase II Development of a Bullnose Guardrail System for Median Applications*, Final Report to the Midwest States' Regional Pooled Fund Program, MwRSF Research Report No. TRP-03-78-98, Midwest Roadside Safety Facility, University of Nebraska-Lincoln, Lincoln, Nebraska, December 1998.
3. Bielenberg, B.W., Faller, R.K., Reid, J.D., Rohde, J.R., Sicking, D.L., Keller, E.A., Holloway, J.C., and Supencheck, L.L., *Phase III Development of a Bullnose Guardrail System for Median Applications*, Final Report to the Midwest States' Regional Pooled Fund Program, MwRSF Research Report No. TRP-03-95-00, Midwest Roadside Safety Facility, University of Nebraska-Lincoln, Lincoln, Nebraska, June 2000.
4. Ross, H.E., Sicking, D.L., Zimmer, R.A., and Michie, J.D., *Recommended Procedures for the Safety Performance Evaluation of Highway Features*, National Cooperative Highway Research Program (NCHRP) Report No. 350, Transportation Research Board, Washington, D.C., 1993.
5. Hinch, J.A., Owings, R.P., and Manhard, G.A., *Safety Modifications of Turned-Down Guardrail Terminals, Volumes 1, 2, and 3*, Final Report to the Federal Highway Administration, Ensco, Inc., Springfield, Virginia, June 1984.
6. Arens, S.W., Sicking, D.L., Faller, R.K., Reid, J.D., Bielenberg, R.W., Rohde, J.R., and Lechtenberg, K.A., *Investigating the Use of a New Universal Breakaway Steel Post*, Final Report to the Minnesota Department of Transportation (MnDOT), MwRSF Research Report No. TRP-03-218-09, Midwest Roadside Safety Facility, University of Nebraska-Lincoln, Lincoln, Nebraska, August 2009.
7. Bielenberg, B.W., Faller, R.K., Rohde, J.R., and Reid, J.D., *Evaluation of an Existing Steel Post Alternative for the Thrie Beam Bullnose Guardrail System*, Letter Report to the Midwest States Regional Pooled Fund Program, MwRSF Research Report No. TRP-03-193-07, Midwest Roadside Safety Facility, University of Nebraska-Lincoln, Lincoln, Nebraska, August 2007.
8. Schmidt, J.D., Sicking, D.L., Faller, R.K., Reid, J.D., Bielenberg, R.W., and Lechtenberg, K.A., *Investigating the Use of a New Universal Breakaway Steel Post – Phase 2*, MwRSF Research Report No. TRP-03-230-10, Midwest Roadside Safety Facility, University of Nebraska-Lincoln, Lincoln, Nebraska, August 2010.
9. Schmidt, J.D., Sicking, D.L., Faller, R.K., Reid, J.D., Bielenberg, R.W., and Lechtenberg, K.A., *Investigating the Use of a New Universal Breakaway Steel Post – Phase 3*, MwRSF

Research Report No. TRP-03-244-10, Midwest Roadside Safety Facility, University of Nebraska-Lincoln, Lincoln, Nebraska, December 2010.

10. *Manual for Assessing Safety Hardware (MASH)*, American Association of State Highway and Transportation Officials (AASHTO), Washington, D.C., 2009.
11. Society of Automotive Engineers (SAE), *Instrumentation for Impact Test—Part 1—Electronic Instrumentation*, SAE/J211/1 MAR95, New York City, NY, July 2007.

6 APPENDICES

Appendix A. Material Certifications



P. O. Box 630 • Sutton, NE 68979
Phone 402-773-4319
FAX 402-773-4513

Invoice # 2589 ? 2598
Shipped To MIDWEST 2, MILWAUKEE, WI

Central Nebraska Wood Preservers, Inc.
Certification of Inspection

Date: 4-19-12

Specifications: Highway Construction Use

Preservative: CCA - C 0.60 pcf

Type: All SYP S4S (unless noted)

Charge #	Date Treated	Grade	Material Size Length	# Pieces	White Moisture Readings	Penetration # of Borings & % Conforming	Actual Retentions % Conforming
330			6x8 6' Rgt H-Hole	140	18%	2/20 90%	.622 pcf
330			6x8 -14" C/P Black	105	18%	2/20 90%	.622 pcf

Number of pieces rejected and reason for rejection:
NONE

Statement: The above reference material was treated and inspected in accordance with the above referenced specifications.

Kurt Andres
Kurt Andres, General Manager

4-19-12
Date

Figure A-1. CRT Wooden Post, Test Nos. UBSPB-1 through UBSPB-4

McMASTER-CARR®

600 County Line Rd
Elmhurst IL 60126-2081
630-600-3600
chi.sales@mcmaster.com

UNIVERSITY OF NEBRASKA
MIDWEST ROADSIDE SAFETY FACILITY
M W R S F
4800 NW 35TH ST
LINCOLN NE 68524-1869
ATTENTION: KEN KRENK

Purchase Order
0827KKRENK

Page 1 of 1

McMaster-Carr Number
8788247-01

08/27/12

Line	Description	Ordered	Shipped
1	92865A677 GRADE 5 ZINC-PLATED STEEL HEX HEAD CAP SCREW 7/16"-14 THREAD, 2-1/2" LONG, FULLY THREADED	3 Pack	3
2	90108A032 ZINC-PLATED STEEL TYPE A USS FLAT WASHER 7/16" SCREW SIZE, 1-1/4" OD, .06"- .11" THICK	1 Pack	1
3	6536K28 INDUSTRIAL-SHAPE HOSE COUPLING SLEEVE-LOCK SCKT, BRASS, 1/4" NPTF FEM, 1/4 CPLG	5 Each	5
4	7527K64 300 VAC/VDC TERMINAL BLOCK 4 CIRCUITS, 7/16" CENTER-TO-CENTER, 20 AMPS	1 Each	1
5	7527K938 COVER FOR 7/16" CTR-TO-CTR, 4 CIRCUIT, 600 & 300 VAC/VDC TERMINAL BLOCK SAME AS 7527K27	1 Each	1
6	9983K12 SURE-CONNECT HEAT-SHRINK RING TERMINAL 22-18 AWG WIRE SIZE, #8 SCREW/STUD SIZE	2 Pack	2
7	9983K18 SURE-CONNECT HEAT-SHRINK RING TERMINAL 16-14 AWG WIRE SIZE, #8 SCREW/STUD SIZE	2 Pack	2
8	7548K362 TERMINALS CONNECTED TO WIRE FEM QUICK-DISCONNECT ON ONE END, 24"L, 14 AWG, BLACK SAME AS 7548K3	1 Pack	1

Certificate of compliance

This is to certify that the above items were supplied in accordance with the description and as illustrated in the catalog. In all other respects this transaction remains subject to our standard terms and conditions of sale, which can be found at www.mcmaster.com.

Gabriel Priyev Gabriel Priyev
Compliance Manager

Figure A-2. Washers, Bolts and Nuts, Test Nos. UBSPB-5 through UBSPB-8B

02Jun09 6:19 TEST CERTIFICATE No: DCR 593215

Sold By: INDEPENDENCE TUBE CORPORATION P/O No 4500121170
6226 W. 74TH STREET Re1
CHICAGO, IL 60638 S/O No DCR 13803-002
Tel: 708-496-0380 Fax: 708-563-1950 B/L No DCR 10325-011 Shp 01Jun09
Inv No Inv

Sold To: (5016) Ship To: (1)
STEEL & PIPE SUPPLY STEEL & PIPE SUPPLY
1003 FORT GIBSON ROAD 1003 FORT GIBSON ROAD
CATOOSA, OK 74015 CATOOSA, OK

Tel: 918-266-6325 Fax: 918 266-4652

CERTIFICATE of ANALYSIS and TESTS Cert. No: DCR 593215
29May09

Part No
TUBING A500 GRADE B(C)
8" X 6" X 3/16" X 40'

		Pcs	Wgt
		6	4,099

Heat Number Tag No Pcs Wgt
A911886 S12697 6 4,099
YLD=60900/TEN=79100/ELG=35

Heat Number *** Chemical Analysis ***
A911886 C=0.2198 Mn=0.4734 P=0.0103 S=0.0021 Si=0.0367 Al=0.0241
Cu=0.0699

WE PROUDLY MANUFACTURE ALL OF OUR HSS IN THE USA.
INDEPENDENCE TUBE PRODUCT IS MANUFACTURED, TESTED,
AND INSPECTED IN ACCORDANCE WITH ASTM STANDARDS.

CURRENT STANDARDS:
..... A500/A500M-07
..... A513-07
..... A252-98 (2002)

Page: 1 Last

Figure A-3. Long Foundation Tube, Test Nos. UBSPB-5 through UBSPB-8B

Bill To:
 STEEL AND PIPE SUPPLY
 P.O. BOX 1088
 MANHATTAN
 66502

KS
 US

Ship To: 3
 STEEL AND PIPE SUPPLY
 SOUTH SMITH ROAD
 JONESBURG
 63351

MO
 US

Order Date: 07/25/2011
 PO No: 45/163745
 Mill Order No: 3914008
 Load No: 1390348
 Manifest No: 2085180

CERTIFIED MATERIAL TEST REPORT
GERDAU AMERISTEEL
 Midlothian Mill
 300 West Road
 Midlothian, TX 76065
 (972) 775-8241



SPECIFICATIONS
 ASTM A6-09, A992-06a, A572-07

SIZE: **W 6 X 9#** / W150 X 13.5
 GRADE: 992/572-50
 LENGTH: 50 FT / 15.24 M
 PRODUCT: WF BEAMS

HEAT NO: 22603040

CHEMICAL ANALYSIS

C	Mn	P	S	Si	Cu	Ni	Cr	Mo	Sn	V	Al	Nb	CE
.06	.90	.026	.012	.23	.39	.08	.15	.028	.009	.002	.003	.018	.28

PHYSICAL PROPERTIES

Yield Strength		Tensile Strength		Specimen Area		Elongation		Bend Test		ROA
KSI	MPa	KSI	MPa	Sq In	Sq cm	%	Gage Length	Dia.	Result	%
63.4	437.1	77.1	531.6	0.269	1.74	24.6	8 In	200 mm		
62.6	431.6	77.6	535.0	0.268	1.73	23.3	8 In	200 mm		

TENSILE TEST RATIOS

YLD/TENS YLD/TENS
 .91 .92

Remarks

MATERIAL COMPLIES WITH ASTM A709-50 & 50S FOR NON-TENSION COMPONENTS.

7886 MT

All manufacturing processes of this product, including electric arc MELTING and continuous CASTING, occurred in the U.S.A. CMTR complies with EN 10204 3.1

"I hereby certify that the contents of this report are correct and accurate. All tests and operations performed by this material manufacturer or its sub-contractors, when applicable, are in compliance with the requirements of the material specifications and applicable purchaser designated requirements."

Signed: Tom L. Harrington Date: Jul. 28, 2011
 Tom L. Harrington: Quality Assurance Manager

Signed: _____
 Notary Public (if applicable)

Date: _____
 Page: 1 of 1

MwRSF Report No. TRP-03-288-14
 April 1, 2014

Figure A-4. Post Material Certification, Test Nos. UBSPB-5 through UBSPB-8B



CARTERSVILLE STEEL MILL
384 OLD GRASSDALE RD NE
CARTERSVILLE GA 30121 USA
(770) 367-3300

Chemical and Physical Test Report
Made and Melted in USA

G-197611

SHIP TO STEEL AND PIPE SUPPLY CO. INC. 1003 FORT GIBSON ROAD 918-266-6325 PORT CATOOSA, OK 74015	INVOICE TO STEEL AND PIPE SUPPLY CO. INC. PO BOX 1688 MANHATTAN, KS 66505-1688	SHIP DATE 04/06/12 CUST. ACCOUNT NO 40130833
--	---	---

PRODUCED IN: CARTERSVILLE

SHAPE + SIZE	GRADE	SPECIFICATION	SALES ORDER	CUST P.O. NUMBER
F1/2 X 7	A36	ASTM A36-08, ASTM A529 GR50-05, ASTM A709 GR36-10	2017907-01	4500175856-01
HEAT I.D.	C	Mn P S Si Cu Ni Cr Mo V Nb B N Sn Al Ti Ca Zn C Eqv		
G122002	.17	.91 .012 .026 .20 .28 .10 .07 .031 .017 .001 .0010 .0070 .011 .000 .00100 .00100 .00300 .41		

Mechanical Test: Yield 54500 PSI, 375.76 MPA Tensile: 75900 PSI, 523.31 MPA %E: 22.1/8in, 22.1/200MM
Customer Requirements CASTING: STRAND CAST
Comment: NO WELD REPAIRMENT PERFORMED. STEEL NOT EXPOSED TO MERCURY.
Mechanical Test: Yield 54500 PSI, 375.76 MPA Tensile: 76100 PSI, 524.69 MPA %E: 21.8/8in, 21.8/200MM
Customer Requirements CASTING: STRAND CAST
Comment: NO WELD REPAIRMENT PERFORMED. STEEL NOT EXPOSED TO MERCURY.

Customer Notes

NO WELD REPAIRMENT PERFORMED. STEEL NOT EXPOSED TO MERCURY.
All manufacturing processes including melt and cast, occurred in USA. MTR complies with EN10204 3.1B

THE ABOVE FIGURES ARE CERTIFIED CHEMICAL AND PHYSICAL TEST RECORDS AS CONTAINED IN THE PERMANENT RECORDS OF COMPANY.

Bhaskar
Bhaskar Yalamanchili
Quality Director
Gerdau

Zachary
Zachary
Metallurgical Services Manager
CARTERSVILLE STEEL MILL

Seller warrants that all material furnished shall comply with specifications subject to standard published manufacturing variations. NO OTHER WARRANTIES, EXPRESSED OR IMPLIED, ARE MADE BY THE SELLER, AND SPECIFICALLY EXCLUDED ARE WARRANTIES OF MERCHANTABILITY AND FITNESS FOR A PARTICULAR PURPOSE. In no event shall seller be liable for indirect, consequential or punitive damages arising out of or related to the materials furnished by seller. Any claim for damages for materials that do not conform to specifications must be made from buyer to seller immediately after delivery of same in order to allow the seller the opportunity to inspect the material in question.

MwRSF Report No. TRP-03-288-14
April 1, 2014

Figure A-5. Upper and Lower Shear Plates, Test Nos. UBSPB-5 through UBSPB-8B

77

Appendix B. Soil Batch Sieve Analysis

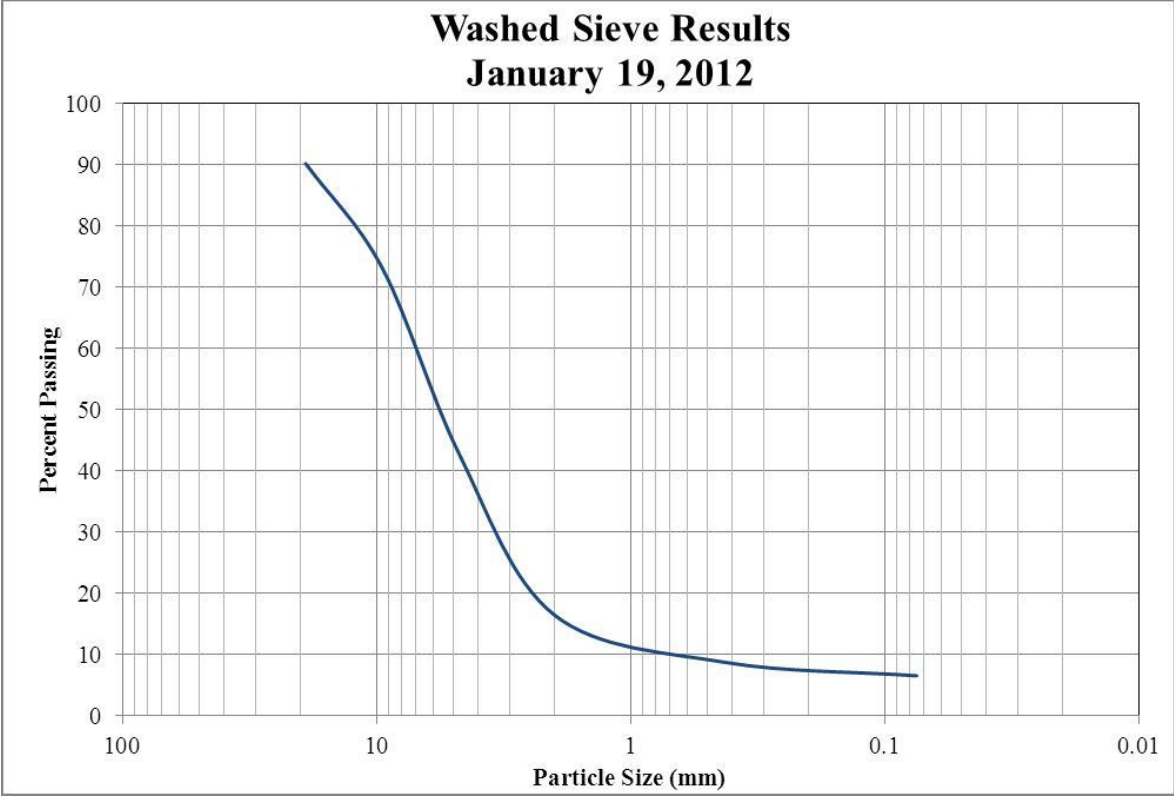


Figure B-1. Soil Gradation for Test Nos. UBSPB-1 through UBSPB-8B

Appendix C. Bogie Test Results

The results of the recorded data from each accelerometer on every dynamic bogie test are provided in the summary sheets found in this appendix. Summary sheets include acceleration, velocity, and displacement vs. time plots as well as force and energy vs. displacement plots.

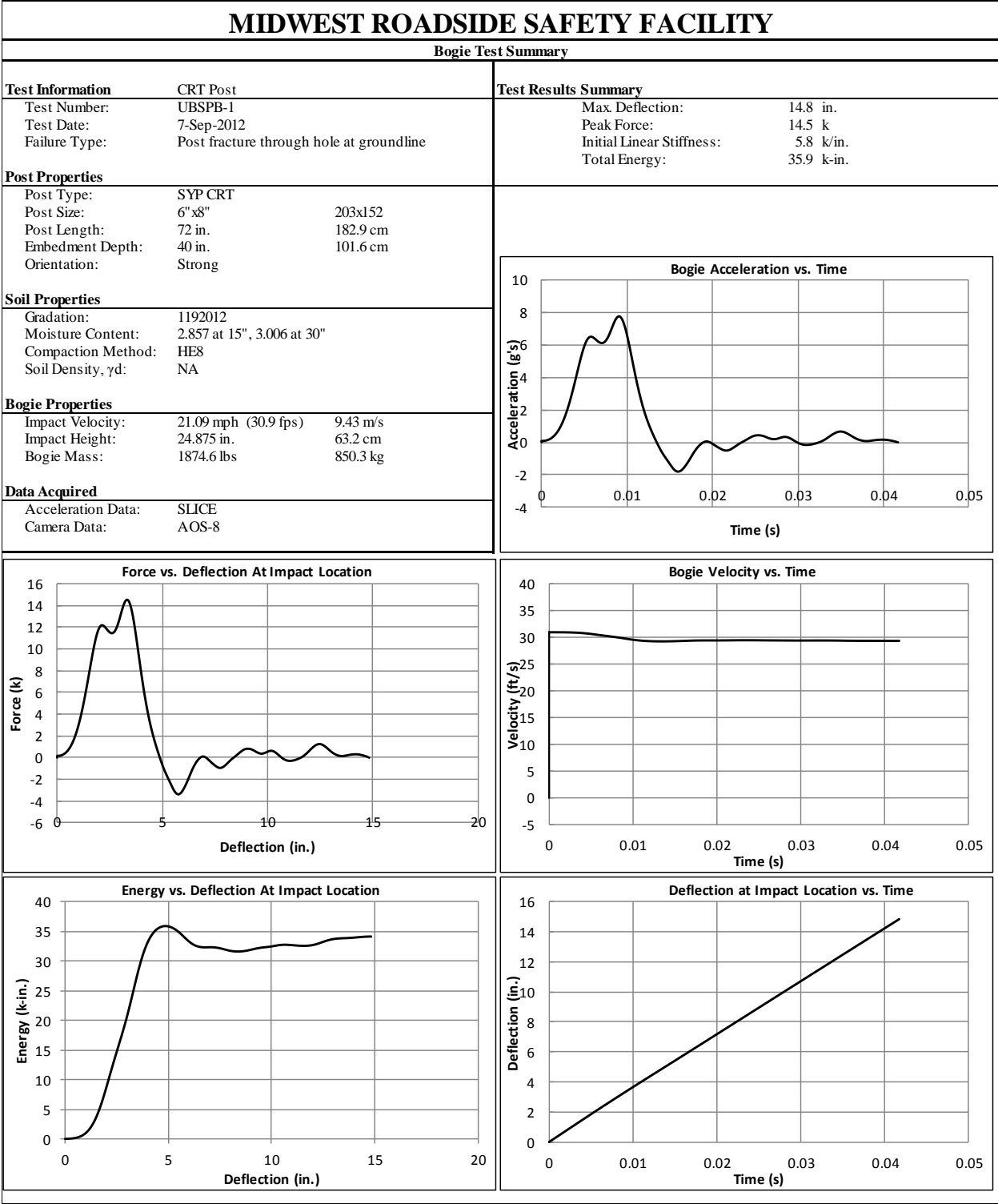


Figure C-1. Results of Test No. UBSPB-1 (SLICE)

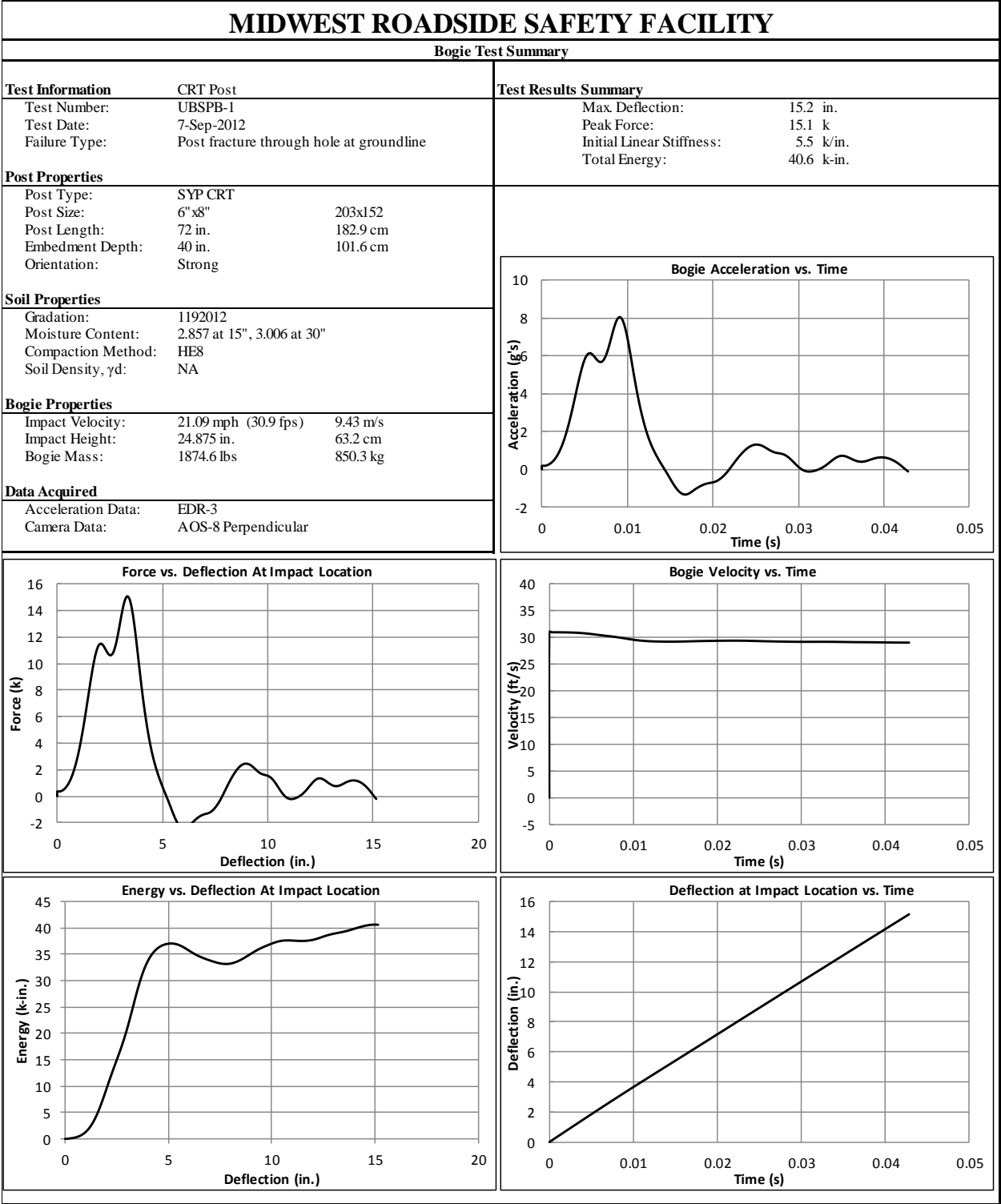


Figure C-2. Results of Test No. UBSPB-1 (EDR-3)

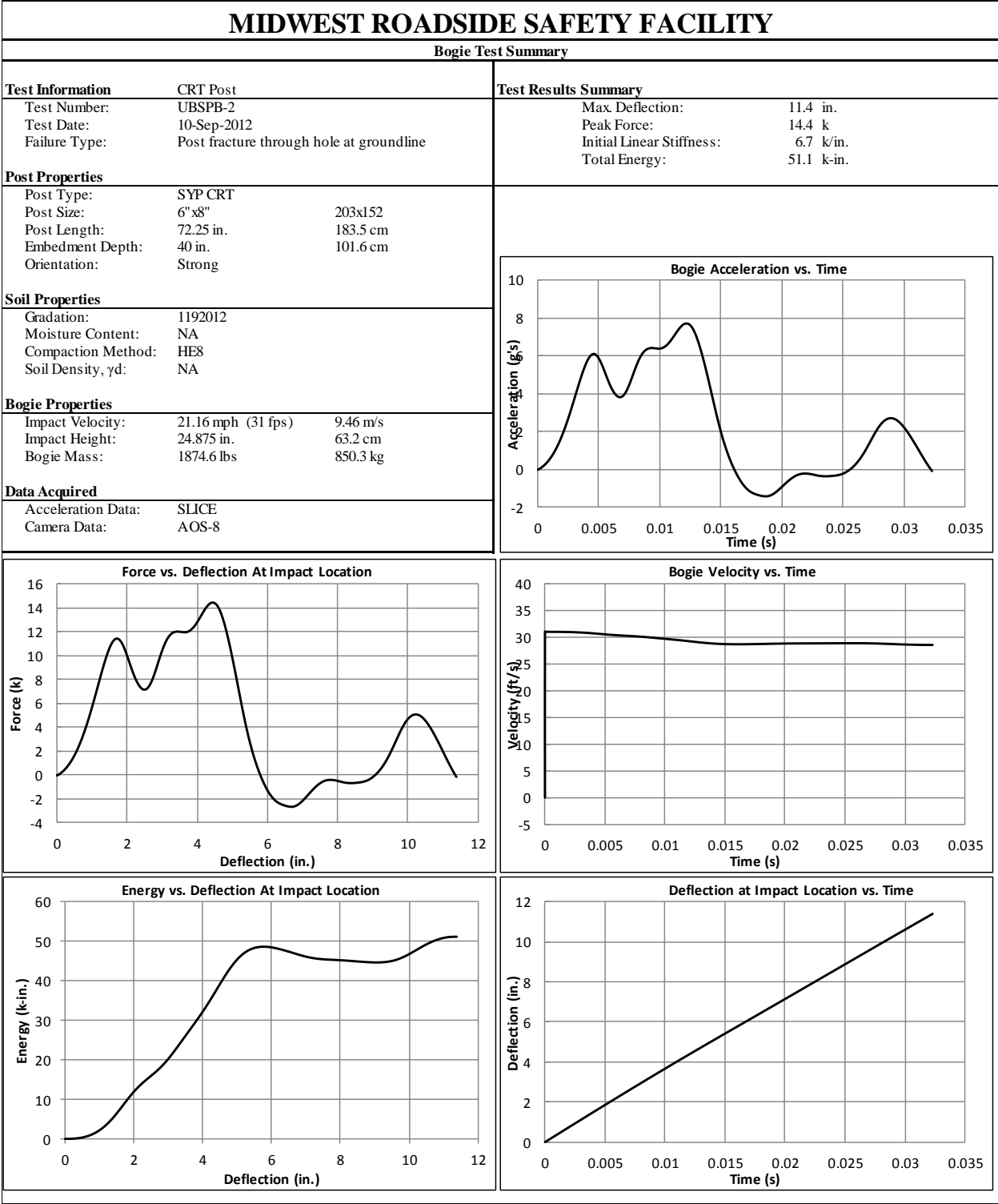


Figure C-3. Results of Test No. UBSPB-2 (SLICE)

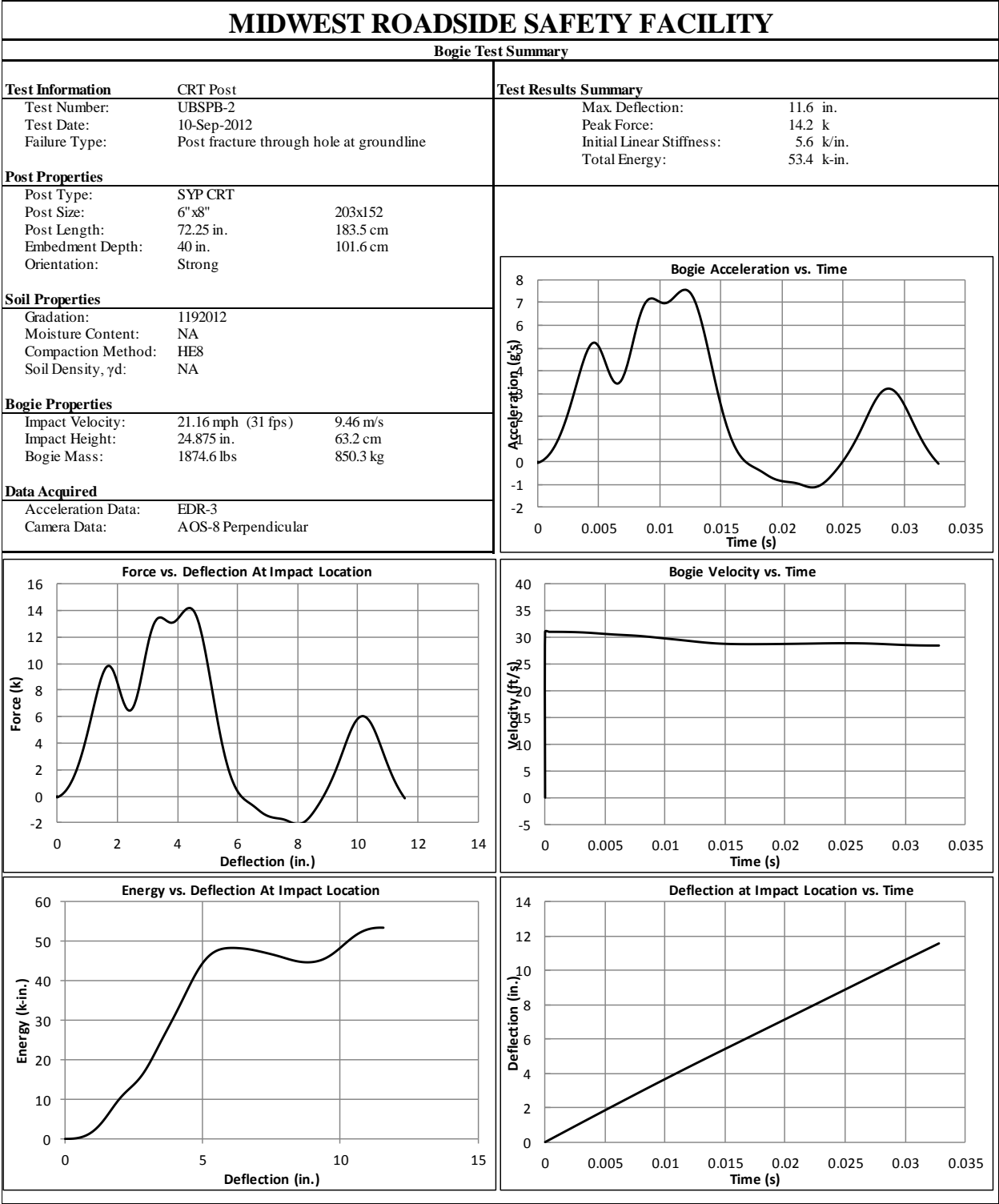


Figure C-4. Results of Test No. UBSPB-2 (EDR-3)

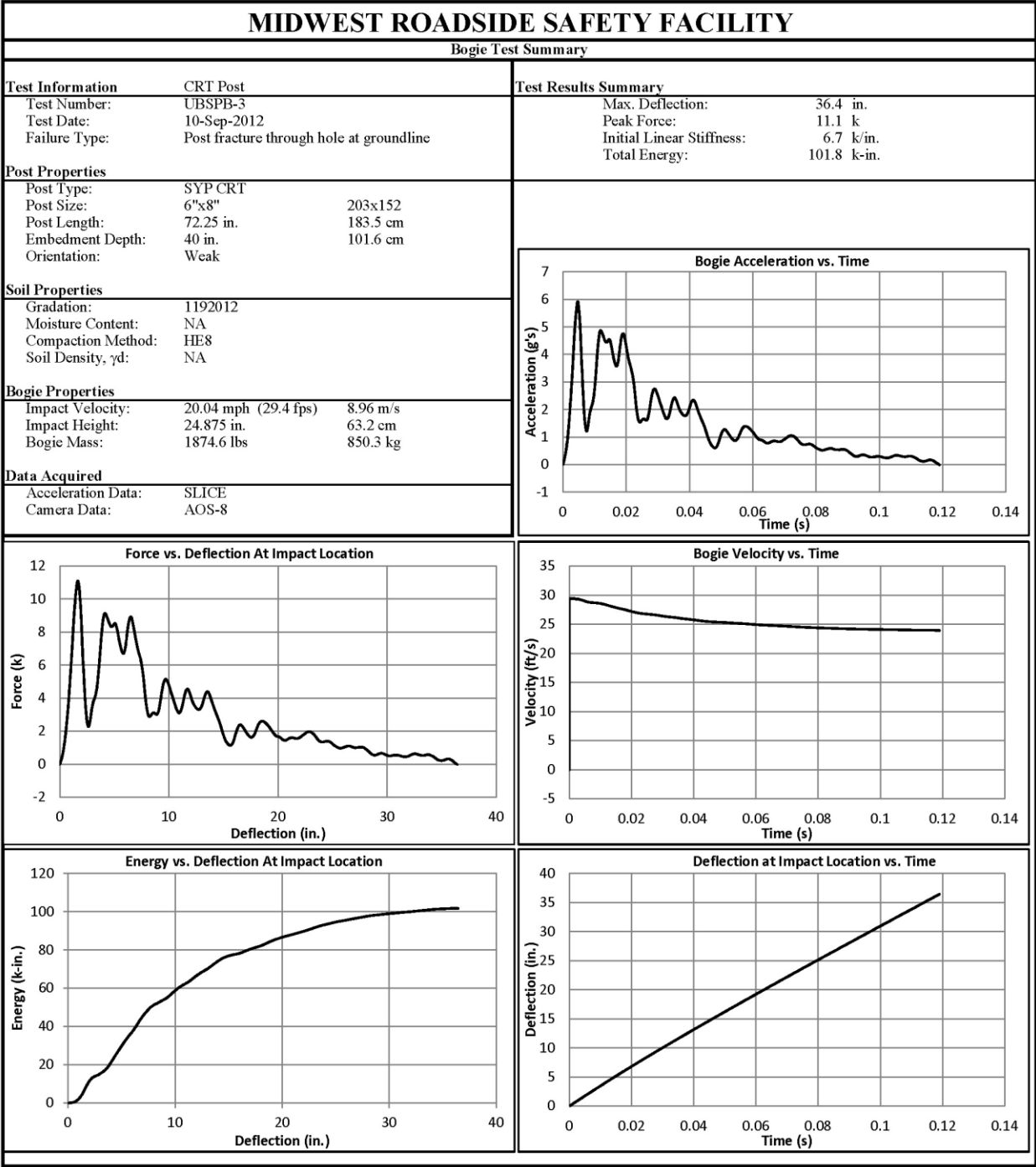


Figure C-5. Results of Test No. UBSPB-3 (SLICE)

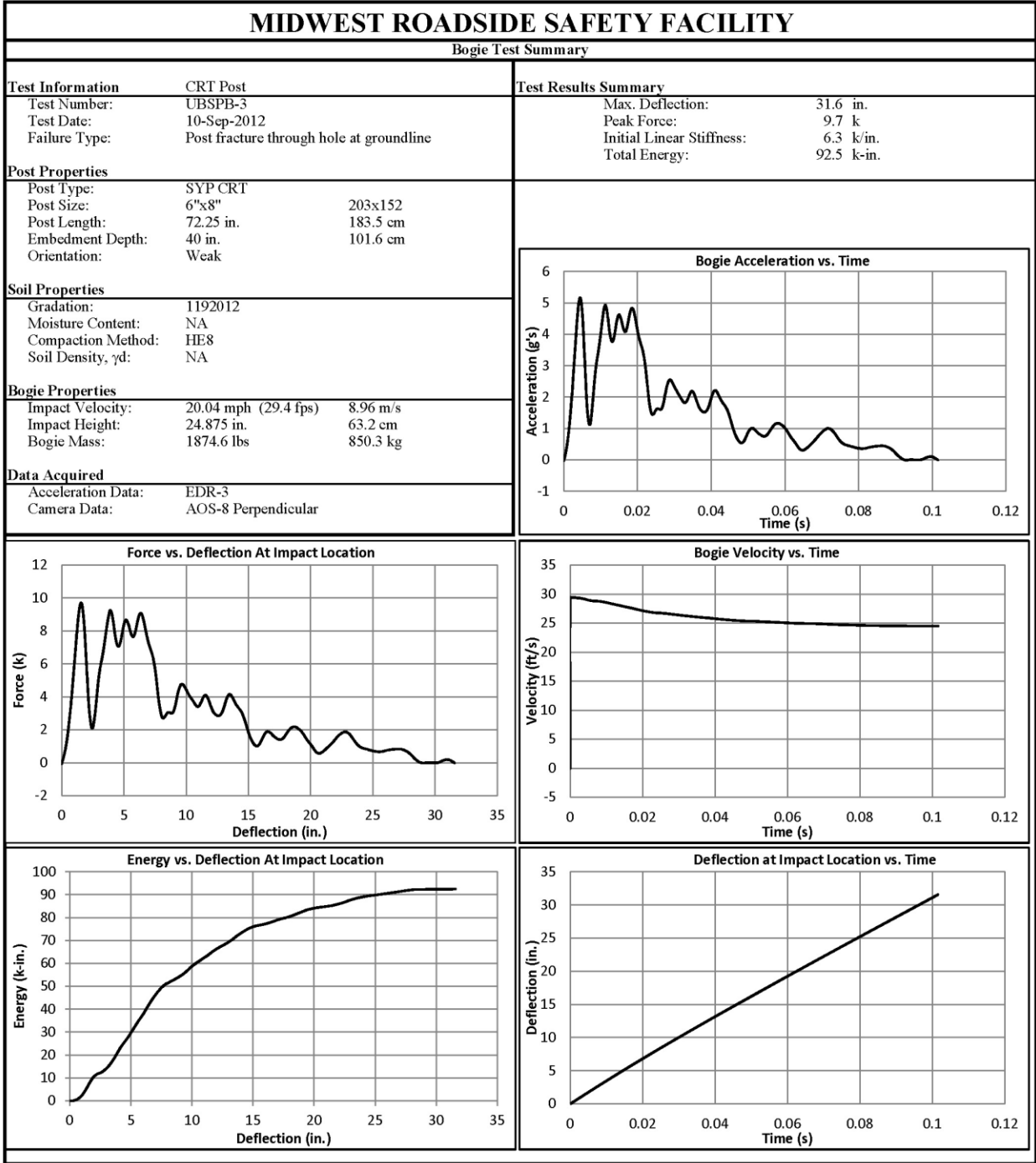


Figure C-6. Results of Test No. UBSPB-3 (EDR-3)

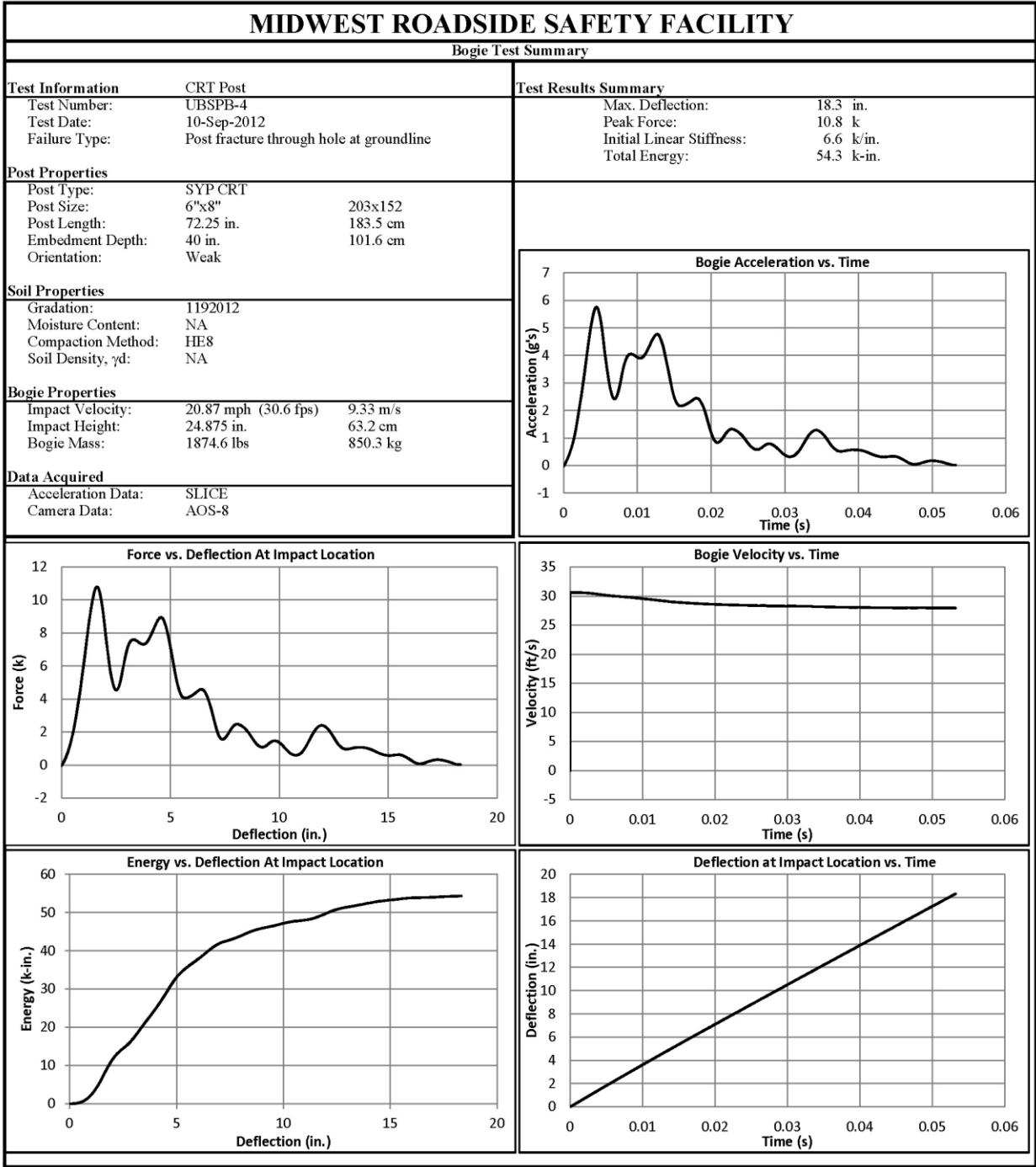


Figure C-7. Results of Test No. UBSPB-4 (SLICE)

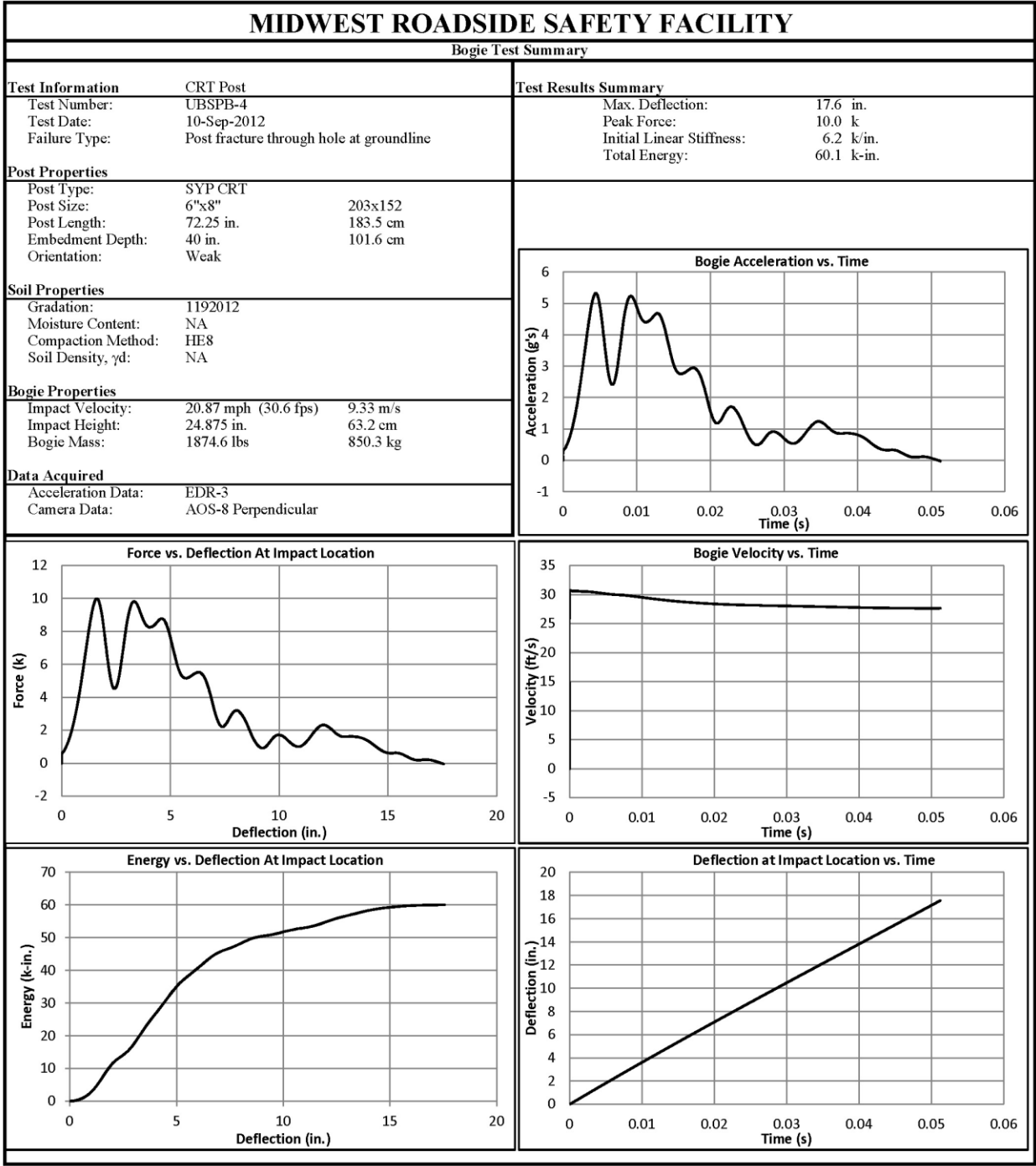


Figure C-8. Results of Test No. UBSPB-4 (EDR-3)

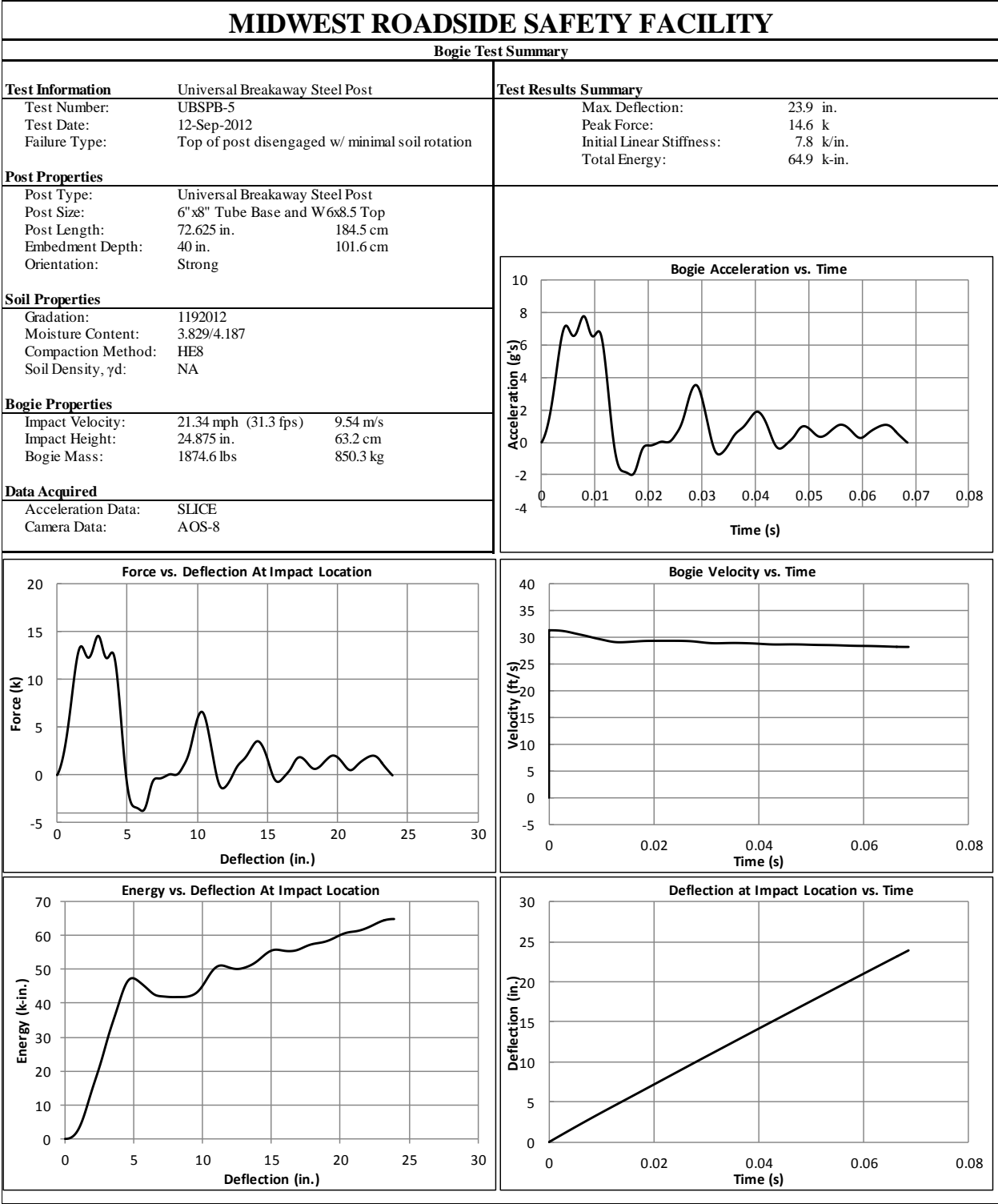


Figure C-9. Results of Test No. UBSPB-5 (SLICE)

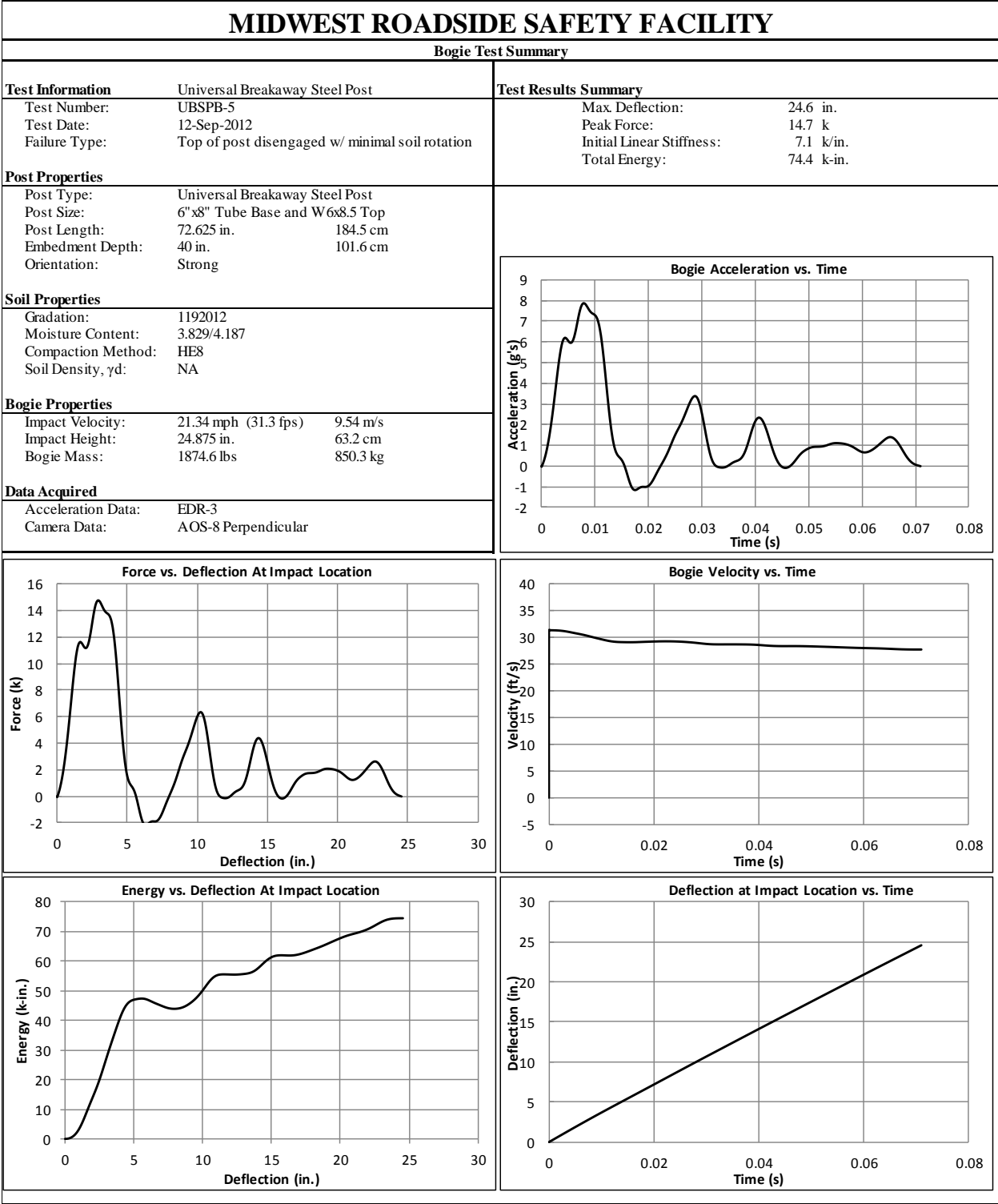


Figure C-10. Results of Test No. UBSPB-5 (EDR-3)

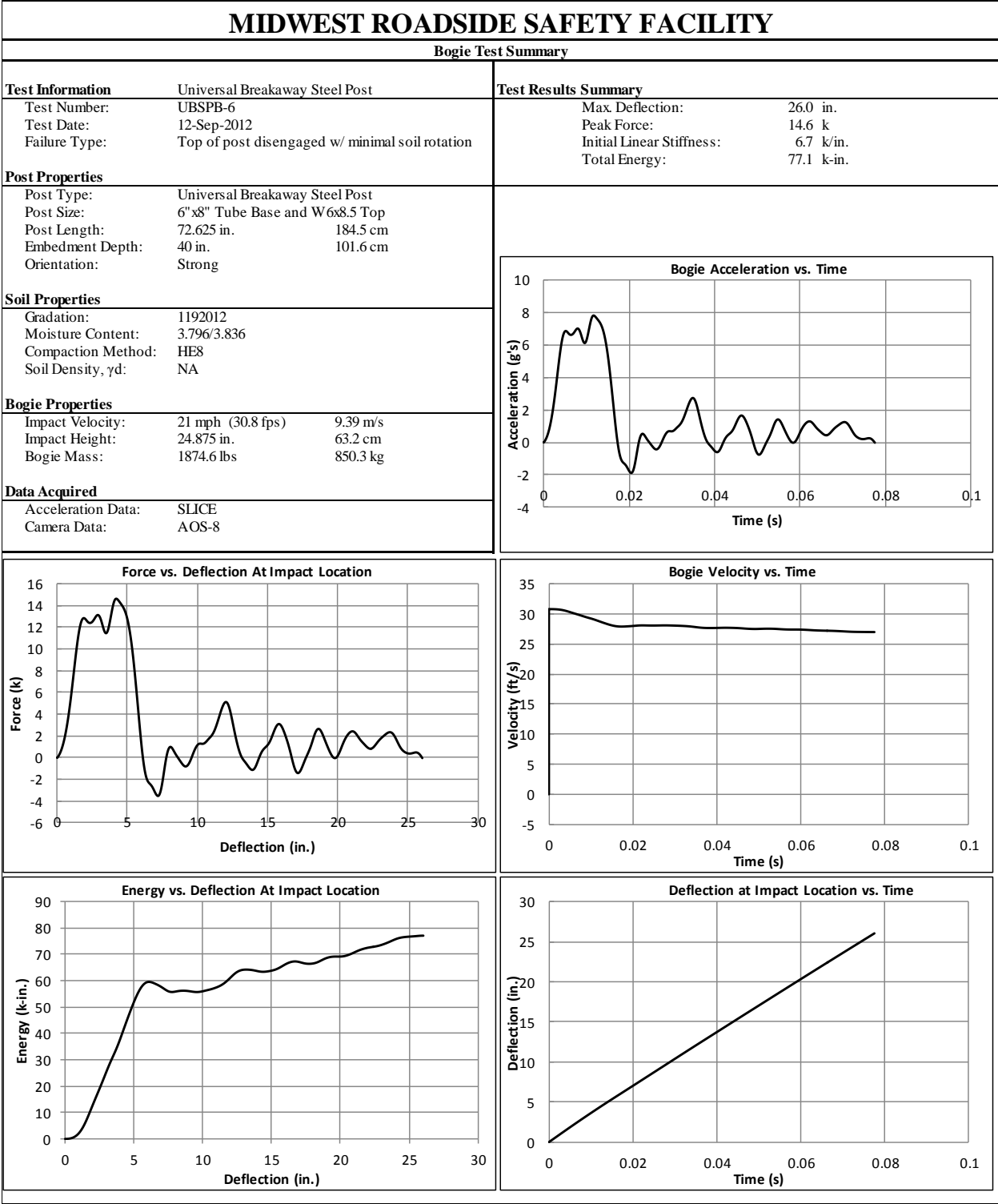


Figure C-11. Results of Test No. UBSPB-6 (SLICE)

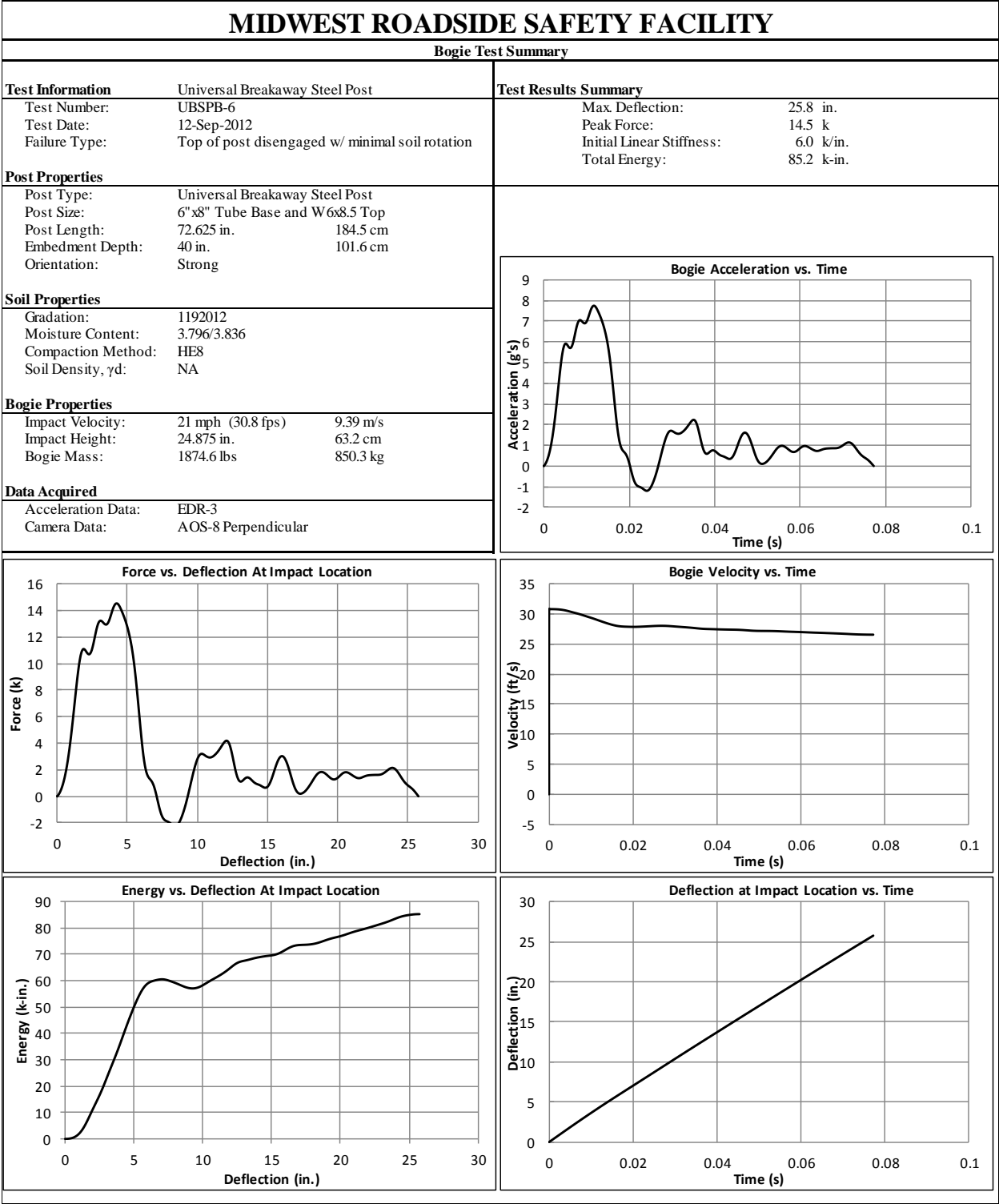


Figure C-12. Results of Test No. UBSPB-6 (EDR-3)

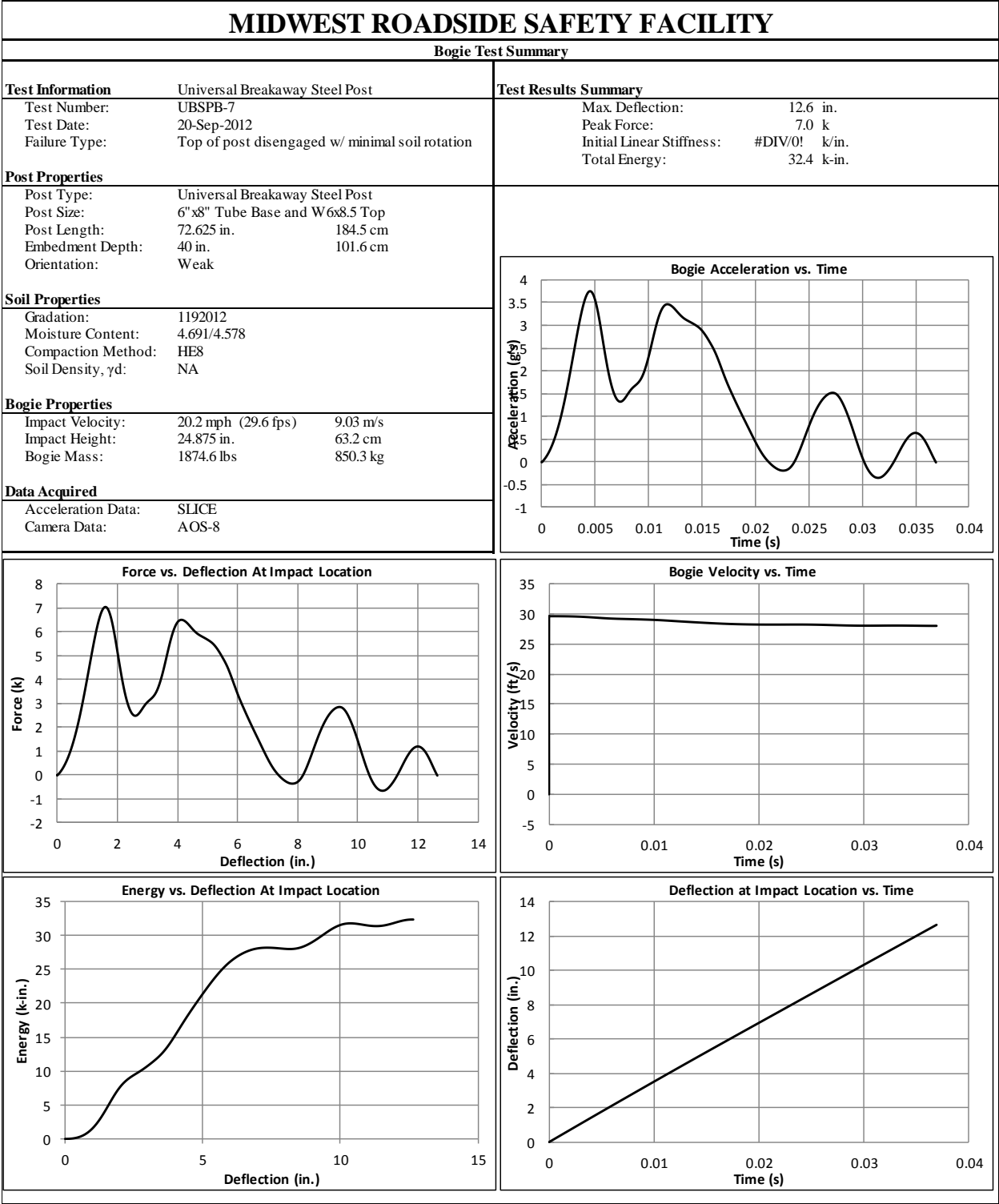


Figure C-13. Results of Test No. UBSPB-7 (SLICE)

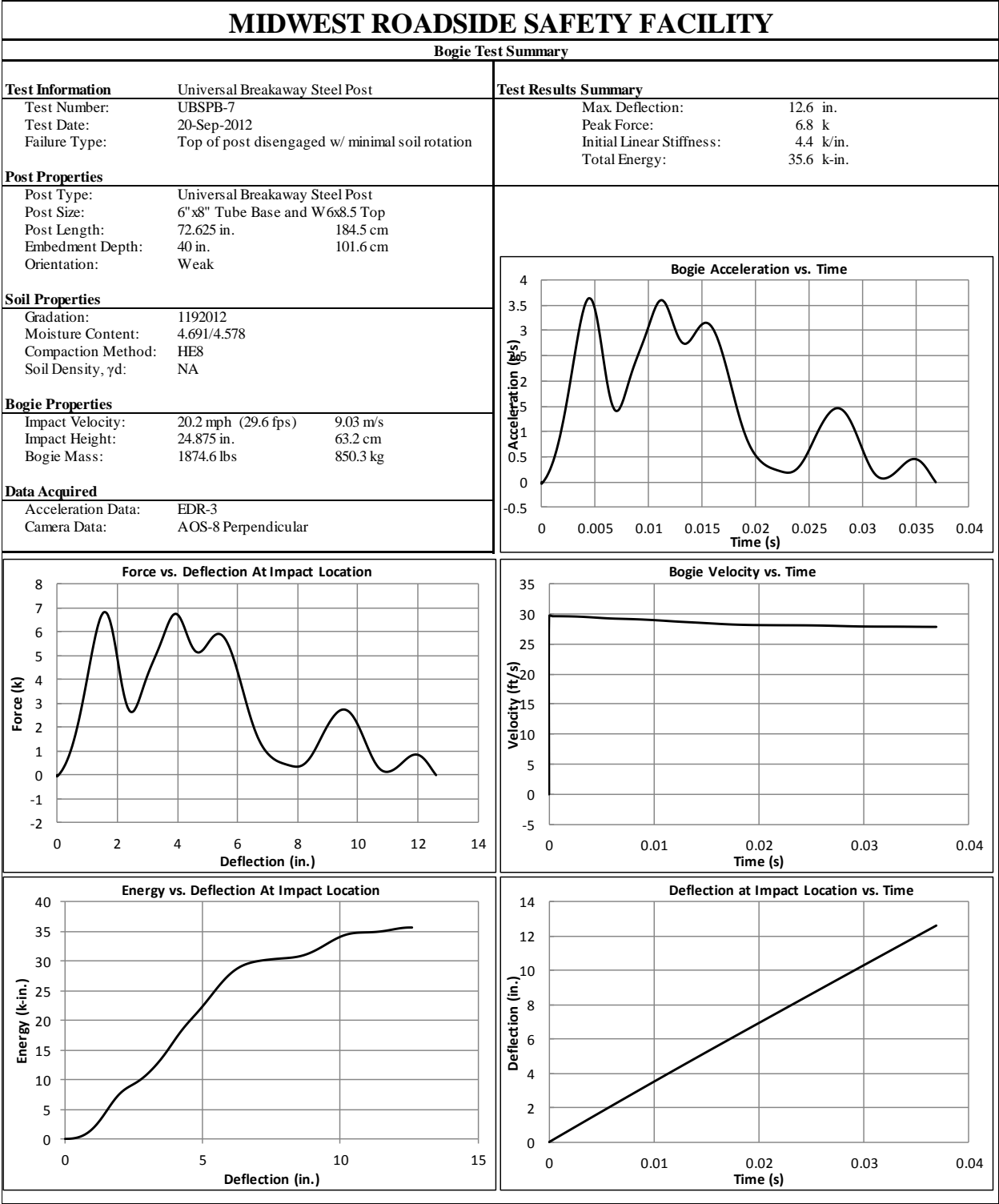


Figure C-14. Results of Test No. UBSPB-7 (EDR-3)

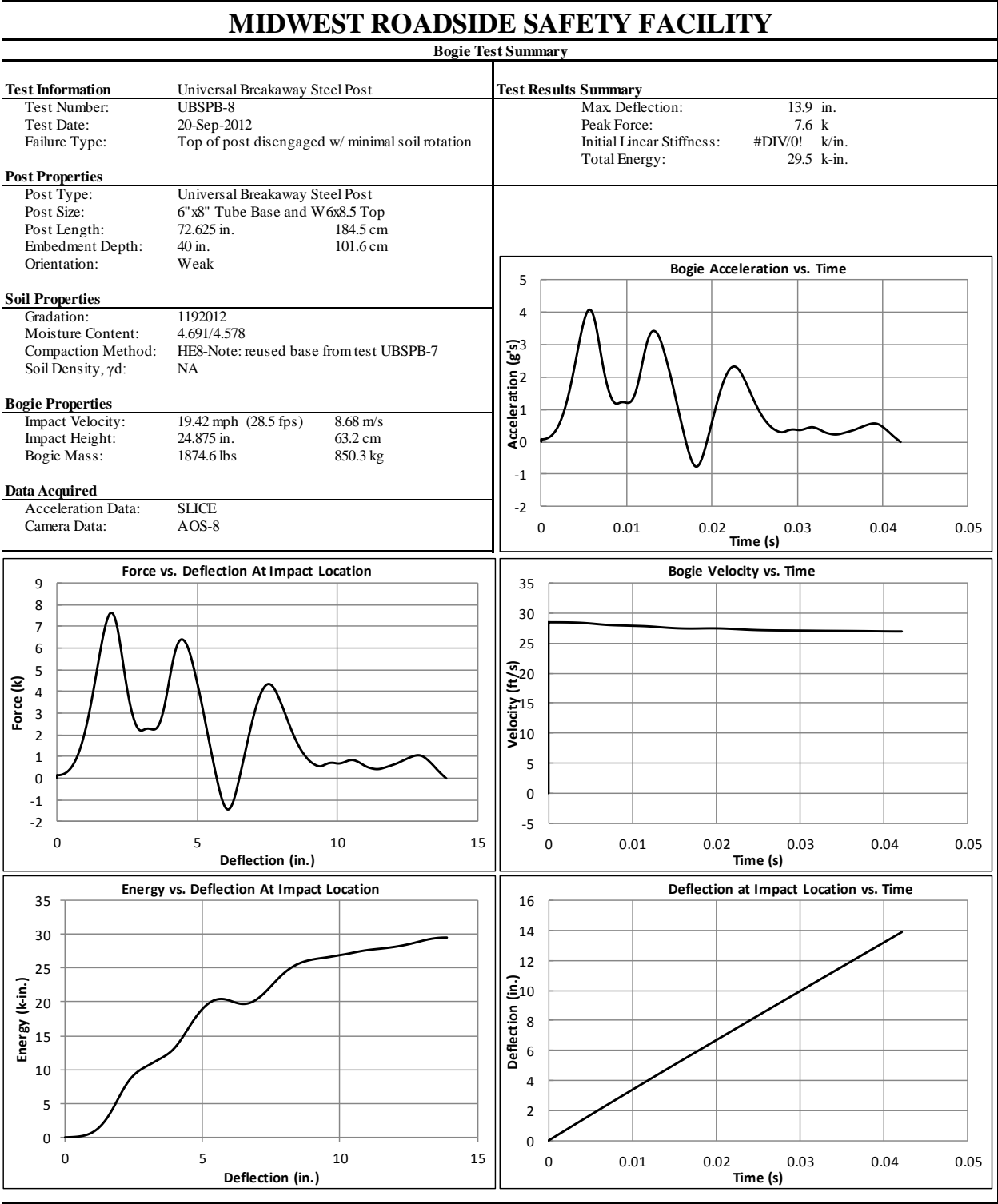


Figure C-15. Results of Test No. UBSPB-8 (SLICE)

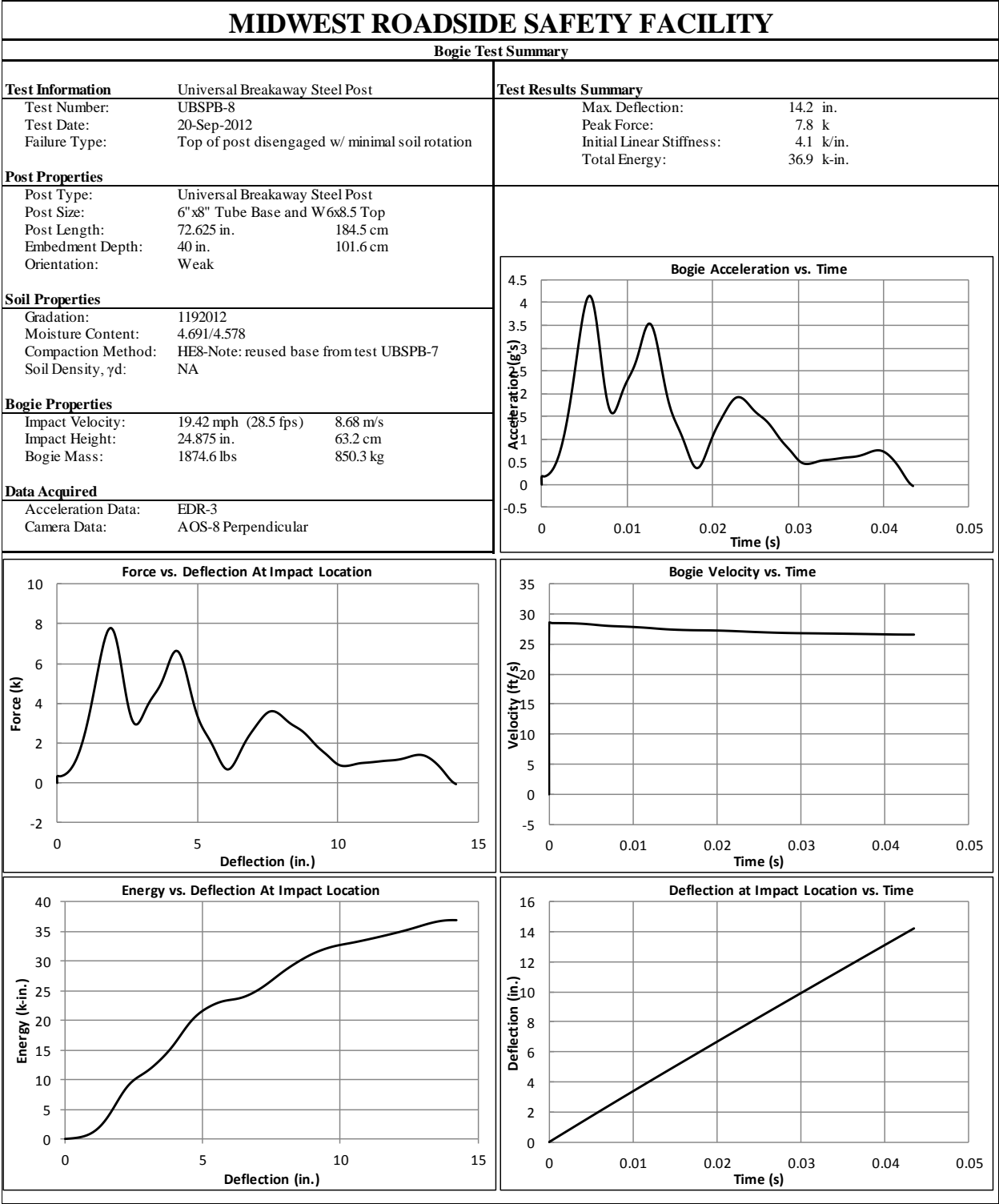


Figure C-16. Results of Test No. UBSPB-8 (EDR-3)

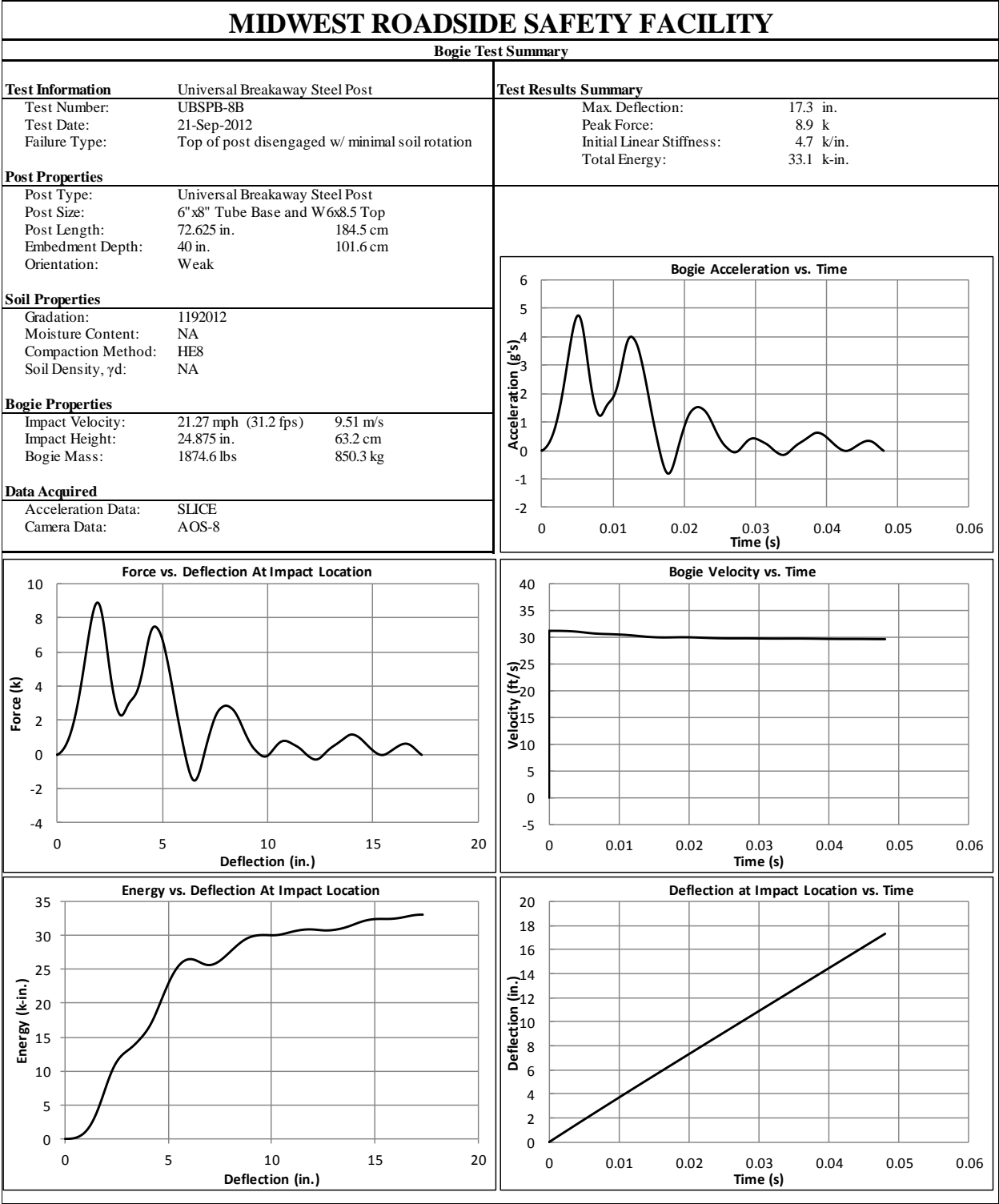


Figure C-17. Results of Test No. UBSPB-8B (SLICE)

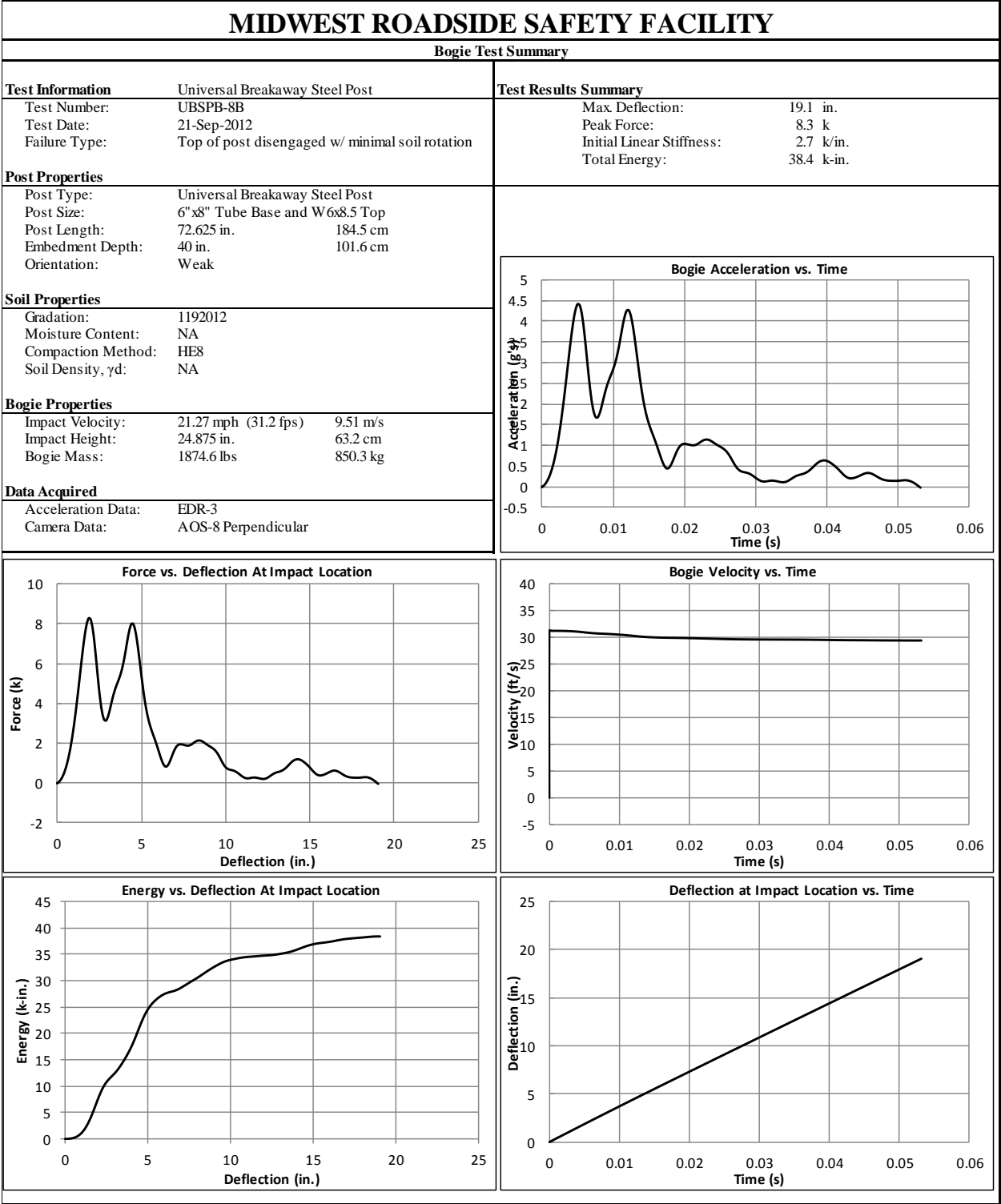


Figure C-18. Results of Test No. UBSPB-8B (EDR-3)

END OF DOCUMENT